This Proposal

entitled

EVENT TRIGGERED STATE ESTIMATION AND OUTPUT FEEDBACK IN CYBER-PHYSICAL SYSTEMS

typeset with NDdiss2$_\varepsilon$ v3.0 (2005/07/27) on April 17, 2011 for

Lichun Li

This LaTeX 2$_\varepsilon$ classfile conforms to the University of Notre Dame style guidelines established in Spring 2004. However it is still possible to generate a non-conformant document if the instructions in the class file documentation are not followed!

> Be sure to refer to the published Graduate School guidelines at `http://graduateschool.nd.edu` as well. Those guidelines override everything mentioned about formatting in the documentation for this NDdiss2$_\varepsilon$ class file.

It is YOUR responsibility to ensure that the Chapter titles and Table caption titles are put in CAPS LETTERS. This classfile does *NOT* do that!

This page can be disabled by specifying the "`noinfo`*" option to the class invocation.* (i.e.,\`documentclass[...,noinfo]{nddiss2e}`)

This page is *NOT* part of the dissertation/thesis, but MUST be turned in to the proofreader(s) or the reviwer(s)!

NDdiss2$_\varepsilon$ documentation can be found at these locations:

`http://www.gsu.nd.edu`
`http://graduateschool.nd.edu`

EVENT TRIGGERED STATE ESTIMATION AND OUTPUT FEEDBACK IN CYBER-PHYSICAL SYSTEMS

A Proposal

Submitted to the Graduate School
of the University of Notre Dame
in Partial Fulfillment of the Requirements
for the Degree of

Doctor of Philosophy in Electrical Engineering

by

Lichun Li, B.S., M.S.

Michael Lemmon, Director

Graduate Program in Electrical Engineering
Notre Dame, Indiana
April 2011

EVENT TRIGGERED STATE ESTIMATION AND OUTPUT FEEDBACK IN CYBER-PHYSICAL SYSTEMS

Abstract

by

Lichun Li

Event triggered approaches to control and estimation have the sensor transmit processed information when a measure of information 'novelty' exceeds a threshold. Prior work has empirically demonstrated that event triggered systems may have significantly longer average sampling intervals than comparably performing periodically triggered systems. There are, however, few results that analytically characterize the tradeoff that event triggering introduces between communication usage and system performance. This proposal studies the tradeoff in event triggered state estimation and output feedback control problems in cyber-physical systems with finite or infinite horizon. We first re-examine event triggered state estimation problems with finite horizon in [17, 36] whose solutions characterize the optimal triggering events that minimize the mean square estimation error over a finite horizon subject to a hard constraint on the number of transmission times. Because the optimal solution is difficult to calculate, this proposal presents an approximate solution with a computational complexity that is polynomial in state-space dimension and horizon length. The same idea is extended to the event triggered output feedback control problem with finite horizon. After that, this proposal discusses event triggered state estimation problems with infinite horizon

is discussed [52]. This work also determines the optimal triggering event that minimizes the mean square estimation error discounted by communication price. We derive a suboptimal solution which extends the work in [11] to unstable systems, and guarantees a specified least average sampling period. This approach is, then, applied to a nonlinear 3 degree-of-freedom helicopter, and achieves better performance than periodic transmission with the same average sampling period. All the previous work serves as the foundation of our future research topics: decoupled event triggered output feedback control, event triggered output feedback systems with delays and dropouts and distributed event triggered state estimation in large scale systems.

CONTENTS

FIGURES

TABLES

CHAPTER 1

INTRODUCTION

The term *cyber-physical systems* (CPS) refers to the tight conjoining of, and coordination between computational and physical resources [19]. Embedded computers and networks monitor and control the physical processes, usually with feedback loops where physical processes affect computations and vice versa. The application of CPS arguably have the potential to dwarf the 20th century IT revolution [20]. Our world will benefit considerably from the research advances of CPS in high confidence medical devices and systems, traffic control and safety, environmental control, power systems, networked building control systems, financial systems, and so on.

The positive impact of CPS in any area above could be enormous. CPS research, however, is still in its infancy [8]. Professional and institutional barriers have resulted in narrowly defined, discipline-specific research. Research is partitioned into isolated subdisciplines such as sensors, communication and networking, control theory, soft engineering and computer science. Systems are designed and analyzed using a variety of modeling formalisms and tools. Each modeling formalism and tool only highlights certain features and disregards others to make analysis tractable. While this method may suffice to support a component-based 'divide and conquer' approach, it neglects the potential benefits of the co-design of CPS and poses a serious problem of verifying overall safety of systems.

Networked control, one of the important topics in CPS, also has the same problem when taking the component-based 'divide and conquer' approach. With this approach, one may restrict oneself to the periodic communication protocol. To reduce the impact of network delay and packet dropout to physical systems, one may need either a shorter sampling period which will result in higher communication usage, or a more aggressive controller which generally would be less robust. But if we break the barrier between disciplines of control and communication, and release ourselves from the periodic communication protocol, we are able to preserve the performance of the physical system without increasing the communication usage or reducing the system's robustness. One method for the co-design of both controller (physical part) and communication protocol (cyber part) is called 'event triggering'.

Event triggering is a communication protocol with which information is transmitted only if some event occurs. In particular, the event is always designed as a measure of data 'novelty' exceeding a threshold. There has been numerous experimental results to support the assertion that event triggering achieves better system performance than periodically triggered systems using the same communication resources [1–3, 6, 7, 12, 15, 21, 26–29, 34, 35, 39–51]. But little substantive work analytically investigates the tradeoff between system performance and communication usage. Our purpose is to analytically examine the tradeoff between system performance and communication usage for event triggered state estimation and observer based output feedback control in CPS.

One of the interesting questions about the tradeoff is what the best system performance is for given communication limitation. This question was first answered in [16–18, 33, 36–38] for event triggered state estimation problem over a

finite horizon. In the finite horizon case, the communication limitation is limited transmission times during the finite horizon, and the system performance is mean square estimation error (MMSE) of a remote observer. It could be seen as an optimal control problem, and dynamic programming was used to solve it. However, it was found that the optimal triggering event could only be calculated numerically, and the computational complexity grew exponentially with respect to the state dimension. This was also the main reason that the prior work only confined their attention to scalar systems. This restriction to scalar systems is of limited use in developing real-life applications of event-triggered systems. A major challenge to be addressed by the research community therefore lies in finding practical ways of extending this analytical framework to multi-dimensional systems.

A computationally effective suboptimal triggering event is then presented in Chapter 2, which is also the main results in [24]. In this work, since the optimal triggering set is not convex, we use the union of several ellipsoids to approximate the optimal triggering set. The computational complexity of the suboptimal triggering event is only cubic with respect to the state dimension, and it is shown from simulation results that the suboptimal triggering set approximates the optimal triggering set very well. We extend the same idea to the output feedback control problem with finite horizon in [22], which will be introduced in Chapter 3.

All the results above are for finite horizon cases. For infinite horizon cases, the event triggered state estimation problem is addressed in this proposal. The main difference between finite and infinite horizon cases is how the communication limitation is expressed. In infinite horizon, the communication limitation, such as average sampling period, average transmission frequency and so on, is reflected by a parameter called communication price. The communication limitation in

infinite horizon can be seen as a 'soft' requirement, because even though higher communication price reflects fewer communication resources, we still don't know exactly what the average sampling period or average transmission frequency is.

[52] discussed the optimal triggering event to minimize the MMSE discounted by the communication price, but the optimal triggering event was computationally complex. A simpler suboptimal approach was proposed in [11] which was able to bound the difference between the performance achieved by the optimal and suboptimal triggering event for stable systems. Since the proposed optimization metric is explicitly discounted by the cost of transmission, it implicitly considers the tradeoff between the performance and the sampling period. That tradeoff, however, was never made explicit in the earlier papers.

Chapter 4 re-examines the problem in [52] using a suboptimal solution similar to that proposed in [11], and extends the earlier work in [11] to unstable systems. Our main results are the design of quadratic suboptimal triggering events that guarantee the required least average sampling period and explicit lower and upper bounds on discounted MSEE [23]. This event triggered state estimator is applied to a highly nonlinear 3 degree-of-freedom helicopter in Chapter 5. The experimental results shows that the event triggered state estimator in Chapter 4 can achieve better performance than the periodically triggered state estimator with the same average sampling period.

There are three research objectives in the future:

1. Decoupled optimal triggering events for output feedback systems with infinite horizon. In these output feedback systems, the whole control loop, which is from sensor to controller and from controller to actuator, is closed over a communication network. Our objective is to design decoupled trig-

gering events for both sensor and controller such that the mean square state of the plant is minimized. By 'decoupled', we mean the transmission of one link doesn't trigger the transmission of the other and both the sensor and the controller can decide when to transmit data by their local information. This decoupled event triggered output feedback systems have never been talked about in the prior work, which considers that either only one part of the control loop is closed over a communication network, or the triggering events in the sensor and the controller are coupled. The main difficulty to get the decoupled triggering events lies on how to make the information of controller decoupled with the decision of sensor. Once the decoupling is done, the triggering events in both sensor and controller can be derived using the same way in our earlier work in Chapter 4.

2. Decoupled event triggered output feedback systems with delays and dropouts. The impact of delays and dropouts to event triggered state feedback systems has already been analyzed in [31, 46–48], but the impact of time delays and packet dropouts to the event triggered output feedback systems has never been studied. This work will study this impact to the event triggered output feedback systems based on user datagram protocol.

3. Distributed event triggered state estimation problem in large scale systems. Recently, there has been great interest in large scale systems, such as power systems, transportation systems and so on. So we would like to extend our work in Chapter 4 to large scale systems. In these large scale systems, there is a data center collecting information from a lot of sensors and making an estimate of the state. Each sensor may only detect a part of the state. Our objective is to design a distributed triggering event for each sensor such

that the mean square estimation error in the data center is minimized. By 'distributed', we mean the triggering event of each sensor only relies on local information. The prior work considering event triggering method in large scale systems mainly studied multi-agent systems without data centers [12, 13, 25, 43, 46–48, 51]. Compared with the multi-agent systems, our structure is more efficient in communication and closer to the practical large systems such as smart transmission grid [10].

We will further discuss how to fulfill these objectives in Chapter 6.

CHAPTER 2

OPTIMAL AND SUBOPTIMAL TRIGGERING SETS OF STATE ESTIMATION PROBLEM WITH FINITE HORIZON

This chapter considers an estimation problem in which a sensor sporadically transmits information to a remote observer. An event triggered approach is used to trigger the transmission of information from the sensor to the remote observer. The event trigger is chosen to minimize the mean square estimation error at the remote observer subject to a constraint on how frequently the information can be transmitted. This problem was recently studied by M. Rabi et al. [36–38] and O. Imer et al. [16–18] where the observed process was a scalar linear system over a finite time interval. This paper relaxes the prior assumption of zero mean initial condition and no measurement noise and extends those earlier results to vector cases and derives a much more computational effective suboptimal threshold which approximates the optimal one very well in our simulations.

2.1 Problem Statement

The event triggering problem in this chapter assumes that a sensor is observing a linear discrete time process over a finite horizon of length $M+1$. The process state $x : \{0, 1, \cdots, M\} \to \mathbb{R}^n$ satisfies the difference equation

$$x(k) = Ax(k-1) + w(k)$$

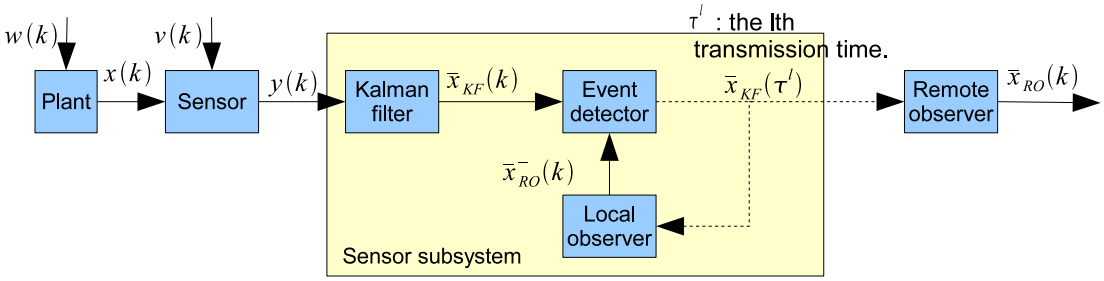

Figure 2.1. Structure of event triggered networked state estimator

for $k \in \{1, 2, \cdots, M\}$ where A is a real $n \times n$ matrix, $w : \{1, 2, \cdots, M\} \to \mathbb{R}^n$ is a zero mean white noise process with variance W. The initial state, $x(0)$, is assumed to be a Gaussian random variable with mean μ_0 and variance Π_0. The sensor generates a measurement $y : \{0, 1, \cdots, M\} \to \mathbb{R}^m$ that is a corrupted output. The sensor measurement at time k is

$$y(k) = Cx(k) + v(k)$$

for $k \in \{0, 1, \cdots, M\}$ and where $v : \{0, 1, \cdots, M\} \to \mathbb{R}^m$ is another zero mean white noise process with variance V that is uncorrelated with the process noise w. The process and sensor blocks are shown on the left hand side of Figure 2.1. In this figure, the output of the sensor feeds into a sensor subsystem that decides when to transmit information to a remote observer.

The sensor subsystem consists of three components: an *event detector*, a *Kalman filter*, and a *local observer*. The event detector decides when to transmit information at $\bar{b} \in \{0, 1, \cdots, M+1\}$ time instants to the remote observer. So $\bar{b}$ represents the total number of transmissions that the sensor is allowed to make to the remote observer. We let the $\tau^0 = \emptyset$ indicate that that there is no

transmission at the beginning, and $\{\tau^\ell\}_{\ell=1}^{\bar{b}}$ denote a sequence of increasing times ($\tau^\ell \in \{0, 1, \cdots, M\}$) when information is transmitted from the sensor to the remote observer. The decision to transmit is based on estimates that are generated by the Kalman filter and local observer.

Let $\mathcal{Y}(k) = \{y(0), y(1), \cdots, y(k)\}$ denote the measurement information available at time k. The *Kalman filter* generates a state estimate $\overline{x}_{KF} : \{0, 1, \cdots, M\} \to \mathbb{R}^n$ that minimizes the mean square estimation error $E\left[\|x(k) - \overline{x}_{KF}(k)\|_2^2 \,|\, \mathcal{Y}(k)\right]$ at each time step conditioned on all of the sensor information received up to and including time k. These estimates, of course, can be computed using the Kalman filter. For the process under study the filter equations are

$$\overline{x}_{KF}(k) = A\overline{x}_{KF}(k-1) + L(k)\left(y(k) - CA\overline{x}_{KF}(k-1)\right) \tag{2.1}$$

for $k \in \{1, 2, \cdots, M\}$. Let $\overline{e}_{KF}(k) = x(k) - \overline{x}_{KF}(k)$ be the filtered state error, and the variance of $\overline{e}_{KF}(k)$, $\overline{P}(k)$, satisfies

$$\overline{P}(k) = A\overline{P}(k-1)A^T + W - L(k)C\left(A\overline{P}(k-1)A^T + W\right), \tag{2.2}$$

where

$$L(k) = \left(A\overline{P}(k-1)A^T + W\right)C^T\left(C\left(A\overline{P}(k-1)A^T + W\right)C^T + V\right)^{-1}.$$

The initial condition are

$$\begin{aligned} \overline{x}_{KF}(0) &= \mu_0 + \Pi_0 C^T (C\Pi_0 C^T + V)^{-1}\left(y(k) - C\mu_0\right) \\ \overline{P}(0) &= \Pi_0 - \Pi_0 C^T\left(C\Pi_0 C^T + V\right)^{-1} C\Pi_0. \end{aligned}$$

The event detector uses the *Kalman filter's* state estimate, $\overline{x}_{KF}$, and another estimate generated by a *local observer* to decide when to transmit the filtered state $\overline{x}_{KF}$ to the *remote observer*. Given a set of transmission times $\{\tau^\ell\}_{\ell=1}^{\bar{b}}$, let $\overline{\mathcal{X}}(k) = \left\{\overline{x}_{KF}(\tau^1), \overline{x}_{KF}(\tau^2), \ldots, \overline{x}_{KF}(\tau^{\ell(k)})\right\}$ denote the filter estimates that were transmitted to the remote observer by time k where $\ell(k) = \max\left\{\ell \,:\, \tau^\ell \leq k\right\}$. We can think of this as the "information set" available to the remote observer at time k. The remote observer generates a posteriori estimate $\overline{x}_{RO} : \{0, 1, \cdots, M\} \to \mathbb{R}^n$ of the process state that minimizes the MSEE, $E\left[\|x(k) - \overline{x}_{RO}(k)\|_2^2 \,|\, \overline{\mathcal{X}}(k)\right]$, at time k conditioned on the information received up to and including time k. The a priori estimate of the remote observer, $\overline{x}_{RO}^- : \{0, 1, \cdots, M\} \to \mathbb{R}^n$, minimizes $E\left[\|x(k) - \overline{x}_{RO}(k)\|_2^2 \,|\, \overline{\mathcal{X}}(k-1)\right]$, the MSEE at time k conditioned on the information received up to and including time $k-1$. These estimates take the form

$$\overline{x}_{RO}^-(k) = E(x(k)|\overline{\mathcal{X}}(k-1)) = A\overline{x}_{RO}(k-1) \tag{2.3}$$

$$\overline{x}_{RO}(k) = \begin{cases} \overline{x}_{KF}(k), & \text{if transmitting at step k;} \\ \overline{x}_{RO}^-(k), & \text{otherwise.} \end{cases} \tag{2.4}$$

where $\overline{x}_{RO}^-(0) = \mu_0$. The event-detection strategy that is used to select the transmission times τ^l is based on observing the *a priori gap*, $e_{KF,RO}^-(k) = \overline{x}_{KF}(k) - \overline{x}_{RO}^-(k)$ between the filter's estimate $\overline{x}_{KF}$ and the remote observer's a priori estimate $\overline{x}_{RO}^-$. Note that even though the gap is a function of the remote observer's estimate, this signal will be available to the sensor. This is because the sensor has access to all of the information, $\overline{\mathcal{X}}(k)$, that it sent to the remote observer. As a result, the sensor can use another *local observer* to construct a copy of $\overline{x}_{RO}^-$ that can be locally accessed by the event detector to compute the gap. This local observer is shown as part of the sensor subsystem in Figure 2.1. The event detector's

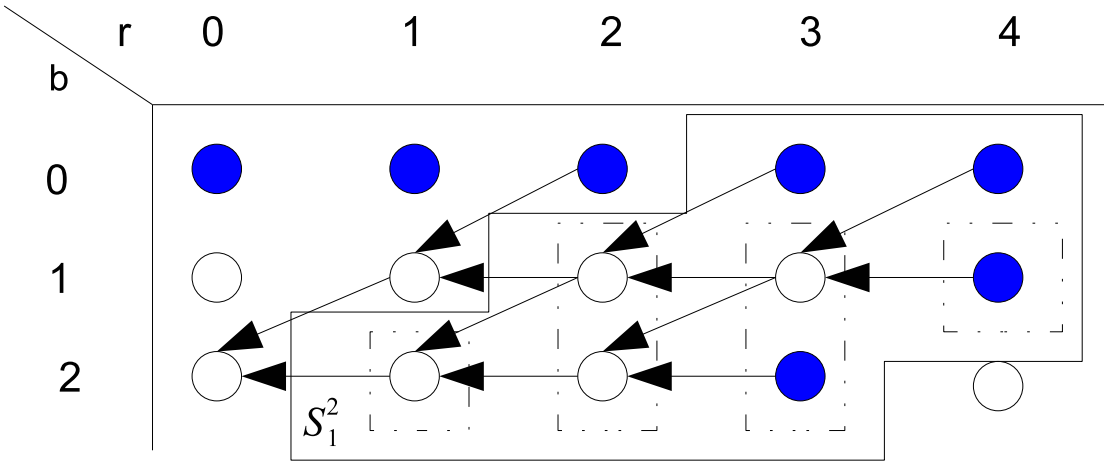

Figure 2.2. Collection of triggering sets and order of calculating value function with M=4, $\bar{b}$=2

decision to transmit is triggered when the estimate's gap $e^-_{KF,RO}(k)$ goes out of a time varying triggering set $S_k^{b(k)}$ where $k \in \{0, 1, \cdots, M\}$ and $b(k)$ is the number of transmissions that are remaining at step k.

For later convenience, the following notational conventions are used throughout this paper. $\mathcal{S}_r^b(k) = \{S_k^{\max\{0,b-k+r\}}, ..., S_k^{\min\{b,M+1-k\}}\}$ are the triggering sets that may be used at step k when b transmissions remaining at step $r \leq k$, and $\mathcal{S}_r^b = \{\mathcal{S}_r^b(r), \cdots, \mathcal{S}_r^b(M)\}$. For example, suppose at step 1 there are 2 transmissions remaining, then at step 1 only $\mathcal{S}_1^2(1) = \{S_1^2\}$ may be used as triggering set, at step 2, $\mathcal{S}_1^2(2) = \{S_2^2, S_2^1\}$ may be used as triggering sets and so on, which are contained by the dashed line in Figure 2.2 and $\mathcal{S}_1^2$ is contained in the solid line. Let $e_{KF,RO}(k) = \overline{x}_{KF}(k) - \overline{x}_{RO}(k)$. $I^-(k) = \{e^-_{KF,RO}(k), b(k)\}$ and $I(k) = \{e_{KF,RO}(k), b(k+1)\}$ are ordered pairs denoting the a priori and posteriori information sets at k respectively.

Let $\overline{e}_{RO}(k) = x(k) - \overline{x}_{RO}(k)$ be the remote state estimation error, and the cost

function is defined as

$$J_M^{\bar{b}}(\mathcal{S}_0^{\bar{b}}) = E\left(\sum_{k=0}^{M} \|\overline{e}_{RO}(k)\|_2^2\right).$$

The expectation is taken over $\{\overline{e}_{RO}(k)\}_{k=0}^{M}$. Our objective is to find the optimal triggering sets $\mathcal{S}_0^{\bar{b}}$ to minimize the cost function:

$$J_M^{\bar{b}*} = \min_{\mathcal{S}_0^{\bar{b}}} J_M^{\bar{b}}(\mathcal{S}_0^{\bar{b}}) \tag{2.5}$$

2.2 Optimal Triggering Sets

The problem in Equation (2.5) can be treated as an optimal control problem of a stochastic process. In our case, the controllable variables are the triggering sets $\mathcal{S}_0^{\bar{b}}$, rather than some "control signal". So it can also be solved using stochastic dynamic programming. After analyzing the properties of optimal triggering set, we find that its computational complexity is exponential with respect to state dimension. So a suboptimal triggering set is derived, which yields to a cubic computational complexity with respect to the state dimension.

The value function is defined in Equation (2.6). It's very similar with how it's defined in stochastic dynamic programming. Because of the Markov property of the information sets $\{I^-(k), I(k)\}_{k=0}^{M}$ (shown in Lemma A.0.2), the expectation is only taken based on the current a priori information set.

$$h(\zeta, b; r) = \min_{\mathcal{S}_r^b} E\left(\sum_{k=r}^{M} \|\overline{e}_{RO}(k)\|_2^2 | I_r^- = (\zeta, b)\right) \tag{2.6}$$

We notice that $J_M^{\bar{b}*} = E(h(e_{KF,RO}^-(0), \bar{b}; r))$.

In Theorem 2.2.1, we show that the value function (2.6) satisfies a backward

recursive equation. The proof is given in the Appendix.

Theorem 2.2.1. *The value function (2.6) satisfies the backward recursive equation:*

$$h(\zeta, b; r) = \min\left\{h_{nt}(\zeta, b, r), h_t(\zeta, b, r)\right\}, \tag{2.7}$$

where

$$h_{nt}(\zeta, b, r) = tr\left(\overline{P}(r)\right) + \|\zeta\|_2^2 + E\left(h(e^-_{KF,RO}(r+1), b; r+1)|I(r) = (\zeta, b)\right)$$

is the cost without transmitting at step r and

$$h_t(\zeta, b, r) = tr\left(\overline{P}(r)\right) + E\left(h(e^-_{KF,RO}(r+1), b-1; r+1)|I(r) = (0, b-1)\right)$$

is the cost with transmitting at step r. Notice that $h_t(\zeta, b, r)$ is independent of ζ.

The initial conditions for the value function are

$$h(\zeta, 0; r) = \zeta^T \Lambda^0_{r,1} \zeta + c^0_{r,1} \tag{2.8}$$

$$h(\zeta, b; M+1-b) = \rho^b_{M+1-b}, \tag{2.9}$$

where

$$\begin{aligned}
\Lambda^0_{r,1} &= \sum_{k=r}^{M} (A^T)^{k-r} A^{k-r}, \\
c^0_{r,1} &= \sum_{k=r}^{M} \left(\sum_{j=r+1}^{k} tr\left(R(j-1)L(j)^T (A^T)^{k-j} A^{k-j} L(j)\right) + tr(\overline{P}(k)) \right); \\
\rho^b_{M+1-b} &= tr\left(\sum_{k=M+1-b}^{M} \overline{P}(k) \right),
\end{aligned}$$

with $R(j) = CA\overline{P}(j)A^TC^T + CWC^T + V$. *The optimal triggering set*

$$S_r^{b*} = \{\zeta : h_{nt}(\zeta, b, r) \leq h_t(\zeta, b, r)\}, \tag{2.10}$$

with $S_r^{0*} = \mathbb{R}^n$ *for all* $r = 0, \cdots, M$ *and* $S_{M+1-b}^{b*} = \emptyset$ *for all* $b = 1, \cdots, \overline{b}$.

What should be apparent in examining Equation (2.7) is that the optimal cost at time step r is based on the choice between the costs of transmitting or not transmitting at step r. The actual values that those two costs take is conditioned on the value $e_{KF,RO}^-(r) = \zeta$, the a priori gap taken at time step r. This means we can use the choice in Equation (2.7) to identify two mutually disjoint sets; the trigger set S_r^{b*} and its complement. If $e_{KF,RO}^-$ is not in the set S_r^{b*}, then we trigger a transmission otherwise the sensor decides not to transmit its information.

Equation (2.7) is a backward recursion that recurses over two sets of indices; the time steps, r, and the remaining transmissions b. The value function, $h(\zeta, b; r)$, at time step r with b remaining transmissions is computed from $h(\zeta, b; r+1)$ and $h(\zeta, b-1; r+1)$, the value functions at time step $r+1$ with b and $b-1$ remaining transmissions respectively. The initial conditions given in Equation (2.8) and (2.9) are the value functions when there is no remaining transmission and when there is a transmission at each step.

We can picture the recursion as shown in Figure 2.2 . This picture plots the indices (b, r) and identifies the initial conditions and the order of computation. The blue dots in the graph show the initial value functions given in Equation (2.8) and (2.9). The arrows show the computational dependencies in the recursion.

According to Theorem 2.2.1, some properties of value function and optimal triggering sets are stated below, and their proofs are shown in the Appendix.

Corollary 2.2.2. *With b and r fixed, the value function $h(\zeta, b; r)$ is symmetric about the origin and nondecreasing with respect to $\|\zeta\|_2$ in the same direction, i.e.*

$$h(\zeta, b; r) = h(-\zeta, b; r);$$
$$h(\alpha_1 d, b; r) \geq h(\alpha_2 d, b; r), \forall \alpha_1 \geq \alpha_2 \geq 0, d \in \mathbb{R}^n$$

Corollary 2.2.3. *Given any direction $d \in \mathbb{R}^n$, the optimal triggering set S_r^{b*} lying in this direction is in the form of $[-\theta_r^b(d), \theta_r^b(d)]$.*

Since there's no closed form for the value functions and optimal triggering sets, they can only be calculated numerically. We will explain the process of computing the optimal triggering sets and their computational complexity below.

First of all, there are $(M+1-\overline{b})\overline{b}$ optimal triggering sets to be calculated. As mentioned above, let $b \in \{1, 2, \cdots, \overline{b}\}$ indicate the remaining transmissions. It is easy to find that only at step $\overline{b}-b, \overline{b}-b, \cdots, M+1-b$, there may be b remaining transmissions. Except the initial condition at step $M+1-b$, there are still $M+1-\overline{b}$ optimal triggering sets needs to be calculated for every $b \in \{1, 2, \cdots, \overline{b}\}$. So we can conclude that there are $(M+1-\overline{b})\overline{b}$ optimal triggering sets to be calculated.

Then, each of these optimal triggering sets can be computed using Corollary 2.2.2 and 2.2.3. According to to Corollary 2.2.2 and 2.2.3, to calculate each of these optimal triggering sets, we first define some directions in $\mathbb{R}^n$, and then find the threshold in each direction using bisection method. After that, the value function is evaluated at several points in each direction, since the value function is necessary to calculate the triggering sets at one step forward.

To define directions in $\mathbb{R}^n$, polar coordinate is used. A state $x \in \mathbb{R}^n$ will be expressed as $[\phi_1, \cdots, \phi_{n-1}, \gamma]$ in polar coordinate, where $\phi_i \in [0, \pi]$ is the ith angle and $\gamma \geq 0$ is the length of x. We assign each angle c_1 values, evenly distributed

from 0 to π. One direction is decided when one of the c_1 values is chosen for each angle. So there are c_1^{n-1} direction.

For each direction, the threshold in this direction is found by bisection method. Let's assume that we are searching for the threshold in direction d at step k with b remaining transmissions. $h_t(\zeta, b, k)$, the cost with transmission, is calculated first. Notice that $h_t(\zeta, b, k)$ is a constant. Here we indicate it as $h_t(b, k)$. Then we use bisection method to search for the threshold $\theta_k^b(d)$ satisfying $h_{nt}(\theta_k^b(d), b, k) = h_t(b, k)$. Assume there are c_2 candidate thresholds in every direction. In the worst case, h_{nt} needs to be evaluated $\log_2^{c_2}$ times. Each evaluation involves $c_3(mn + 2n)$ multiplications, where c_3 is the number of random variables in Monte-Carlo method which is used to calculate the expectation in $h_n t$. So in the worst case, $\log_2^{c_2} c_3(mn+2n)$ multiplications are needed to calculate the threshold in direction d at step k with b remaining transmissions.

After the threshold in a direction is computed, we still need to compute the value function along this direction, so the value function at current step can be used to calculate the optimal triggering sets at one step forward. When ζ is beyond the threshold, the value function , $h_t(b, k)$, is already known. When ζ is within the threshold, the value function is calculated at c_4 points along this direction. For each calculation, there are $c_3(mn + 2n)$ multiplications, where c_3 is as mentioned above. So the value function in direction d at step k with b remaining transmissions can be calculated with $c_4 c_3(mn + 2n)$ multiplications.

Therefore, we will need $(M+1-\overline{b})\overline{b}c_1^{n-1}(\log_2^{c_2} + c_4)c_3(mn+2n)$ multiplications in all to obtain the optimal triggering sets for all steps with all possible remaining transmissions, which is exponential with respect to the state dimension n.

2.3 Suboptimal Triggering Sets

Because the computational complexity of optimal triggering sets is an exponential function of the state dimension, we turn to the suboptimal triggering sets whose computational complexity is only cubic in the state dimension.

Theorem 2.3.1. *The value function (2.6) is upper bounded by*

$$\bar{h}(\zeta, b; r) = \min\{\bar{h}_{nt}(\zeta, b, r), \bar{h}_t(\zeta, b, r)\},$$

where

$$\bar{h}_{nt}(\zeta, b, r) = \min_{j=1,\cdots,l_r^b}\{\zeta^T \Lambda_{r,j}^b \zeta + c_{r,j}^b\}, \text{for } b \neq 0 \tag{2.11}$$

$$\bar{h}_t(\zeta, b, r) = \rho_r^b. \tag{2.12}$$

$\Lambda_{r,j}^b$,$c_{r,j}^b$ *and* ρ_r^b *can be calculate backward recursively as*

$$\Lambda_{r,j}^b = \begin{cases} A^T \Lambda_{r+1,j}^b A + I, & j < M+1-b-r; \\ I, & j = M+1-b-r, \end{cases}$$

$$c_{r,j}^b = \begin{cases} \delta_{r+1,j}^b + tr(\overline{P}(r)), & j < M+1-b-r; \\ \rho_{r+1}^b + tr(\overline{P}(r)), & j = M+1-b-r, \end{cases}$$

$$\rho_r^b = \begin{cases} tr(\overline{P}(r)) + \delta_{r+1,1}^{b-1}, & \text{if } b = 1; \\ tr(\overline{P}(r)) + \min\{\delta_{r+1,1}^{b-1}, \cdots, \delta_{r+1,l_r^b}^{b-1}, \rho_{r+1}^{b-1}\}, & \text{otherwise.} \end{cases}$$

where $\delta_{r+1,j}^b = tr(R(r)L(r+1)^T \Lambda_{r+1,j}^b L(r+1)) + c_{r+1,j}^b$ *and* $l_r^b = M+1-b-r$. *The initial conditions for* $\bar{h}_{nt}$ *and* $\bar{h}_t$ *are described by equations (2.8) and (2.9)*

respectively. The suboptimal triggering sets

$$S_r^{b+} = \{\zeta : \bar{h}_{nt}(\zeta, b, r) \leq \bar{h}_t(\zeta, b, r)\}$$

with $S_r^{0+} = \mathbb{R}^n$ *for all* $r = 0, \cdots, M$ *and* $S_{M+1-b}^{b+} = \emptyset$ *for all* $b = 1, \cdots, \overline{b}$.

The value function's upper bound and the suboptimal triggering set are derived mainly from the fact that

$$E(\min\{h_{nt}(\zeta, b, r), h_t(\zeta, b, r)\}) \leq \min\{E(h_{nt}(\zeta, b, r)), E(h_t(\zeta, b, r))\}.$$

The main difficulty in calculating the value function efficiently is the expectation part of h_{nt} and h_t in Theorem 2.2.1. With the fact mentioned above, we are able to derive an upper bound of the value function which is in closed form and much easier to calculate than the value function.

The suboptimal triggering set is the union of the ellipses $\zeta^T \Lambda_{r,j}^b \zeta + c_{r,j}^b \leq \rho_r^b$ for $j = 1, \cdots, M + 1 - b - r$. What we do in Theorem 2.3.1 can also be seen as using a set of ellipses to approximate the optimal triggering sets.

Given r and b, to calculate the suboptimal triggering set, we need $M + 1 - b - r$ quadratic forms in $\bar{h}_{nt}(\zeta, b; r)$, and $M - b - r$ of them need to do matrix multiplication. To calculate $\Lambda_{r,j}^b$ and $c_{r,j}^b$, $2n^3$ and $mn^2 + m^2n$ scalar multiplications are needed. So the computational complexity of computing calculating all $\bar{h}_{nt}$ in $\mathcal{S}_0^{\bar{b}+}$ is $\frac{1}{2}(M + 1 - \overline{b})(M - \overline{b})\overline{b}(2n^3 + mn^2 + m^2n)$. Since $\bar{h}_t$ is only a constant, the computational complexity of all $\bar{h}_t$ is $(M+1-\overline{b})\overline{b}(mn^2+m^2n)$. Compared with the exponential computational complexity of optimal triggering set, the computation of suboptimal triggering sets is much more efficient.

2.4 Simulation Results

In this section, the optimal triggering sets, suboptimal triggering sets, and periodic transmission are used in a two dimensional example. The mean square estimation errors of the three strategies are compared.

Consider the system

$$\begin{aligned} x(k) &= \begin{bmatrix} 0 & -1 \\ 1 & \sqrt{2} \end{bmatrix} x(k-1) + w(k) \\ y(k) &= \begin{bmatrix} 1 & 1 \end{bmatrix} x(k) + v(k). \end{aligned} \tag{2.13}$$

The mean and variance of initial condition are $\begin{bmatrix} 1 \\ 0 \end{bmatrix}$ and I(identity matrix) respectively. The variance of w and v are $\begin{bmatrix} 1 & 2 \\ 2 & 5 \end{bmatrix}$ and 1 respectively. The terminal step $M = 4$ and $\overline{b} = 1$. According to Theorem 2.2.1 and Theorem 2.3.1, we first calculate the value functions and their upper bounds, and then compare the optimal triggering set with the suboptimal one.

Figure 2.3 gives the cross-section plots of value functions and their upper bounds on the left side. The red and white line are the value function and its upper bound respectively. We can see that the difference between them is small, especially at the points where h_{nt} and h_t are equal. These points are very important, because they form the edge of the optimal triggering set. The right side is the optimal and suboptimal triggering sets. We can see that the union of the ellipses which is the suboptimal triggering set fits the optimal triggering set very well.

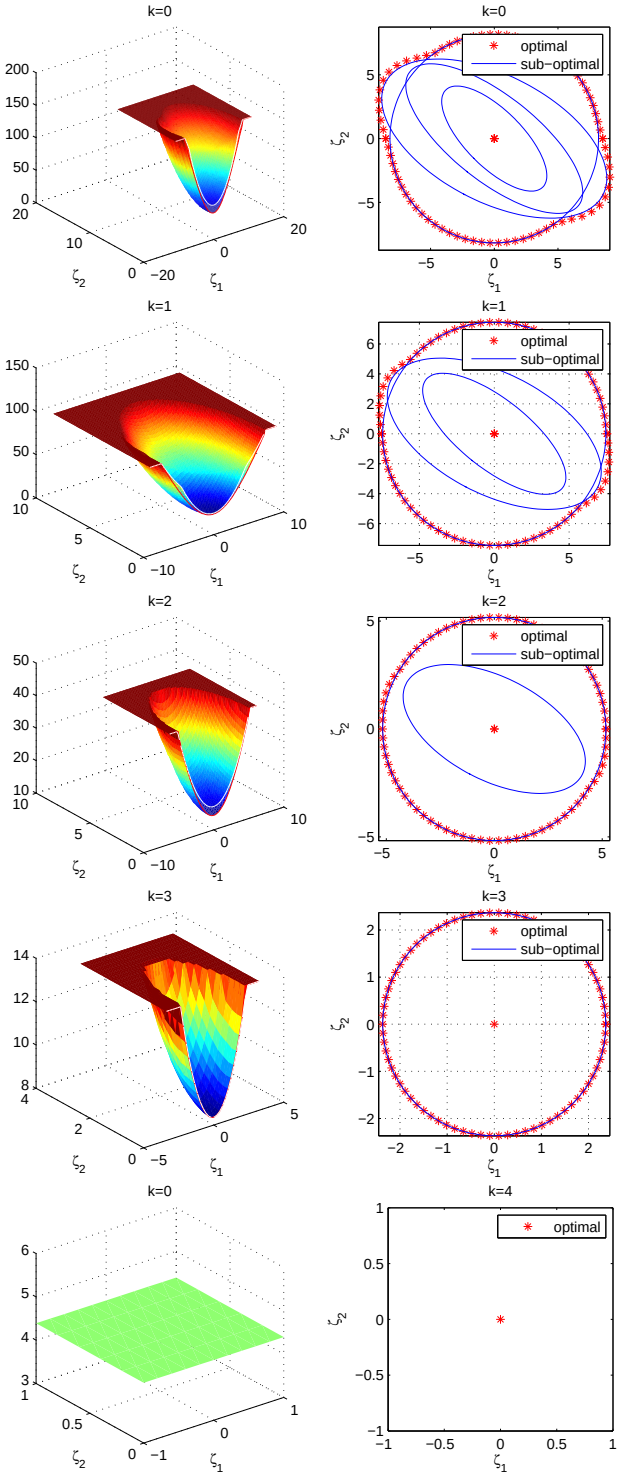

Figure 2.3. Value functions and their upper bound; optimal and suboptimal triggering sets

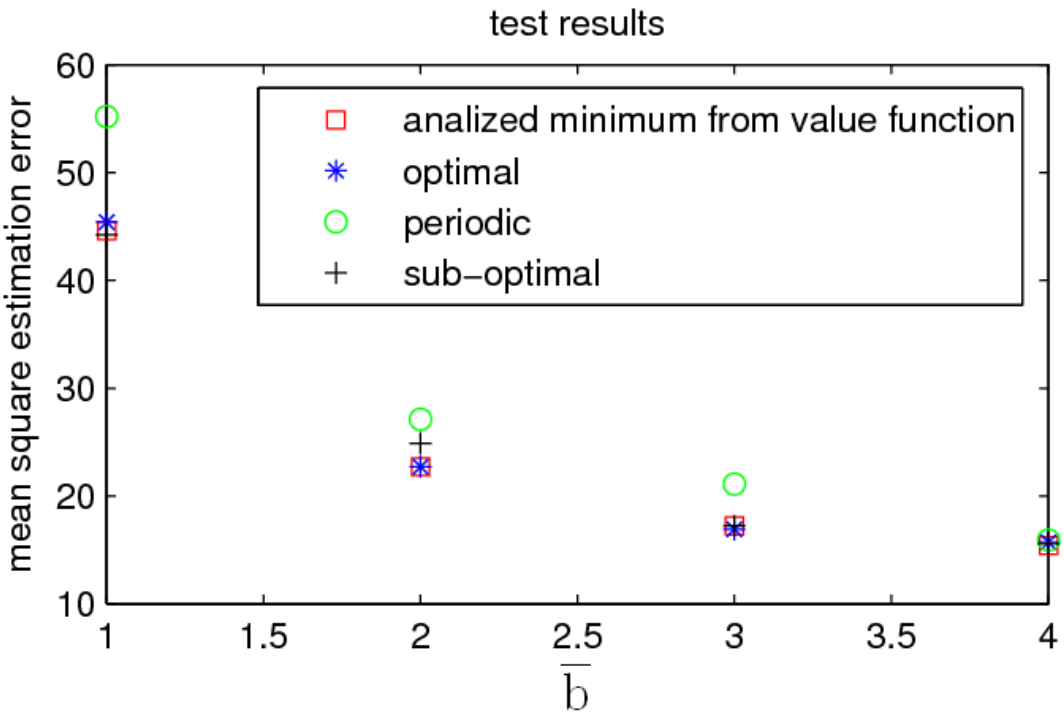

Figure 2.4. MSEEs of optimal, suboptimal and periodic triggered transmissions

Now, we vary the number of transmissions from 1 to 4, and calculate the optimal and suboptimal triggering sets. We'll use them and the periodic triggering to trigger transmission respectively and compare the mean square estimation errors of the three strategies. The results are shown in Figure 2.4. The x-axis is the allowed number of transmissions, and y-axis is the mean square estimation error. First, we notice that the mean square estimation error provided by the optimal triggering sets (blue star) matches the analyzed minimum mean square estimation error (red square). we can also see that the suboptimal triggering sets (black cross) give almost the same mean square estimation error as the optimal triggering sets (blue star), and the mean square estimation error of optimal and suboptimal triggering sets are both no greater than the mean square estimation error given by the periodic transmission (green circle).

2.5 Summary

This chapter first provides the minimum mean square estimation error and the optimal triggering events given limited transmissions over a finite horizon for a event triggered state estimator. This work recovers and extends the earlier results in [16–18, 33, 36–38] to vector cases. However, the computation of the optimal triggering sets is found to be very expensive, which is the main reason that prevents the earlier work from exploring the vector cases. This chapter then derives suboptimal triggering sets which is in closed form and much easier to compute. In the example, the suboptimal triggering sets approximate the optimal ones very well, and have similar behavior with the optimal triggering sets. Based on the same method of the event triggered state estimator with finite horizon discussed in this chapter, we will closed the control loop and discuss the event

triggered output feedback control problem in the next chapter.

CHAPTER 3

OPTIMAL AND SUBOPTIMAL TRIGGERING SETS OF OUTPUT FEEDBACK PROBLEM WITH FINITE HORIZON

In chapter 2, we talked about the optimal triggering sets for state estimation problem with finite horizon. Because the calculation of optimal triggering sets is exponential with respect to the state dimension, suboptimal triggering sets are derived which are more computationally effective. This chapter will first answer the question about what the best performance is given limited transmissions in event triggered output feedback systems. The computation of the optimal triggering sets, however, is still complex as we mentioned in the event triggered state estimation problem. Based on the same method in state estimation problem, a union of several sets in quadratic forms is used to approximate the optimal triggering sets. This suboptimal triggering set is shown, in our example, to approximate the optimal triggering sets very well.

3.1 Problem Statement

Consider a linear discrete time process over a finite horizon of length $M+1$, during which only $\bar{b} \in \{0, 1, \cdots, M+1\}$ transmissions are allowed. A block diagram of the closed loop system is shown in Figure 3.1. This closed loop system consists of a discrete time linear *plant* which generates a measurement sequence, a

sensor subsystem which processes the measurement sequence and decide when to transmit the processed data and an actuator subsystem which uses the information sent by the sensor subsystem to compute the control signal.

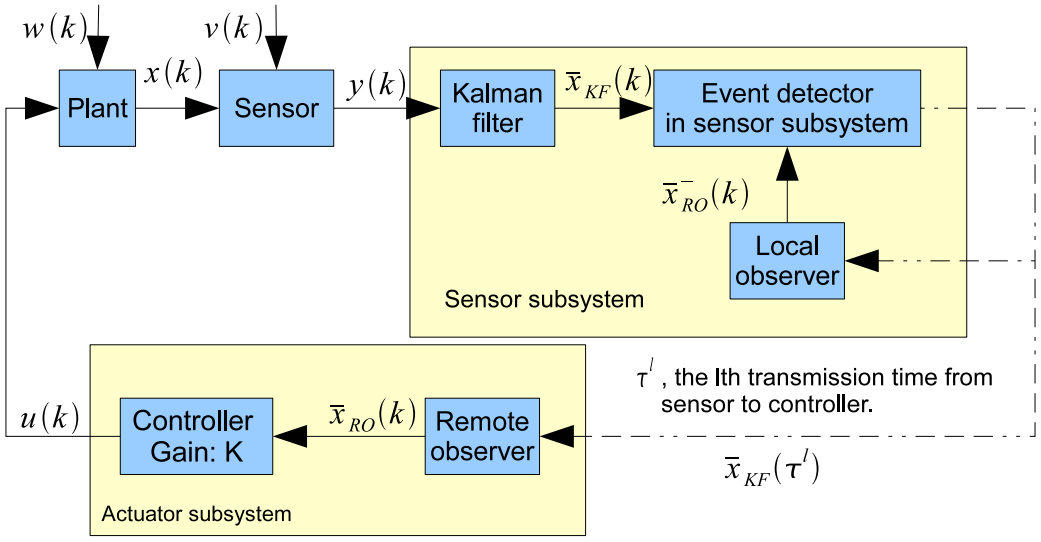

Figure 3.1. Event triggered output feedback Control System

The plant satisfies the difference equation below

$$\begin{aligned} x(k+1) &= Ax(k) + Bu(k) + w(k), \\ y(k) &= Cx(k) + v(k) \end{aligned}$$

for $k \in [0, 1, \ldots, M]$ where A is a $n \times n$ real matrix, B is a $n \times p$ real matrix, u is

the control input, and $w : [0, 1, \ldots, M] \to \mathbb{R}^n$ is a zero mean white noise process with covariance matrix W. The initial state, x_0, is a Gaussian random variable with mean μ_0 and variance Π_0. $y(k)$ is the sensor measurement at time k. C is a real $m \times n$ matrix and $v : [0, 1, \ldots, M] \to \mathbb{R}^m$ is another zero mean white noise process with variance V. w,v and x_0 are uncorrelated with each other. We assume that (A, B, C) is controllable and observable. The sensor outputs are fed into a sensor subsystem that decides when to transmit information to the actuator subsystem

The sensor subsystem consists of three components:, a *Kalman filter*, a *local observer*, and an *event detector*. Let $\mathbb{Y}(k) = \{y(0), y(1), \ldots, y(k)\}$ denote the sensor information available at time k. The *Kalman filter* generates a state estimate $\overline{x}_{KF}$ that minimizes the mean square estimation error $E\left[\|x(k) - \overline{x}_{KF}(k)\|_2^2 \,|\, \mathbb{Y}(k)\right]$ at each time step conditioned on all of the sensor information received up to and including time k. These estimates are computed using a Kalman filter. The filter equations for the system are,

$$\begin{aligned}
\overline{x}_{KF}(k) &= E\left[x(k) \,|\, \mathbb{Y}(k)\right] = \overline{x}^-_{KF}(k) + L(k)(y(k) - C\overline{x}^-_{KF}(k)) \\
\overline{x}^-_{KF}(k) &= A\overline{x}_{KF}(k-1) + Bu(k-1) \\
\overline{P}(k) &= E\left[\overline{e}_{KF}(k)\overline{e}^T_{KF}(k) \,|\, \mathbb{Y}(k)\right] \\
&= A\overline{P}(k-1)A^T + W - L(k)C(A\overline{P}(k-1)A^T + W)
\end{aligned}$$

for $k = 1, 2, \ldots, M$ where $L(k)$ is the Kalman filter gain and $\overline{e}_{KF}(k) = x(k) - \overline{x}_{KF}(k)$ is the estimation error at the Kalman filter. The initial condition $\overline{x}_{KF}(0)$ is the first posteriori update based on $y(0)$ and $\overline{P}(0)$ is the covariance of this initial estimate.

Because the sensor subsystem has access to the information received by actuator subsystem, the *local observer* can duplicate the state estimate, $\overline{x}_{RO}$, made by the remote observe in the actuator subsystem. The behavior of the local and remote observers will be explained later in the description of the actuator subsystem.

The *event detector* observes the filtered state, $\overline{x}_{KF}(k)$ and the gap between filtered state and the remote estimated state, $e^{-}_{KF,RO}(k) = \overline{x}_{KF}(k) - \overline{x}^{-}_{RO}(k)$. If the vector $\begin{bmatrix} \overline{x}_{KF}(k) \\ e^{-}_{KF,RO}(k) \end{bmatrix}$ lies outside the specified triggering set S^{b}_{k}, where b is the remaining transmission times, the filtered state $\overline{x}_{KF}(k)$ will be transmitted to the actuator subsystem. Given a set of transmission times $\{\tau^{\ell}\}^{\bar{b}}_{\ell=1}$, let $\overline{\mathbb{X}}(k) = \left\{\overline{x}_{KF}(\tau^{1}), \overline{x}_{KF}(\tau^{2}), \ldots, \overline{x}_{KF}(\tau^{\ell(k)})\right\}$ denote the filter estimates that were transmitted to the remote observer by time k where $\ell(k) = \max\{\ell \,:\, \tau^{\ell} \leq k\}$. This is the information set available to the remote observer at time k.

The actuator subsystem consists of two components; a *remote observer* and a *controller gain*. The remote observer uses the received information to compute a posteriori estimate $\overline{x}_{RO}$ of the process state that minimizes the MSEE, $E\left[\|x(k) - \overline{x}_{RO}(k)\|^{2}_{2} \,|\, \overline{\mathbb{X}}(k)\right]$, at time k conditioned on the information received up to and including time k. The a priori estimate of the remote observer, $\overline{x}^{-}_{RO} : [0, 1, \ldots, M] \to \mathbb{R}^{n}$, minimizes $E\left[\|x(k) - \overline{x}_{RO}(k)\|^{2}_{2} \,|\, \overline{\mathbb{X}}(k-1)\right]$, the MSEE at time k conditioned on the information received up to and including time $k-1$. These

estimates take the form

$$\overline{x}_{RO}^{-}(k) = E\left[x(k) \,|\, \overline{\mathbb{X}}(k-1)\right] = A\overline{x}_{RO}(k-1) + Bu(k-1) \tag{3.1}$$

$$\overline{x}_{RO}(k) = E\left[x(k) \,|\, \overline{\mathbb{X}}(k)\right] = \begin{cases} \overline{x}_{RO}^{-}(k) & \text{if no transmission at step } k \\ \overline{x}_{KF}(k) & \text{if transmission occurs at step } k \end{cases} \tag{3.2}$$

where $\overline{x}_{RO}^{-}(0) = \mu_0$. This estimate is then used to compute the control, $u(k) = K\overline{x}_{RO}(k)$, for $k = 0, 1, \ldots, M$ where K is some real $p \times n$ matrix.

For convenience, we let

$$\mathcal{S}_r^b(k) = \left\{S(k)^{\max\{0, b-k+r\}}, \ldots, S(k)^{\min\{b, M+1-k\}}\right\}$$

denote the triggering sets to be used at step k with b transmissions remaining. We let $\mathcal{S}_r^b = \{\mathcal{S}_r^b(r), \ldots, \mathcal{S}_r^b(M)\}$ be the collection of all triggering sets that will be used by the sensor subsystem after and including time step r.

We are now in a position to formally state the problem being addressed. Consider the cost function

$$J_M(\mathcal{S}_0^{\bar{b}}) = E\left[\sum_{k=0}^{M} z(k)^T Z z(k)\right]$$

where $Z = \begin{bmatrix} Z_{11} & Z_{12} \\ Z_{21} & Z_{22} \end{bmatrix}$ is a symmetric and positive semi-definite $2n$ by $2n$ matrix and $z(k) = \begin{bmatrix} x(k) \\ \overline{e}_{RO}(k) \end{bmatrix}$ is the system state at time k, where $\overline{e}_{RO}(k) = x(k) - \overline{x}_{RO}(k)$, is the remote state estimation error. The objective is to find the collection, $\mathcal{S}_0^{\bar{b}}$, of triggering-sets that minimizes the cost function. The optimal

cost then becomes

$$J_M^* = \min_{\mathcal{S}_0^{\bar{b}}} J_M(\mathcal{S}_0^{\bar{b}})$$

3.2 Optimal Triggering Sets

The problem is an optimal control problem whose controls are the triggering-sets in $\mathcal{S}_0^{\bar{b}}$, as we mentioned in state estimation problem. The difference is that the triggering set in the output feedback system is a subset of $\mathbb{R}^{2n}$ instead of a subset of $\mathbb{R}^n$ in state estimation problem. The solution may be characterized using dynamic programming techniques, and we define the problem's value function as

$$h(\theta, b; r) = \min_{\mathcal{S}_r^b} \left(\sum_{k=r}^{M} z(k)^T Z z(k) \,|\, I^-(r) = (\theta, b) \right).$$

For convenience, indicate $\begin{bmatrix} \overline{x}_{KF}(r) \\ e^-_{KF,RO}(r) \end{bmatrix}$ by $q^-(r)$ and $\begin{bmatrix} \overline{x}_{KF}(r) \\ e_{KF,RO}(r) \end{bmatrix}$ by $q(r)$. $I^-(r)$ is the a priori information set at time step r consisting of an ordered pair $(q^-(r), b)$ with b the remaining transmissions. The value function is defined as the minimum cost conditioned on $q^-(r) = \theta = \begin{bmatrix} \eta_{n\times 1} \\ \zeta_{n\times 1} \end{bmatrix}$ with b remaining transmissions.

Theorem 3.2.1. *The value function satisfies*

$$h(\theta, b; r) = \min \{h_{nt}(\theta, b, r), h_t(\theta, b, r)\} \tag{3.3}$$

where h_{nt} is the cost function without transmitting at step r and h_t is the cost

function if transmitting at step r. Both of them are defined as

$$\begin{aligned} h_{nt}(\theta, b, r) &= E\left[h(q^-(r+1), b; r+1) \,|\, I(r) = (\theta, b)\right] \\ &\quad +\theta^T Z\theta + \beta(r) \qquad (3.4) \\ h_t(\theta, b, r) &= E\left[h(q^-(r+1), b-1; r+1) \,|\, I(r) = (\theta_0, b-1)\right] \\ &\quad +\theta_0^T Z\theta_0 + \beta(r) \qquad (3.5) \end{aligned}$$

where $I(r)$ is the posteriori information set with ordered pair $(q(r), b)$. $\theta = \begin{bmatrix} \eta \\ \zeta \end{bmatrix}$ and $\theta_0 = \begin{bmatrix} \eta \\ 0 \end{bmatrix}$ are the actual values of a posteriori random variable, $q(r)$. The scalar $\beta(r)$ equals $\mathrm{tr}(\overline{P}(r)\,(Z_{11} + Z_{12} + Z_{21} + Z_{22}))$.

This theorem indicates that the value function chooses the smaller one between the two cost functions (3.4) and (3.5).

The preceding theorem shows that $h(\theta, b, r)$ can be computed through a recursion that ranges over the indices b (number of remaining transmissions) and r (current time). The initial conditions for this recursion occur when $b = 0$ or $b = M + 1 - r$ for all values of r. For the first case ($b = 0$), this corresponds to the cost of never transmitting after time step r. The other case ($b = M + 1 - r$) corresponds to transmitting at every single remaining time step. In both cases, the value function can be computed in closed form, and the expressions are given in the Appendix.

Given these initial conditions, the value function at index (b, r) may be computed from the value function at indices $(b, r + 1)$ and $(b - 1, r + 1)$. This computational dependence on the recursion is illustrated in Figure 3.2. This Figure

shows the indices including the the triggering set collection $\mathcal{S}_1^2$. The indices for the initial value functions are filled in. The order of computation used to compute $\mathcal{S}_1^2$ is shown by the arrows.

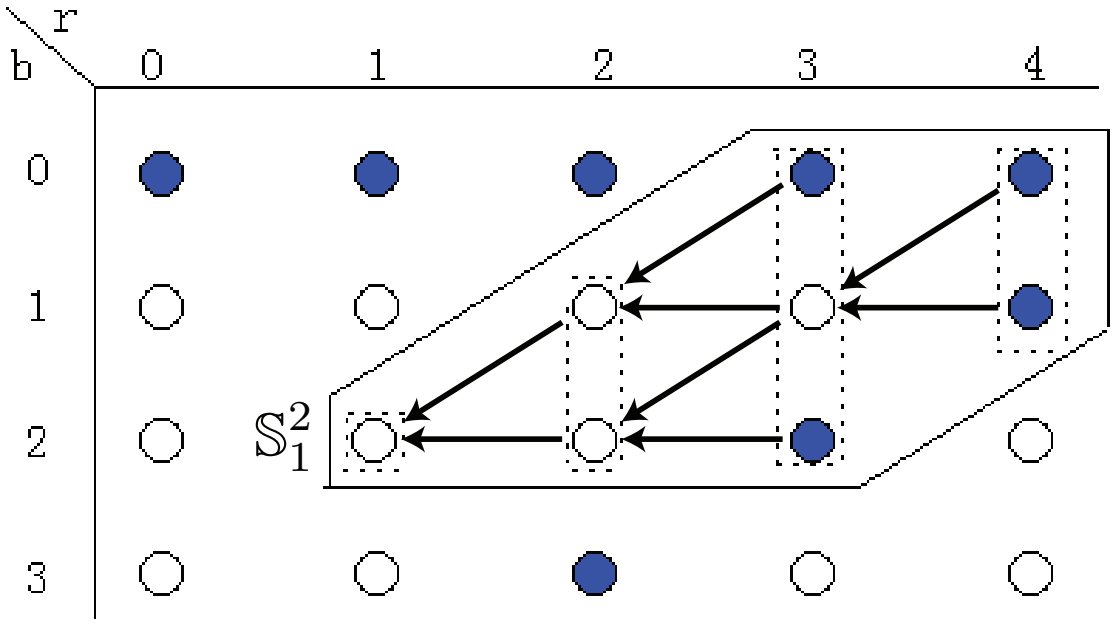

Figure 3.2. Index Sets for Value Function Recursion

Corollary 3.2.2. *The optimal triggering set used at time step r with b transmissions remaining will be*

$$S_r^{b*} = \left\{ \theta = \begin{bmatrix} \eta \\ \zeta \end{bmatrix} \in \mathbb{R}^{2n} \,|\, h_{nt}(\theta, b, r) \leq h_t(\theta, b, r) \right\} \tag{3.6}$$

The initial triggering sets are $S_r^{0*} = \mathbb{R}^{2n}$ *and* $S_r^{(M+1-r)*} = \emptyset$.

The recursion used in Equation (3.4) and (3.5) may only be tractable for first order linear systems. In this case, the triggering sets are subsets of $\mathbb{R}^{2n}$ and the bisection search from [24] may be employed to determine the triggering-sets S_r^{b*}. This is done for a specific example below. Extending this approach to multi-dimensional systems is impractical. The approach used in [24] involves computing the value function over a grid of points in the state space. Overall, there are $\overline{b}(M+1-\overline{b})$ triggering sets in the collection $\mathcal{S}_0^{\overline{b}*}$. If each value function is evaluated in a $2n$-dimensional space over a range of $[-c/2, c/2]$ with a granularity of ϵ, then there are a total of $\left(\frac{c}{\epsilon}\right)^{2n}$ points at which the value functions are computed. This means the computational effort required to compute $h(\theta, b; r)$ will be on the order of $O\left(\overline{b}(M+1-\overline{b})\left(\frac{c}{\epsilon}\right)^{2n}\right)$. This is exponential in the state space dimension and generally $\frac{c}{\epsilon}$ will be very large. As a result this approach is impractical for all but scalar linear systems.

3.3 Suboptimal Triggering Sets

Since the computational complexity of the recursion in Equation (3.4) and (3.5) will be prohibitively large, one must resort to approximation methods. One useful approximation in [11] was developed for the infinite horizon problem considered in [52]. This approximation used a single quadratic form to over bound the value function. While this method works well for infinite horizon problems, it seems to be ill-suited for finite horizon problems. In particular, recent work [24] for the finite horizon estimation problem [17] shows that the value functions are non-convex and are therefore poorly approximated by a single quadratic form. The work in [24] suggested that a family of quadratic forms provide a much better way

of approximating the value function for the estimation problem. This approach can also be adopted for the output feedback control problem considered in this paper.

The basic idea behind the approximations used in [24] is as follows. While the value function, h, is inherently non-convex due to the choice in Equation 3.3, the functions h_t and h_{nt} may be well approximated by quadratic forms. This conjecture is based on two observations. First the initial value functions $h(\theta, b, r)$ for $b = 0$ and $b = M + 1 - r$ are quadratic and second that the recursion in Equation (3.4) and (3.5) are nearly quadratic. It therefore seems possible that we can bound $h_{nt}(\theta, b, r)$ and $h_t(\theta, b, r)$ from above by a family of quadratic forms.

Propsition 3.3.1. *There exist* $\Lambda^b_{r,j} \in \mathbb{R}^{2n\times 2n}$, $\Psi^b_r \in \mathbb{R}^{n\times n}$, *and scalars* $c^b_{r,j}$, d^b_r *for* $r \in [0, 1, \ldots, M]$, $b \in [0, 1, \ldots, \overline{b}]$, *and* $j \in [1, 2, \ldots, \rho^b_r]$ *such that*

$$h_{nt}(\theta, b, r) \leq \overline{h}_{nt}(\theta, b, r) = \min_{j\in[1,\ldots,\rho^b_r]} \left\{\theta^T \Lambda^b_{r,j}\theta + c^b_{r,j}\right\} \tag{3.7}$$

$$h_t(\theta, b, r) \leq \overline{h}_t(\theta, b, r) = \eta^T \Psi^b_r \eta + d^b_r, \tag{3.8}$$

where ρ^b_r *is a finite integer associated with step* r *and remaining transmissions* b.

With the upper bounds of the true value functions, $\overline{h}_{nt}$ and $\overline{h}_t$, we can construct a suboptimal triggering set S^{b+}_r of the form

$$S^{b+}_r = \left\{\theta \in \mathbb{R}^{2n} \,:\, \overline{h}_{nt}(\theta, b, r) \leq \overline{h}_t(\theta, b, r)\right\} \tag{3.9}$$

which is an approximation of the optimal triggering sets, S^{b*}_r, in Equation (3.6).

We notice that (3.4) and (3.5) add a quadratic value to the expected minimum of h_t and h_{nt}. The approximation can be done by interchanging the expectation and minimization operators as $h_{nt} = \theta^T Z\theta + \beta + E\left[\min(h_t, h_{nt})\right] \leq$

$\theta^T Z\theta + \beta + \min\{E[h_t], E[h_{nt}]\}$, where the expected values can again be represented by a family of quadratic forms. Provided the variances of the noise processes are relatively small, this approximation can be made tight.

For convenience, we let $\overline{A} = \begin{bmatrix} A+BK & -BK \\ 0 & A \end{bmatrix}$, $\overline{L}(k) = \begin{bmatrix} L(k) \\ L(k) \end{bmatrix}$, $\beta(k) = \mathrm{tr}(\overline{P}(k)(Z_{11}+Z_{12}+Z_{21}+Z_{22}))$ and $R(k) = CA\overline{P}(k)A^TC^T + CWC^T + V$. It can be easily shown by using mathematical induction and the fact that $E[\min(h_t, h_{nt})] \leq \min\{E[h_t], E[h_{nt}]\}$ that

Lemma 3.3.2. *Equation (3.7) and (3.8) hold, if for all $b \geq 1$ and all $\bar{b} - b \leq r \leq M - b$,*

$$\Lambda^b_{r,j} = \begin{cases} Z + \overline{A}^T \Lambda^b_{r+1,j} \overline{A} & j = 1, \ldots, \rho^b_{r+1} \\ Z + \overline{A}^T \begin{bmatrix} \Psi^b_{r+1} & 0 \\ 0 & 0 \end{bmatrix} \overline{A} & j = \rho^b_r \end{cases} \tag{3.10}$$

$$c^b_{r,j} = \begin{cases} c^b_{r+1,j} + \beta(r) + \mathrm{tr}(\overline{\Lambda}^b_{r+1,j}) & j = 1, \ldots, \rho^b_{r+1} \\ d^b_{r+1} + \beta(r) + \mathrm{tr}(\overline{\Psi}^{b-1}_{r+1}) & j = \rho^b_r \end{cases} \tag{3.11}$$

$$\Psi^b_r = Z_{11} + (A+BK)^T \Psi^{b-1}_{r+1} (A+BK) \tag{3.12}$$

$$d^b_r = \min\{\hat{\Lambda}^{b-1}_{r+1}, \hat{\Psi}^{b-1}_{r+1}\} + \beta(r) \tag{3.13}$$

where

$$\begin{aligned}
\overline{\Lambda}^{b}_{r+1,j} &= R(r)\overline{L}^{T}(r+1)\Lambda^{b}_{r+1,j}\overline{L}(r+1) \\
\overline{\Psi}^{b-1}_{r+1} &= R(r)L^{T}(r+1)\Psi^{b}_{r+1}L(r+1) \\
\hat{\Lambda}^{b-1}_{r+1} &= \min_{j\in[1,\rho^{b-1}_{r+1}]}\left[\mathrm{tr}(\overline{\Lambda}^{b-1}_{r+1,j}) + c^{b-1}_{r+1,j}\right] \\
\hat{\Psi}^{b-1}_{r+1} &= \mathrm{tr}(\overline{\Psi}^{b-1}_{r+1}) + d^{b-1}_{r+1}.
\end{aligned}$$

In this case, ρ^{b}_{r} *equals* $M+1-b-r$ *for* $b \geq 1$*, and* 1 *for* $b = 0$*. The initial condition is the same as defined in Theorem 3.2.1.*

Because the recursion used above mimics the recursions used for the original value function, we expect these bounds to be relatively tight. Precisely how tight these bounds are is still being quantified.

Computing the suboptimal triggering sets involves a $2n$ by $2n$ matrix-matrix multiplication with a computational complexity $O((2n)^3)$. The computation of $\overline{h}_{nt}$ dominates the effort since it has the most quadratic forms to compute. One can therefore show that the effort associated with computing the suboptimal triggering set S^{b+}_{r} will be $O(\bar{b}(M+1-\bar{b})(M+2-\bar{b})(2n)^3)$. This has a complexity that is polynomial in n and quadratic in M (the length of the horizon window). The complexity is much lower than that used in computing the value functions, so these approximations may represent a practical way of implementing optimal event-triggered controllers provided the approximations are tight. Preliminary simulation results are given below to experimentally evaluate how good the approximation really is.

3.4 Simulation Results

As stated above, we'd like to experimentally evaluate how closely the approximations in Equation (3.7) and (3.8) approximate the value function computed using the Equation (3.4) and (3.5). We'll do this for a specific example. Because we can only compute the exact value function for scalar systems, this example focuses only on the scalar system.

The system under study is a scalar system where $A, B, C, D = 1$, $W = V = 1$, $\mu_0 = \Pi_0 = 1$, $K = -0.95$, $M = 4$ and $\overline{b} = 1$. We consider a control problem without a penalty on the control input, so that $Z = \begin{bmatrix} 1 & 0 \\ 0 & 0 \end{bmatrix}$. The value functions and their bounds were computed using the recursions described in the preceding section. The results from this comparison are shown below in Figure 3.3.

The left column of Figure 3.3 shows the value functions and their upper bounds. While it may be difficult to see, both the value function and the upper bound are shown in these graphs. If one looks closely along the plane where $\eta = 0$, one may see a white line that marks the upper bound. For $k = 0$ and $k = 1$, these plots show a small difference between h and its bound appears. For the other values of k it is nearly impossible to see any difference. The triggering-sets are easily identified as the boundary of the deep values in these plots. These boundaries mark where h_t and h_{nt} are equal to each other. The triggering sets are more clearly seen in the contour plots on the right column of Figure 3.3. The boundary of the optimal triggering-set is marked by the asterisks. The boundary of the suboptimal triggering sets are marked by the solid lines. These figures show that the suboptimal and optimal triggering-sets are nearly identical with only small variations appearing for $k = 0$ and $k = 1$.

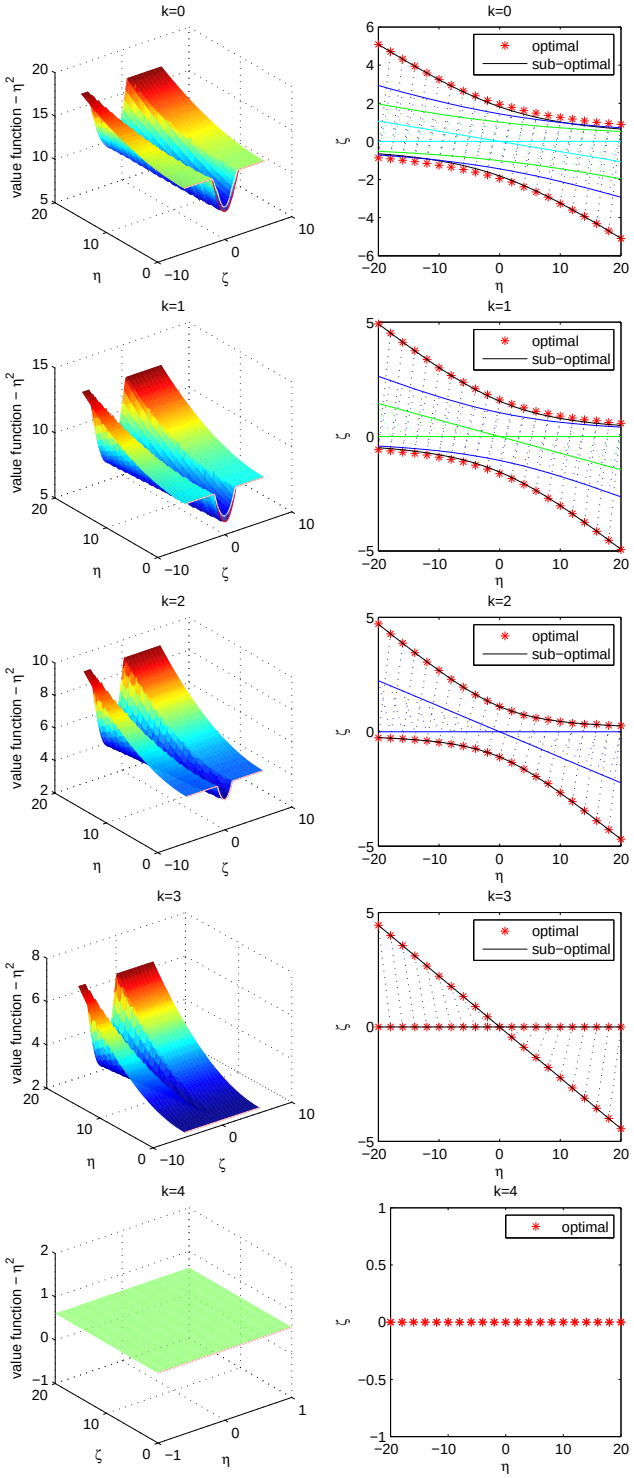

Figure 3.3. Value functions and optimal/suboptimal triggering sets.

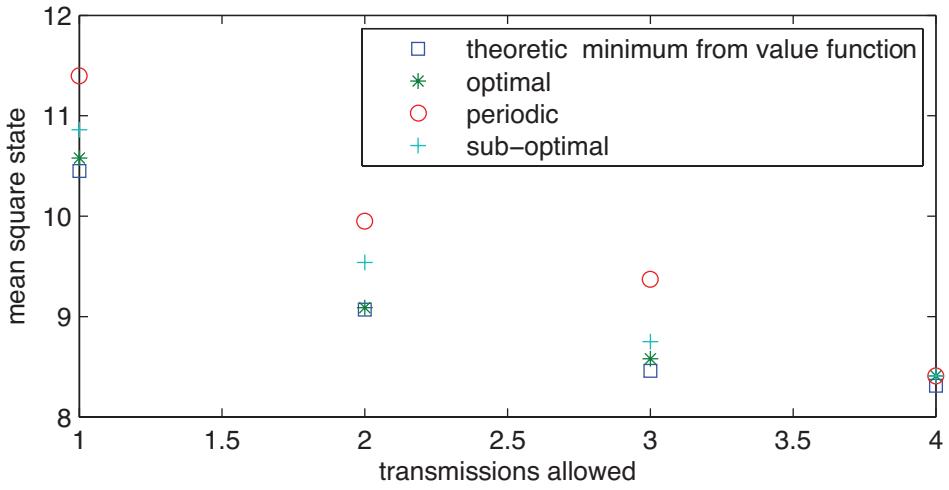

Figure 3.4. Mean square state of optimal, suboptimal and periodic transmissions

We can evaluate the performance of the system under periodic, optimal, and suboptimal event-triggering. In particular, let's vary the number of allowed transmissions, $\bar{b}$, between 1 and 4. For these values of $\bar{b}$, we compute the optimal and suboptimal triggering sets and then use these sets in a simulation of the system. The results of these simulations are shown in Figure 3.4. This figure plots the mean square state with respect to $\bar{b}$, when transmission is done using the optimal, suboptimal and periodic triggering. One can see that the suboptimal event triggers performance are only slightly worse than the optimal event triggering sets, and both of them have smaller mean square state errors than periodic triggering. Finally, we determine the actual mean square state that should have been achieved. This value matches what was achieved using the optimal event triggers.

In this example, the complexity associated with computing and using the optimal triggering sets is a thousand times greater than the complexity of the suboptimal triggering sets. In particular, the optimal triggering sets are characterized over

a range of $[-20, 20]$ with a quantization level of 0.2. This requires 4×10^4 points per value function. Since there are $M+1-\overline{b}$ value functions, computing the thresholds requires us to store 1.6×10^5 points. These points are then used in a bisection search to determine the thresholds. This search requires $\lceil 2\log_2(40/0.2)\rceil = 16$ steps to achieve an accuracy consistent with the quantization level of 0.2, so a total of 25×10^5 computations are needed to determine the triggering set thresholds. For this example there are a total of $\left(\frac{40}{0.2}\right)2\left(M+1-\overline{b}\right)\overline{b} = 1600$ thresholds to be used and checking whether a given θ lies in the triggering set or not requires $(40/0.2)2 = 400$ comparisons.

In contrast, we only need $\frac{1}{2}(M+1-\overline{b})(M+2-\overline{b}) = 10$ matrices to characterize the bounds on the value functions. Determining these matrices requires matrix-matrix multiplications on the order of $(2n)^3$ multiplies, so the total computational cost required to determine the upper bounds is $10(2n)^3 = 80$ multiplies. Evaluating the event triggering bounds, requires all 10 matrices with a computational cost of $(2n)^2(M+1-r-b)$ multiplies if the current event index is (r, b). The second term represents the number of quadratic forms used in evaluating $\overline{h}_{nt}$. The worst-case occurs when $r = b = 0$, so the worst-case computational cost is $(2n)^2(M+1) = 20$ multiplies.

From the preceding discussion it is clear that the total space-complexity of the optimal approach is on the order of 25×10^5 whereas the space-complexity of the suboptimal approach is $10(2n)^3 = 80$. The cost of evaluating an event-trigger for the optimal case is 400 whereas the suboptimal case only requires 20 multiplies. For this example, the proposed suboptimal method clearly has a much smaller computational cost than the optimal method. Moreover, the suboptimal thresholds work nearly as well as the optimal ones as indicated in Figure 3.4.

3.5 Summary

This chapter first presents the minimum mean state and the optimal triggering sets of the event triggered output feedback systems with limited transmissions over a finite horizon. Since both the minimum mean state and the optimal triggering sets are not in closed forms, they can only be calculated numerically. By a computation analysis, the computation of the optimal triggering sets is shown to have an exponential complexity with respect to the state dimension. With the concern about the exponential computation complexity of the optimal triggering set with respect to the state dimension, this chapter then provide suboptimal triggering sets which is more computationally tractable. These suboptimal triggering sets, based on the same idea obtaining the suboptimal triggering sets in event triggered state estimation, relies on using a family of quadratic forms to characterize the value functions in the problem's optimal dynamic program. Our example shows that this suboptimal sets is much more computational effective and have the similar performance as the optimal triggering sets.

Both work in Chapter 2 and 3 are for finite horizon cases. In the next chapter, we will talk about the event triggered state estimation problem with limited communication over infinite horizon.

CHAPTER 4

OPTIMAL AND SUBOPTIMAL TRIGGERING SETS OF STATE ESTIMATION PROBLEM WITH INFINITE HORIZON

In infinite horizon cases, the communication limitation is reflected by a constant called communication price. The cost of event triggered state estimator is defined as the average mean square estimation discounted by the communication price. The minimum cost and the optimal triggering sets were obtained in [52]. Realizing the computation of the optimal triggering sets is difficult, Cogill et.al provided a suboptimal solution in [11]. Their suboptimal solution could guarantee that for stable systems, the cost of suboptimal solution won't be greater than six times of the minimum cost. Although we know that the higher communication price reflects fewer communication resources, the trade of between communication and performance was never clearly stated in earlier papers.

This chapter examines another suboptimal solution to the constrained state estimation problem considered in [52]. The suboptimal solution is comparable to that used by Cogill [11] for the Xu/Hespanha problem, and extends the earlier work to unstable systems. In particular, this chapter derives a suboptimal solution that guarantees the specified least average sampling period. The chapter also derives upper and lower bounds on the event triggered estimator performance. Simulation results are used to demonstrate the utility of these bounds.

4.1 Problem Statement

The event triggering problem assumes that a sensor is observing an observable linear discrete time process. The process state $x : \mathbb{Z}^+ \to \mathbb{R}^n$ satisfies the difference equation

$$x(k) = Ax(k-1) + w(k)$$

for $k \in \mathbb{Z}^+$ where A is a real $n \times n$ matrix, $w : \mathbb{Z}^+ \to \mathbb{R}^n$ is a zero mean white Gaussian noise process with variance W. The initial state, x_0, is assumed to be a Gaussian random variable with mean μ_0 and variance Π_0. The sensor generates a measurement $y : \mathbb{Z}^+ \to \mathbb{R}^m$ that is a corrupted output. The sensor measurement at time k is

$$y(k) = Cx(k) + v(k)$$

for $k \in \mathbb{Z}^+$ and where $v : \mathbb{Z}^+ \to \mathbb{R}^m$ is another zero mean white Gaussian noise process with variance V that is uncorrelated with the process noise w. The process and sensor blocks are shown on the left hand side of Figure 4.1. In this figure, the output of the sensor feeds into a sensor subsystem that decides when to transmit information to a remote observer. The subsystem consists of three components: a *Kalman filter*, a *local observer* and an *event detector*.

Let $\mathcal{Y}(k) = \{y(0), y(1), \cdots, y(k)\}$ denote the measurement information available at step k. The *Kalman filter* generates a state estimate $\overline{x}_{KF} : \mathbb{Z}^+ \to \mathbb{R}^n$ that minimizes the weighted MSEE $E\left[\|x(k) - \overline{x}_{KF}(k)\|_Z^2 \,|\, \mathcal{Y}(k)\right]$ at each step conditioned on all of the sensor information received up to and including step k, where $Z \geq 0$ is the weight matrix and $\|\theta\|_Z^2 = \theta^T Z \theta$. Let $Z = P_Z^T P_Z$. For the process

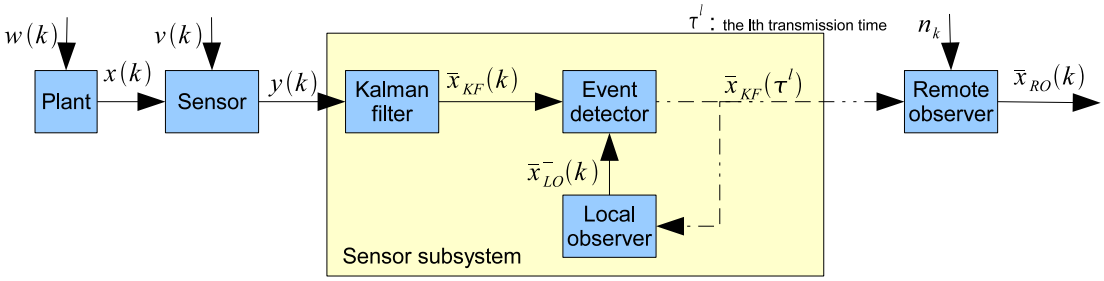

Figure 4.1. Structure of event triggered networked state estimator

under study the filter equation is

$$\overline{x}_{KF}(k) = A\overline{x}_{KF}(k-1) + P_Z^{-1}L\left(y(k) - CA\overline{x}_{KF}(k-1)\right),$$

where $L = \overline{A}X\overline{C}^T(\overline{C}X\overline{C}^T + V)^{-1}$, $\overline{A} = P_Z A P_Z^{-1}$, $\overline{C} = CP_Z^{-1}$, $\overline{W} = P_Z A P_Z^{-1}$ and X satisfies the discrete linear Riccati equation

$$\overline{A}X\overline{A}^T - X - \overline{A}X\overline{C}^T(\overline{C}X\overline{C}^T + V)^{-1}\overline{C}X\overline{A}^T + \overline{W} = 0.$$

The steady state estimation error $\overline{e}_{KF}(k) = x(k) - \overline{x}_{KF}(k)$ is a Gaussian random variable with zero mean and weighted variance $E(\overline{e}_{KF}Z\overline{e}_{KF}^T) = Q = (I - L\overline{C})X$.

Let $\{\tau^\ell\}_{\ell=1}^{\infty}$ denote a sequence of increasing times ($\tau^\ell \in [0, +\infty]$) when information is transmitted from the sensor to the local and the remote observers. We require that τ^ℓ is forward progressing, i.e. for any $k \geq 0$, there always exists a ℓ such that $\tau^\ell \geq k$. Let $\overline{\mathcal{X}}(k) = \left\{\overline{x}_{KF}(\tau^1), \overline{x}_{KF}(\tau^2), \ldots, \overline{x}_{KF}(\tau^{\ell(k)})\right\}$ denote the filter estimates that are transmitted to the local and the remote observers by step k where $\ell(k) = \max\left\{\ell : \tau^\ell \leq k\right\}$. We can think of this as the "information set" available to both the local observer and the remote observer at time k. The local

observer generates a posteriori estimate $\overline{x}_{LO} : \mathbb{Z}^+ \to \mathbb{R}^n$ of the process state that minimizes the weighted MSEE, $E\left[\|x(k) - \overline{x}_{LO}(k)\|_Z^2 \,|\, \overline{\mathcal{X}}_k\right]$, at time k conditioned on the information received up to and including time k. The a priori estimate of the local observer, $\overline{x}_{LO}^- : \mathbb{Z}^+ \to \mathbb{R}^n$, minimizes $E\left[\|x(k) - \overline{x}_{LO}^-(k)\|_Z^2 \,|\, \overline{\mathcal{X}}_{k-1}\right]$, the weighted MSEE at time k conditioned on the information received up to and including step $k-1$. These estimates take the form

$$\begin{aligned}
\overline{x}_{LO}^-(k) =& A\overline{x}_{LO}(k-1) \\
\overline{x}_{LO}(k) =& \begin{cases} \overline{x}_{LO}^-(k), & \text{if no transmission at step } k; \\ \overline{x}_{KF}(k), & \text{otherwise ,} \end{cases}
\end{aligned}$$

where $\overline{x}_{LO}^-(0) = \mu_0$.

Let $e_{KF,LO}^-(k) = \overline{x}_{KF}(k) - \overline{x}_{LO}^-(k)$ and $S(k) \subseteq \mathbb{R}^n$ be a *triggering set* at step k. The *event detector* detects the a priori gap $e_{KF,LO}^-(k)$ and compares the gap with the triggering set $S(k)$. If the gap is inside the triggering set $S(k)$, then no data is transmitted. Otherwise, the state estimate in Kalman filter $\overline{x}_{KF}(k)$ is sent to both the local and the remote observers.

The *remote observer* and the local observer have similar behavior. It produces an a priori state estimate $\overline{x}_{RO}^-(k)$ and an a posteriori state estimate $\overline{x}_{RO}(k)$ to minimize the weighted MSEE at step k based on the information received by step $k-1$ and by step k with weight matrix Z, respectively. Because there is communication error, the remote observer receives the corrupted state estimate of the Kalman filter when transmission occurs. The dynamics of the state estimate

$\overline{x}^{-}_{RO}(k)$ and $\overline{x}_{RO}(k)$ in the remote observer are

$$\overline{x}^{-}_{RO}(k) = A\overline{x}_{RO}(k-1) \tag{4.1}$$

$$\overline{x}_{RO}(k) = \begin{cases} \overline{x}^{-}_{RO}(k), & \text{if no transmission at step } k; \\ \overline{x}_{KF}(k) + n(k), & \text{otherwise ,} \end{cases} \tag{4.2}$$

where $\overline{x}^{-}_{RO}(0) = \mu_0$, $n(k)$ is a zero mean white Gaussian noise with variance N and independent with w and v.

The *communication* between the sensor and the remote observer is limited in the sense that the communication channel can only reliably transport a limited number of packets over the channel. This limitation on channel capacity means that the average interval between any consecutive packets is greater than or equal to a number $T_r \geq 1$. Formally, we express it as

$$\min\{t : E(e^{-}_{KF,LO}(t+\tau^{\ell})) \notin S(t+\tau^{\ell})\} \geq T_r, \forall \ell \in \mathbb{Z}^{+}. \tag{4.3}$$

Let $\mathcal{S}$ be the collection of all triggering sets. The average cost is

$$J(\{S(k)\}_{k=0}^{\infty}) = \lim_{M\to\infty} \frac{1}{M} \sum_{k=0}^{M-1} E\left(c(\overline{e}^{T}_{RO}(k), S(k))\right), \tag{4.4}$$

where $\overline{e}_{RO}(k) = x(k) - \overline{x}_{RO}(k)$ is the remote state estimation error, $\lambda \in \mathbb{R}^{+}$ is the communication price and the cost function $c : \mathbb{R}^n \times \mathcal{S} \to \mathbb{R}^{+}$ is defined as

$$c(\overline{e}^{T}_{RO}(k), S(k)) = \|\overline{e}_{RO}(k)\|^2_Z + \lambda 1_{e^{-}_{KF,LO}(k) \notin S(k)}, \tag{4.5}$$

with $1_{\{.\}}$ a characteristic function which is the weighted mean square estimation error discounted by the cost of transmitting data.

Our objective is to find the optimal triggering sets $\{S(k)\}_{k=0}^{\infty}$ to minimize the average cost $J\left(\{S(k)\}_{k=0}^{\infty}\right)$ subject to the communication requirement (4.3), and the optimal cost is denoted by J^*.

4.2 The Optimal Cost and Upper and Lower Bounds on It

For the convenience of the rest of this paper, we define

$$\begin{aligned}
e_{KF,LO}^{-}(k) =& \overline{x}_{KF}(k) - \overline{x}_{LO}^{-}(k), \\
e_{KF,LO}(k) =& \overline{x}_{KF}(k) - \overline{x}_{LO}(k), \\
e_{LO,RO}^{-}(k) =& \overline{x}_{LO}^{-}(k) - \overline{x}_{RO}^{-}(k), \\
e_{LO,RO}(k) =& \overline{x}_{LO}(k) - \overline{x}_{RO}(k).
\end{aligned}$$

The variances of these random variables are denoted by $U_{KF,LO}^{-}(k)$, $U_{KF,LO}(k)$, $U_{LO,RO}^{-}(k)$ and $U_{LO,RO}(k)$, respectively. Note that $\overline{e}_{RO}(k) = (\overline{e}_{KF} + e_{KF,LO} + e_{LO,RO})(k)$. Since $\overline{e}_{KF}(k)$, $e_{KF,LO}(k)$ and $e_{LO,RO}(k)$ are uncorrelated with each other, it can be shown that

$$\begin{aligned}
J_a(\{S(k)\}_{k=0}^{\infty}) =& J(\{S(k)\}_{k=0}^{\infty}) - tr(Q) \\
=& \lim_{M\to\infty} \frac{1}{M} \sum_{k=0}^{M-1} E(c_a(e_{KF,LO}^{-}(k), S(k))),
\end{aligned}$$

where

$$
\begin{aligned}
&c_a(e^-_{KF,LO}(k), S(k)) \\
=&tr(ZU_{LO,RO}(k)) + \lambda 1_{e^-_{KF,LO}(k)\notin S(k)} + \|e^T_{KF,LO}(k)\|^2_Z \\
=&\left[\|e^-_{KF,LO}(k)\|^2_Z + tr(ZU^-_{LO,RO}(k))\right] 1_{e^-_{KF,LO}(k)\in S(k)} + \left[\lambda + tr(ZN)\right] 1_{e^-_{KF,LO}(k)\notin S(k)}.
\end{aligned}
\tag{4.6}
$$

So finding $\{S(k)\}_{k=0}^{\infty}$ to minimize $J(\{S(k)\}_{k=0}^{\infty})$ in (4.4) subject to the communication requirement (4.3) is equivalent to finding $\{S(k)\}_{k=0}^{\infty}$ to minimize $J_a(\{S(k)\}_{k=0}^{\infty})$ with (4.3) satisfied, and the optimal cost of $J_a(\{S(k)\}_{k=0}^{\infty})$ is denoted by J_a^*. The problem stated above is an optimal average cost problem, and a method for solving it was given in [5].

This section states the optimal average cost and the corresponding optimal triggering sets in Lemma 4.2.1. Then, an upper bound on the cost of any triggering sets $\{S(k)\}_{k=0}^{\infty}$ is given in Lemma 4.2.2. Finally, Lemma 4.2.3 presents a lower bound on the optimal cost. The triggering sets discussed in this section can be any subsets of $\mathbb{R}^n$, and the next subsection will focus explicitly on quadratic ones.

Lemma 4.2.1. *If there exist two sequences of bounded functions* $\{J_k : \mathbb{R}^n \to \mathbb{R}\}$ *and* $\{h_k : \mathbb{R}^n \to \mathbb{R}\}$ *for* $k = 0, 1, \cdots$ *such that*

$$
J_{k+1}(e^-_{KF,LO}(k)) + h_k(e^-_{KF,LO}(k)) = G\left(h_{k+1}(e^-_{KF,LO}(k))\right)
$$

where

$$
G\left(h(\theta)\right) = \min_{S(k)} \left\{E(h(e^-_{KF,LO}(k+1))|e_{KF,LO}(k) = \theta) + c_a(\theta, S(k))\right\},
$$

then the optimal cost is

$$J_a^* = \lim_{N\to\infty} \frac{1}{N} \sum_{k=0}^{N-1} E(J_{k+1}(e^-_{KF,LO}(k))), \tag{4.7}$$

and the optimal triggering set

$$\begin{aligned} S^*(k) = \big\{\theta : E(h_{k+1}(e^-_{KF,LO}(k+1))|e_{KF,LO}(k) = \theta) + \|\theta\|_Z^2 + tr(ZU^-_{LO,RO}(k)) \\ \leq \lambda + tr(ZN) + E(h_{k+1}(e^-_{KF,LO}(k+1))|e_{KF,LO}(k) = 0)\big\}. \end{aligned} \tag{4.8}$$

Proof. Given any $S(k)$,

$$\begin{aligned} &J_{k+1}(e^-_{KF,LO}(k)) + h_k(e^-_{KF,LO}(k)) \\ \leq &E\left(h_{k+1}(e^-_{KF,LO}(k+1))|e^-_{KF,LO}(k)\right) + c_a(e^-_{KF,LO}(k)). \end{aligned}$$

Taking the expect action of both sides, we have

$$\begin{aligned} &E(J_{k+1}(e^-_{KF,LO}(k)) + E\left(h_k(e^-_{KF,LO}(k))\right) \\ \leq &E(c_a(e^-_{KF,LO}(k))) + E\left(h_{k+1}(e^-_{KF,LO}(k+1))\right). \end{aligned}$$

Then adding the inequalities from step 0 to $M-1$ and taking the limit of M as it goes to infinity, we have

$$\lim_{M\to\infty} \frac{1}{M} \sum_{k=0}^{M-1} E(J_{k+1}(e^-_{KF,LO}(k))) \leq J_a(S(k)).$$

We know that the equality holds if $S(k) = S^*(k)$, so equation (4.7) holds and the optimal triggering set is (4.8). □

With the optimal triggering set $S^*(k)$ described in (4.8), transmission occurs when the average cost with transmission is less than the average cost without transmission. Based on the current information $e^-_{KF,LO}(k)$ and the current decision to transmit or not, the average cost consists of two parts: the current cost and the estimated future cost. If no transmission occurs at step k, the current cost is $\|\theta\|^2_Z + tr(ZU^-_{LO,RO}(k))$, and the estimated future cost is

$$E(h_{k+1}(e^-_{KF,LO}((k+1))|e_{KF,LO}(k) = e^-_{KF,LO}(k)).$$

The left side of the inequality in (4.8) is the average cost if no transmission occurs at step k. With the same analysis as above, the right side of the inequality in (4.8) is the average cost if transmission occurs at step k. Therefore, if $e^-_{KF,LO}(k)$ lies in $S(k)$, the average cost without transmission must be less than the average cost with transmission, and no data is transmitted. Otherwise, $\overline{x}_{KF}(k)$ is transmitted to both the local and the remote observers.

If the optimal strategy exists, it must be time varying, because the cost function c_a is a time varying function. If there is no communication noise, i.e. $N = 0$, the optimal strategy is the same as the strategy in [52] with time invariant function h_k and time invariant constant J_k.

It is difficult to calculate the optimal triggering sets $\{S^*(k)\}_{k=0}^{\infty}$ described in (4.8). There is, therefore, great interest in identifying computable approximations $\{S(k)\}_{k=0}^{\infty}$ of the optimal triggering sets . To characterize the performance of $\{S(k)\}_{k=0}^{\infty}$, an upper bound on the cost of $\{S(k)\}_{k=0}^{\infty}$ and the difference between the cost and the optimal cost should be derived. Lemma 4.2.2 and 4.2.3 derive an upper bound on the cost of $\{S(k)\}_{k=0}^{\infty}$ and a lower bound on the optimal cost, respectively. These two bounds can be used to characterize the performance of

$\{S(k)\}_{k=0}^{\infty}$.

Lemma 4.2.2. *Given the triggering set $\{S(k)\}_{k=0}^{\infty}$, if there exists a sequence of bounded function $\{f_k : \mathbb{R}^n \to \mathbb{R}\}$ and a sequence of finite constants $\{\overline{J}_k\}$ such that*

$$E\left(f_{k+1}(e^-_{KF,LO}(k+1))|e^-_{KF,LO}(k)=\theta, S(k)\right) + c_a\left(\theta, S(k)\right) \leq \overline{J}_{k+1} + f_k(\theta), \quad (4.9)$$

for any $k \in \mathbb{Z}^+$, then

$$J_a(\{S(k)\}_{k=0}^{\infty}) \leq \lim_{M\to\infty} \frac{1}{M} \sum_{k=1}^{M} \overline{J}_k < \infty \quad (4.10)$$

Lemma 4.2.3. *If there exists a sequence of bounded function $\{g_k : \mathbb{R}^n \to \mathbb{R}\}$ and a sequence of nonnegative constants $\{\underline{J}_k\}$ such that*

$$\underline{J}_{k+1} + g_k(e^-_{KF,LO}(k)) \leq G\left(g_{k+1}(e^-_{KF,LO}(k))\right), \quad (4.11)$$

for any $k \in \mathbb{Z}^+$, then

$$J_a(\{S(k)\}_{k=0}^{\infty}) \geq J_a^* \geq \lim_{M\to\infty} \frac{1}{M} \sum_{k=1}^{M} \underline{J}_k \geq 0$$

Proof. We can follow the same steps in the proof of Lemma 4.2.1 to get the two lemmas above. □

Lemma 4.2.2 and 4.2.3 are very similar to Lemma 4 and 5 in [11]. One of the differences is that we allow time varying functions f_k, g_k and time varying constants $\overline{J}_k$ and $\underline{J}_k$. If there is no communication noise, then the cost function c_a becomes time invariant and all the time varying parameters f_k, $\overline{J}_k$, g_k and $\underline{J}_k$ should be time invariant, too. The other difference is that the functions f_k and g_k

need to be bounded from both below and above while [11] only required that f_k was bounded from below and g_k was bounded from above. It seems that we have a more strict assumption, but in fact the property of being bounded from both below and above is an intrinsic property of the cost function, $c_a \in [0, \lambda + tr(ZU^-_{LO,RO})]$. Since f_k and g_k are approximations of the cost function, they should be bounded, too.

Lemma 4.2.2 and 4.2.3 can be used for any triggering sets $\{S(k)\}_{k=0}^{\infty}$. The next subsection makes use of these two lemmas, and considers the case where these sets are defined by quadratic forms. We are interesting in quadratic sets, because they are easy to compute.

4.3 Quadratic Sets, Their Average Period and Performance

The quadratic sets are analyzed in this section. Theorem 4.3.1 first states how to design quadratic sets such that the communication requirement (4.3) is satisfied, and then gives the upper bounds on the cost of the quadratic sets and its difference from the optimal cost. Please see the appendix for the proof.

Theorem 4.3.1. *Given a quadratic triggering set*

$$S(k) = \{e^-_{KF,LO}(k) : \|e^-_{KF,LO}(k)\|^2_H \leq \lambda + tr(ZN) - \zeta(k)\}, \tag{4.12}$$

where the $n \times n$ matrix $H \geq 0$ satisfies the generalized Lyapunov inequality

$$\frac{A^T H A}{1+\delta^2} - H + \frac{Z}{1+\delta^2} \leq 0, \tag{4.13}$$

for some $\delta^2 \geq 0$, *and*

$$\zeta(k) = \frac{\delta^2(\lambda + tr(ZN)) + tr(ZU^-_{LO,RO}(k)) + tr(HR)}{1+\delta^2} \tag{4.14}$$

with

$$\begin{aligned}\lambda \geq \max_{t=1,\cdots,T_r-1} \Bigg[& (1+\delta^2)\sum_{i=1}^{t} tr(HA^{t-i}R(A^T)^{t-i}) \\ & -tr(ZN) + tr(ZA^tR(A^T)^t) + tr(HR)\Big],\end{aligned} \tag{4.15}$$

and $R = P_Z^{-1}L(CAQA^TC^T + CWC^T + V)L^T(P_Z^{-1})^T$, *the statements below are true.*

1. *the communication requirement (4.3) is satisfied;*

2. $J_a(\{S(k)\}_{k=0}^{\infty})$ *is bounded above by*

$$\begin{aligned} & \overline{J}_a(\{S(k)\}_{k=0}^{\infty}) \\ = & \lim_{M\to\infty} \frac{1}{M}\sum_{k=1}^{M} E(f_k(e^-_{KF,LO}(k))|e_{KF,LO}(k-1)=0) \\ \leq & \lim_{M\to\infty} \frac{1}{M}\sum_{k=1}^{M} \min\{tr(HR)+\zeta(k), \lambda + tr(ZN)\}\end{aligned} \tag{4.16}$$

   where $f_k(\theta) = \min\{\|\theta\|_H^2 + \zeta(k), \lambda + tr(ZN)\}$;

3. *The difference between the cost of* $\{S(k)\}_{k=0}^{\infty}$ *and the optimal cost is bounded above by*

$$\overline{J}_a(\{S(k)\}_{k=0}^{\infty}) - J_a^* \leq \min\{D_1, D_2\},$$

where

$$D_1 = \lim_{M\to\infty} \frac{1}{M} \sum_{k=1}^{M} \max\{\zeta(k) - tr(ZU^{-}_{LO,RO}(k)), 0\} + tr(YR),$$

$Y \geq 0$ *is the matrix which has the smallest trace such that* $Y \geq H - Z$*,*

$$D_2 = \lambda + tr(ZN) - \lim_{M\to\infty} \frac{1}{M} \sum_{k=1}^{M} \min\{tr(ZU^{-}_{LO,RO}(k)), \lambda + tr(ZN)\}.$$

Remark 4.3.2. *For any* A *and* $Z > 0$*, there always exists an* $H > 0$ *and a* $\delta^2 \geq 0$ *such that the generalized Lyapunov inequality (4.13) holds. We should notice that the greatest singular value of* A*,* $\overline{\sigma}(A)$*, is always greater than or equal to the absolute value of any eigenvalue of* A*. So if we set* δ^2 *to be the value such that* $\overline{\sigma}(A) \leq \sqrt{1+\delta^2}$*,* $A/\sqrt{1+\delta^2}$ *is always stable, and there always exists* $H \geq 0$ *such that (4.13) holds for any semi-positive definite matrix* Z*.*

According to the triggering set $S(k)$ in (4.12), if the approximated cost of no transmission at step k is less than the approximated cost of transmission, transmission will not occur at step k. Put $\zeta(k)$ defined in (4.14) into the triggering set $S(k)$ in (4.12), and the triggering event is

$$\|e^{-}_{KF,LO}(k)\|^2_H \leq \frac{(\lambda + tr(ZN)) - (tr(HR) + tr(ZU^{-}_{LO,RO}(k)))}{1+\delta^2},$$

where $tr(HR)+tr(ZU^{-}_{LO,RO}(k))$ is an approximation of the cost of no transmission at step k, and $\lambda + tr(ZN)$ is an approximation of the cost of transmission. If the cost of no transmission is less, the right side of the inequality above is negative, and the inequality never holds, which implies that transmission will not occur at step k.

The lower bound on communication price λ in (4.15) is calculated numerically. Basically, the value in the bracket of (4.15) is calculated from step 1 to step $T_r - 1$, and λ is chosen to be the greatest one. But as T_r grows, one may want to find a more efficient way to calculate λ. Corollary 4.3.3 gives explicit description of λ.

Propsition 4.3.3. *Let $P_H^T P_H = H$, $P_R P_R^T = R$, $P_Z^T P_Z = Z$ and $P_N P_N^T = N$. If*

$$\begin{aligned}
\lambda &= tr(HR) - tr(ZN) \\
&+ \begin{cases} (1+\delta^2) n\overline{\sigma}^2(P_H)\overline{\sigma}^2(P_R)\frac{1-\overline{\sigma}^{2(P_r-1)}(A)}{1-\overline{\sigma}^2(A)}, & \text{if } \overline{\sigma}(A) \neq 1; \\ (1+\delta^2) n\overline{\sigma}^2(P_H)\overline{\sigma}^2(P_R)(P_r-1)\overline{\sigma}^2(A) & \text{otherwise,} \end{cases} \\
&+ \begin{cases} n\overline{\sigma}(P_Z)\overline{\sigma}(P_N), & \text{if } \overline{\sigma}(A) \leq 1; \\ n\overline{\sigma}(P_Z)\overline{\sigma}(P_N)\overline{\sigma}^{2(T_r-1)}(A), & \text{otherwise,} \end{cases}
\end{aligned} \tag{4.17}$$

then the inequality (4.15) holds.

Proof. Equation (4.17) can be derived by finding the upper bound of the right side of inequality (4.15). From the fact that $tr(HA^iR(A^T)^i) = tr(P_H A^i P_R (A^T)^i P_H^T) \leq n\overline{\sigma}^2(P_H A^i P_R) \leq n\overline{\sigma}^2(P_H)\overline{\sigma}^2(P_R)\overline{\sigma}^{2i}(A)$, it can be shown that (4.17) is an upper bound on the right hand side of (4.15), and Proposition 4.3.3 is true. □

4.4 Simulation Results

An example is used to demonstrate that the proposed quadratic triggering sets can guarantee the communication requirement (4.3) and that the average cost triggered by the quadratic sets is bounded by the upper and lower bound derived in Theorem 4.3.1. We then compare the average cost of the quadratic sets in this paper against the average cost of the quadratic sets used in [11].

Let's consider the system with A to be $\begin{bmatrix} 0.95 & 1 \\ 0 & 1.01 \end{bmatrix}$, and C to be $\begin{bmatrix} 0.1 & 1 \end{bmatrix}$. The variances of the system noises are $W = \begin{bmatrix} 0.2 & 0 \\ 0 & 0.2 \end{bmatrix}$, $V = 0.3$, and $N = \begin{bmatrix} 0.02 & 0 \\ 0 & 0.02 \end{bmatrix}$. The weight matrix Z is chosen to be an identity matrix.

Given δ to be the greatest singular value of A, we calculate the quadratic triggering sets, and run the state estimation system with the quadratic triggering sets. In Figure 4.2, T_{sim} and J_{sim} are the average sampling period and the average cost of quadratic triggering set. J_{up} and D_{up} are upper bounds of the average cost and difference from the optimal cost, respectively. In the top plot of Figure 4.2, the x-axis is the required least average sampling period T_r, and the y-axis is the average sampling period in our experiment. We can find that the average sampling period T_{sim} (solid line) is always greater than or equal to the required least average sampling period T_r (dashed line). In the bottom plot of Figure 4.2, the x-axis denotes the required least average sampling period, and y-axis denotes the average cost. It shows that the average cost J_{sim} (solid line) is always bounded from below by $J_{up} - D_{up}$ (dotted line), and bounded from above by J_{up} (dot-dashed line). The simulation results confirm the statements in Theorem 4.3.1.

Comparing against the result in [11] is of interest since they also approximated the optimal triggering set with a quadratic form. Since their results can only be applied to stable systems without communication noise, we let A be $\begin{bmatrix} 0.95 & 1 \\ 0 & 0.95 \end{bmatrix}$, and N be 0. Because there is no result in [11] showing how λ is related with communication requirement T_r, the comparison is made given the same communication price, λ. To derive our quadratic triggering set, we let $\delta^2 = 1.5$. Figure 4.3

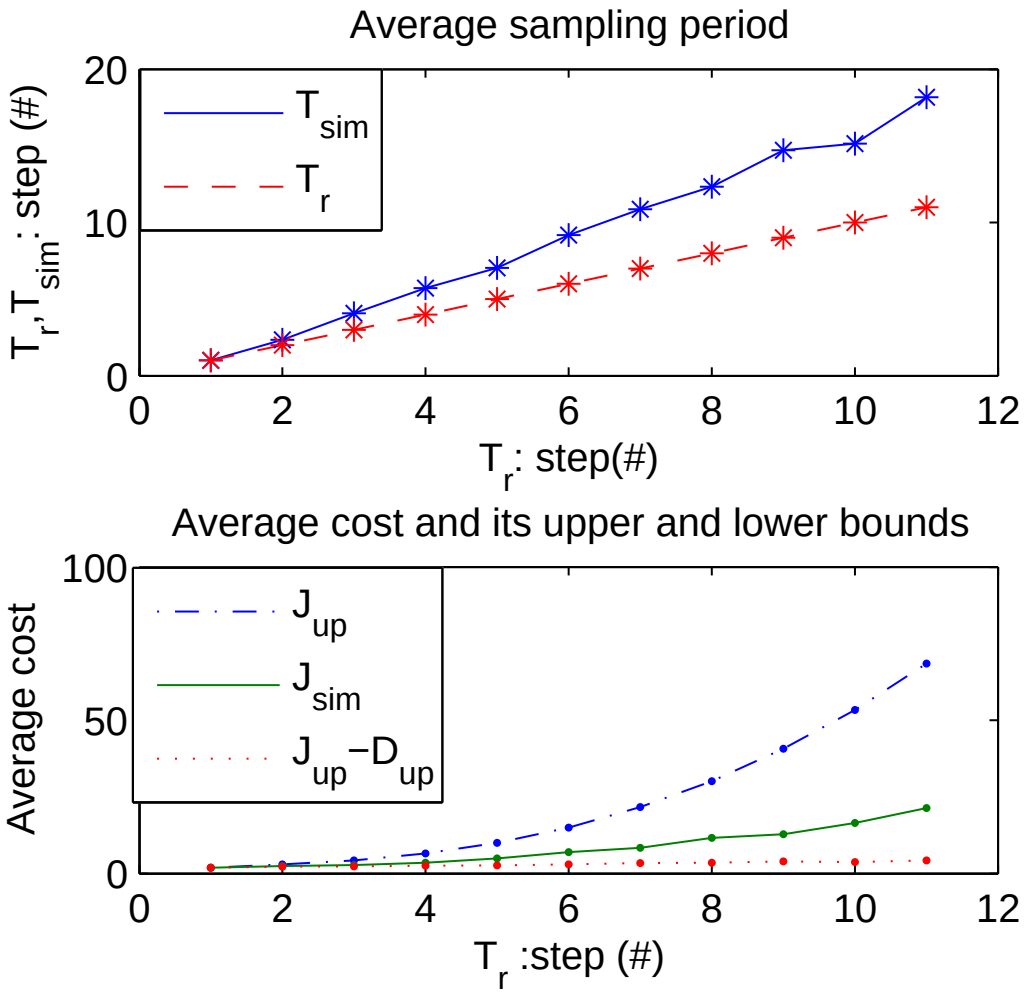

Figure 4.2. The average sampling period of the quadratic sets and the upper and lower bounds of the average cost.

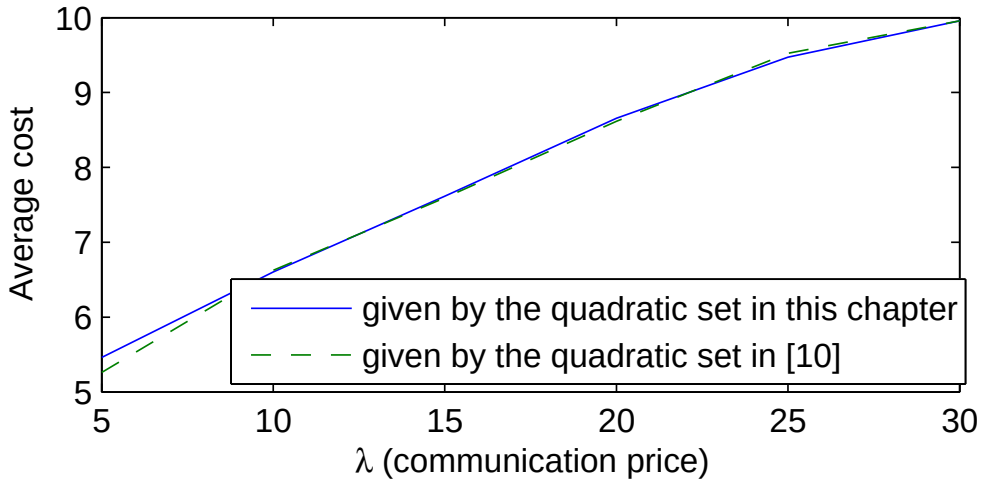

Figure 4.3. Comparison of the average costs of the triggering sets in this paper and [10]

shows the average costs of both quadratic triggering sets in this paper and [11]. The x-axis is the communication price λ, and the y-axis is the average cost. The average cost of the quadratic triggering set in this paper is indicated by the solid line, and the average cost of the quadratic triggering set in [11] is indicated by the dashed line. Figure 4.3 shows that these two costs are almost the same. Our quadratic triggering set, however, can be applied to unstable linear time invariant systems while the results in [11] can not.

4.5 Summary

The minimum average mean square estimation error discounted by communication price and the optimal triggering set has already been solved in [52]. Because the computation of the optimal triggering set is really complex, a suboptimal solution for stable systems was proposed in [11]. The tradeoff between communication

and the average mean square estimation error discounted by communication price, however, was never made explicit in the earlier papers.

This chapter explicitly states the relationship between the performance of the state estimation system and the least average sampling period when communication is triggered by quadratic events. Upper and lower bounds on the cost of the quadratic triggering sets are derived. The simulation results agree on the theoretic results, and indicates that the quadratic set in this paper is comparable with the quadratic set used in [11] for stable systems while our triggering sets can be applied to unstable systems.

Based on the same structure of the event triggered state estimator discussed in this chapter, one of our future work is to close the control loop with another networked communication link to build a decoupled event triggered output feedback system. The decoupled event triggered output feedback system is proposed in Section 6.1.

CHAPTER 5

APPLICATION OF EVENT TRIGGERED STATE ESTIMATOR WITH INFINITE HORIZON TO *QUANSER*© 3DOF HELICOPTER

In this chapter, the event triggered state estimator in Chapter 4 is applied to the highly nonlinear real time system, *Quanser*© 3 degree-of-freedom (3DOF) helicopter. The use of this highly non-linear mechanical plant contrasts with the linear (mainly non-mechanical) implementations of previous works. The controller/estimator is implemented on a standard PC using the real-time S.Ha.R.K. kernel. A detailed analysis of the performance as well as the improvements achieved by the event triggered state estimator is presented.

5.1 Experimental Setup

The real time system used consists primarily of a *Quanser*© 3DOF helicopter model as the main plant, an ISA MultiQ-3 board for data acquisition, two UMP-2405 modules as power amplifiers for the helicopter DC motors and a standard single processor PC running on a Free-DOS system. *Matlab*© and *Simulink*© are extensively used for system simulation during plant modeling and the design of the controllers.

The 3DOF helicopter model, shown in Figure 5.1, has three main components mounted on a table top; a main beam, a twin rotor assembly and a counterweight.

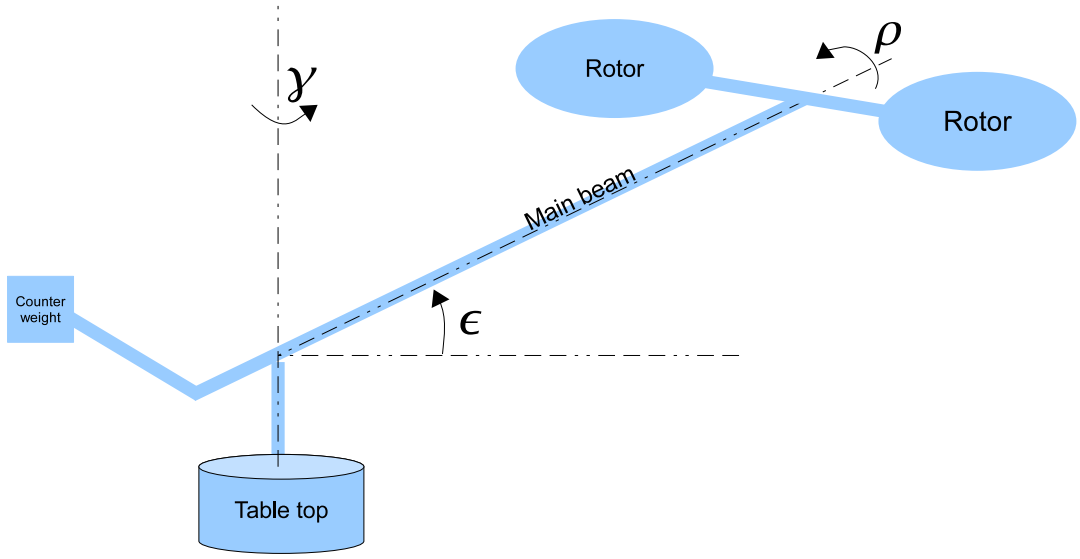

Figure 5.1. Schematic of the 3DOF helicopter

The system is actuated by two rotors driven each by an electric DC motor. Encoders for position measurements are mounted in each of the three axis of the system: elevation ($\epsilon(t)$), pitch ($\rho(t)$), and travel ($\gamma(t)$).

The elevation subsystem is shown in Figure 5.2. The dotted model indicates the initial position of 3DOF helicopter, and the solid line is the position after apply some control input to it. Let ϵ_m and ϵ_0 denote the measured and initial elevation, respectively. The dynamics of the elevation subsystem can be characterize as

$$\begin{aligned} J_\epsilon \ddot{\epsilon_m} = &- \sqrt{((ml_w - Ml_a)g)^2 + ((m+M)gd)^2}\sin(\epsilon_m) \\ &+ T_{col}\cos(\rho)(l_a + d\tan(\epsilon_m + \epsilon_0)) - c_\epsilon \dot{\epsilon}_m \end{aligned}$$

where m is the gross counter weight at the tail, M is the gross weight at the head, l_w is the length from connecting point to the tail while l_a is the length from connecting point to the head, d is the length from connecting point to the fixed

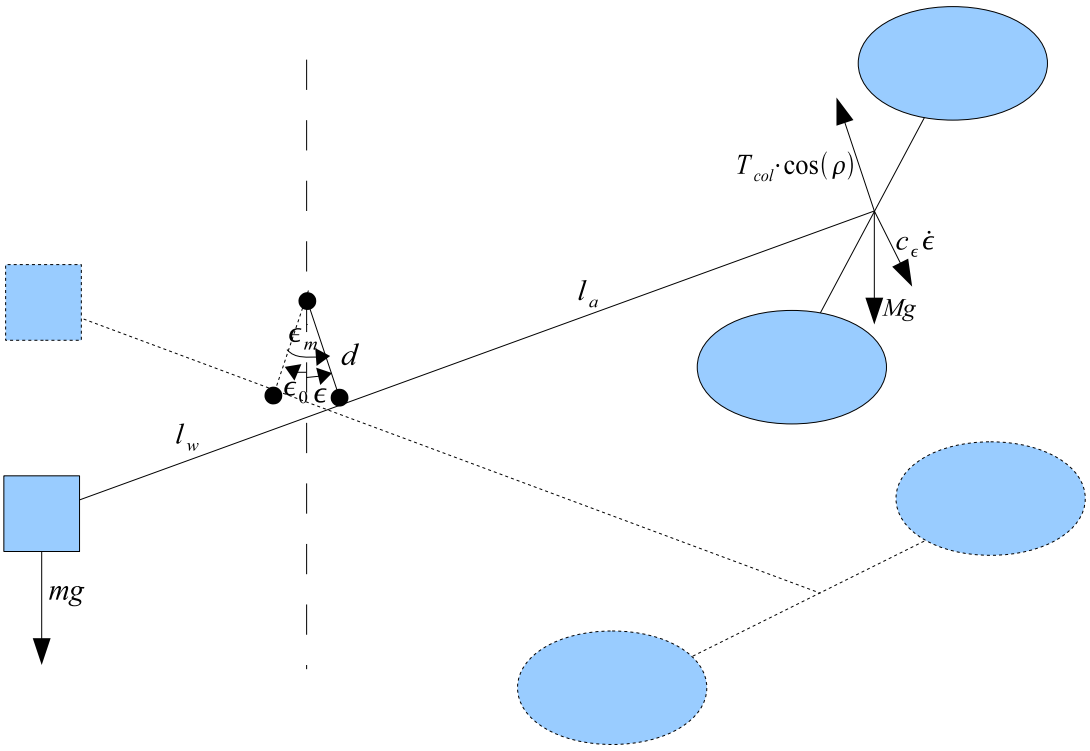

Figure 5.2. Elevation of the 3DOF helicopter

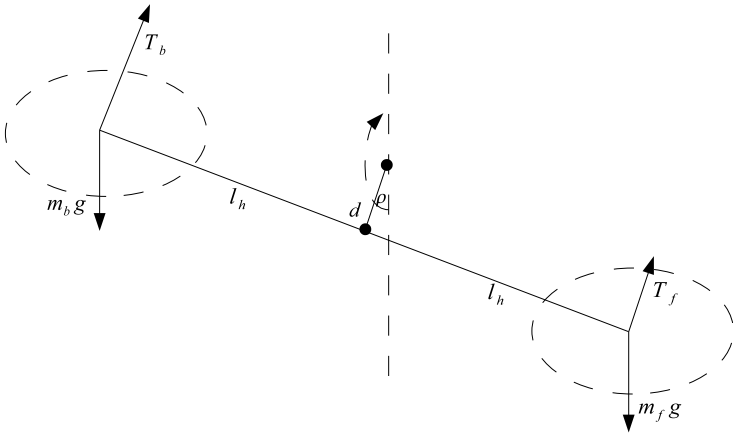

Figure 5.3. Pitch of the 3DOF helicopter

point, $T_{col} = T_f + T_b$ is the collective thrust generated by both front and back motors, J_ϵ is the inertia moment for elevation, and $c_\epsilon \dot{\epsilon}$ is the drag generated by air.

The pitch subsystem shown in Figure 5.3 has the behavior as

$$J_\rho \ddot{\rho} = T_{cyc} l_h - M_{bf} g d \sin(\rho) - c_\rho \dot{\rho} + c_{\gamma\rho} \dot{\gamma},$$

where $M_{bf} = m_b + m_f$ is the sum mass of the two motors, l_h is the length from the center to each motor while d is the length from connecting point to the fixed point, ρ is the angle of pitch while γ is the angle of travel, $T_{cyc} = T_b - T_f$ is the cyclic thrust generated by back and front motor, J_ρ is the inertia moment of pitch, and $c_\rho \dot{\rho}$ is the drag due to the change of pitch while $c_{\gamma\rho} \dot{\gamma}$ is the drag due to the change of travel.

The travel subsystem shown in Figure 5.4 has the dynamic behavior as

$$J_\gamma \ddot{\gamma} = -l_a T_{col} \sin\rho \cos\epsilon - c_\gamma \dot{\gamma},$$

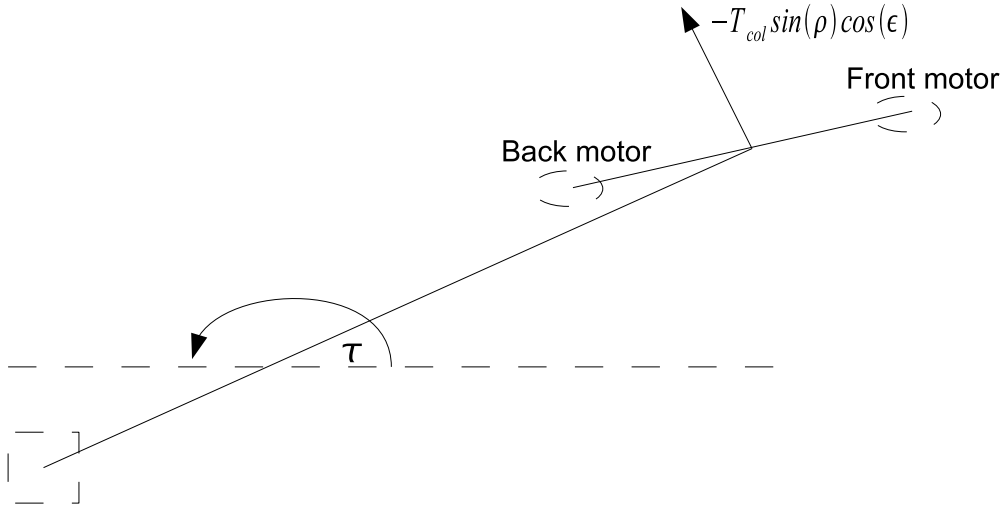

Figure 5.4. Travel of the 3DOF helicopter

where γ is the angle of travel, J_γ is the inertia moment of travel and $c_\gamma\dot{\gamma}$ is the drag due to the change of travel.

With the model of the 3DOF helicopter described above, we notice that this is a highly nonlinear model. To apply our event triggering methods in Chapter 4 to this system, we need to linearize it first. Neglecting the non-dominant terms and under the assumption that $\sin(\rho) \approx \rho$ and $\sin(\epsilon_m) \approx \epsilon_m$, the model of 3DOF helicopter can be simplified as

$$\begin{aligned} J_\epsilon\ddot{\epsilon}_m &= -\sqrt{((ml_w - Ml_a)g)^2 + ((m+M)gd)^2}\epsilon_m + c_\epsilon\dot{\epsilon_m}l_aT_{col}\cos(\rho) \\ J_\rho\ddot{\rho} &= -M_{bf}gd\rho - c_\rho\dot{\rho} + l_hT_{cyc} \\ J_\gamma\ddot{\gamma} &= -c_\gamma\dot{\gamma} - l_aT_{col}\sin(\rho)\cos(\epsilon) \end{aligned}$$

l_a	0.67 m	ϵ_0	-0.136 rad
l_h	0.177 m	c_ϵ	0.18 $kg.m^2/s$
l_w	0.48 m	c_ρ	0.003 $kg.m^2/s$
d	0.04 m	c_γ	0.25 $kg.m^2/s$
M	1.4611 kg	$c_{\gamma\rho}$	0.003 $kg.m^2/s$
m	2 kg	J_ϵ	3.5 $kg.m^2$
M_bf	0.29 kg	J_ρ	0.01 $kg.m^2$
g	9.8 m/s^2	J_γ	4 $kg.m^2$

TABLE 5.1

3DOF HELICOPTER PARAMETER VALUES

Let

$$u_\epsilon = T_{col}\cos(\rho) \tag{5.1}$$

$$u_\rho = T_{cyc} \tag{5.2}$$

$$u_\gamma = T_{col}\sin(\rho)\cos(\epsilon). \tag{5.3}$$

We have

$$\begin{aligned} J_\epsilon \ddot{\epsilon}_m &= -\sqrt{((ml_w - Ml_a)g)^2 + ((m+M)gd)^2}\epsilon_m + c_\epsilon \dot{\epsilon_m} + l_a u_\epsilon \\ J_\rho \ddot{\rho} &= -M_{bf} g d\rho + l_h u_\rho \\ J_\gamma \ddot{\gamma} &= -l_a u_\gamma - c_\gamma \dot{\gamma}, \end{aligned}$$

where all the system parameters can be found in Table 5.1.

Our objective of this experiment is to set the helicopter body to a commanded elevation ($\epsilon_c(t)$) and a commanded travel rate ($\dot{\gamma}_c(t)$), and compare the system performance of event triggered state estimator against the system performance of periodically triggered state estimator when both of them have the same average sampling period.

Now that the experiment is set up and the system is linearized, we will design the event triggered and periodically triggered state estimators according to the linearized model, and then compare their performances in our experiment.

5.2 Event and Periodically Triggered State Estimators

The event triggered state estimator in Chapter 4 is applied to the 3DOF helicopter assuming that there is no communication noise. Its framework is shown in Figure 5.5. The measurements of elevation, pitch and travel subsystems are sampled every 0.005 seconds, and then fed into the elevation, pitch and travel sensor subsystem, respectively. These sensor subsystems process the measurement and decide when to transmit the processed measurements to the corresponding remote observers. These remote observers generate remote state estimates for the three subsystems (elevation, pitch and travel) which, together with the commanding signals, are used by the controllers of elevation, pitch and travel to produce control inputs of these subsystems. A motor input generator, then, transforms these control inputs to the front and back motor thrusts which are fed back to the 3DOF helicopter.

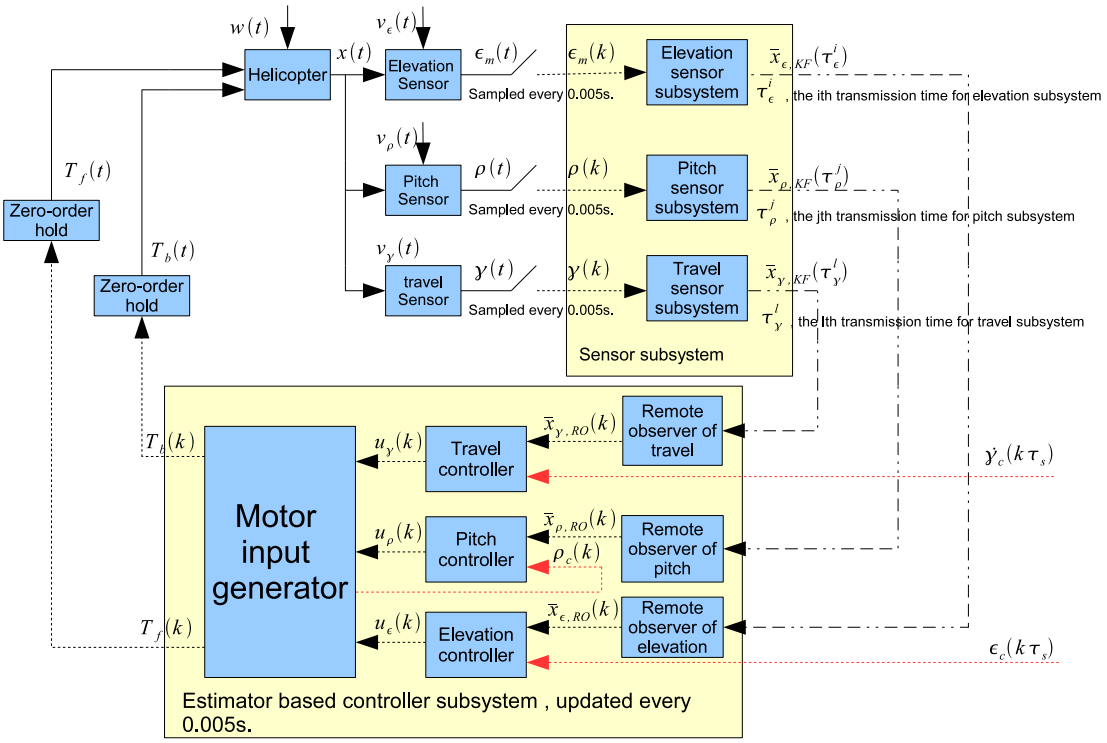

Figure 5.5. Framework of event triggered state estimator for 3DOF helicopter

Let's define the states of elevation, pitch and travel subsystem as

$$
\begin{aligned}
x_\epsilon(t) =&[\int_{s=0}^{t} \epsilon_m(s)ds \ \epsilon_m(t) \ \dot{\epsilon_m}(t)]^T, \\
x_\rho(t) =&[\int_{s=0}^{t} \rho(s)ds \ \rho(t) \ \dot{\rho}(t)]^T, \\
x_\gamma(t) =&[\gamma(t) \ \dot{\gamma}(t)]^T,
\end{aligned}
$$

respectively. For each subsystem, we will build a sensor subsystem to process measurements and decide when to transmit the processed measurements to the corresponding remote observer. Take the elevation subsystem as an example. The elevation sensor subsystem is designed the same as the sensor subsystem as described in Chapter 4. There is a Kalman filter to process the elevation measurements with the Kalman gain $\begin{bmatrix} 1 & 0.0016 \\ 0 & 0.3563 \\ 0 & 10.7707 \end{bmatrix}$. The filtered state of elevation is denoted by $\overline{x}_{\epsilon,KF} : \mathbb{R} \to \mathbb{R}^n$. It will be transmitted to the remote observer of elevation when $\|e^-_{\epsilon,KF,LO}\|^2_{H_\epsilon} > \lambda_\epsilon - \zeta_\epsilon$, where $e^-_{\epsilon,KF,LO}$ is defined as $e^-_{KF,LO}$ in Chapter 4 for the elevation subsystem, H_ϵ, λ_ϵ and ζ_ϵ can be calculated the same as H, λ and ζ in Chapter 4. The same strategy is applied to the pitch and travel sensor subsystems. The filtered state of pitch subsystems $\overline{x}_{\rho,KF}$ is calculated by a Kalman filter with the Kalman gain $\begin{bmatrix} 1 & 0.0015 \\ 0 & 0.3177 \\ 0 & 8.6804 \end{bmatrix}$ and transmitted to the remote observers of pitch when $\|e^-_{\rho,KF,LO}\|^2_{H_\rho} > \lambda_\rho - \zeta_\rho$, while The filtered state of travel subsystem $\overline{x}_{\gamma,KF}$ is calculated by a Kalman filter with the Kalman gain $\begin{bmatrix} 0.4083 \\ 13.8375 \end{bmatrix}$ and transmitted to the remote observers of travel when $\|e^-_{\gamma,KF,LO}\|^2_{H_\gamma} > \lambda_\gamma - \zeta_\gamma$.

Remote observers, controllers and motor input generator compose the estimator based controller subsystem. The remote observers generate remote state estimates of elevation $\overline{x}_{\epsilon,RO}$, pitch $\overline{x}_{\rho,RO}$ and travel subsystems $\overline{x}_{\gamma,RO}$, and are built the same as the remote observer in Chapter 4.

The subsystem controllers use the remote state estimate together with the commanded signal of elevation, pitch and travel rate, ϵ_c, ρ_c and $\dot{\gamma}_c$, to calculate the control inputs u_ϵ, u_ρ and u_γ which are expressed formally as

$$
\begin{aligned}
u_\epsilon(k) &= \begin{bmatrix} 7 & 44 & 68 \end{bmatrix} \left(\overline{x}_{\epsilon,RO}(k) - \begin{bmatrix} \int_{s=0}^{k\tau_s} \epsilon_c(s)ds \\ \epsilon_c(k\tau_s) \\ 0 \end{bmatrix} \right); \\
u_\rho(k) &= \begin{bmatrix} 3.54 & 30.65 & 11.54 \end{bmatrix} \left(\overline{x}_{\rho,RO}(k) - \begin{bmatrix} \sum_{j=0}^{k} \tau_s \rho_c(k) \\ \rho_c(k) \\ 0 \end{bmatrix} \right); \\
u_\gamma(k) &= \begin{bmatrix} 14.03 & 22.6 \end{bmatrix} \left(\overline{x}_{\epsilon,RO}(k) - \begin{bmatrix} \gamma_c(k\tau_s) \\ \dot{\gamma}_c(k\tau_s) \end{bmatrix} \right),
\end{aligned} \tag{5.4}
$$

where ϵ_c and $\dot{\gamma}_c$ are commanded elevation and travel rate given by user, and ρ_c, the commanded pitch, together with the front and back thrusts is calculated by the motor input generator.

The motor input generator calculates ρ_c, T_f and T_b according to Equation (5.1), (5.2), (5.3) and the equation $T_{col} = T_f + T_b$ and $T_{cyc} = T_b - T_f$. ρ_c, T_f and

T_b are explicitly expressed as

$$\begin{aligned}\rho_c(k) =& \frac{u_\tau(k)}{T_{col}(k-1)\cos(\overline{\epsilon}_{RO}(k)-\epsilon_0)} \\ T_f(k) =& \frac{\frac{u_\epsilon(k)}{\cos(\overline{\rho}_{RO}(k))}-u_\rho(k)}{2} \\ T_b(k) =& \frac{\frac{u_\epsilon(k)}{\cos(\overline{\rho}_{RO}(k))}+u_\rho(k)}{2}.\end{aligned} \tag{5.5}$$

where $\overline{\epsilon}_{RO}$ is the estimated elevation in remote observer of elevation, the second element of $\overline{x}_{\epsilon,RO}$ and $\overline{\rho}_{RO}$ is the estimated pitch in remote observer of pitch , the second element of $\overline{x}_{\rho,RO}$

The outputs of the estimator based controller subsystem, T_f and T_b, are then fed back to the helicopter to control the helicopter body to the commanded elevation ($\epsilon_c(k)$) and travel rate ($\dot{\gamma}_c(k)$).

The framework of periodic feedback controller is the same as the event triggered state estimator, except that the transmission rule is set to be periodic. To be explicit, $\overline{x}_{\epsilon,KF}$, $\overline{x}_{\rho,KF}$ and $\overline{x}_{\gamma,KF}$ are transmitted every T_ϵ, T_ρ and T_γ seconds, respectively.

5.3 Experimental Results

We run the system for 90 seconds using event triggered and periodic transmission methods, respectively. We'd like to compare the system performance of both transmission methods with the same average transmission period.

We first calculate the triggering event for the event triggered state estimators of the elevation, pitch and travel subsystems given the required least average transmission period to be $0.5s$ for the elevation subsystem, $0.2s$ for the pitch subsystem and $0.25s$ for the travel subsystem. Based on these required least

average transmission period, the triggering events for the elevation, pitch and travel subsystems are

$$\|e^-_{\epsilon,KF,LO}\|^2_{H_\epsilon} > 2.9189e-004, \text{where } H_\epsilon = \begin{bmatrix} 0.9942 & 0.0049 & 0.0000 \\ 0.0049 & 0.9943 & 0.0030 \\ 0.0000 & 0.0030 & 0.9938 \end{bmatrix},$$

$$\|e^-_{\rho,KF,LO}\|^2_{H_\rho} > 0.0197, \text{where } H_\rho = \begin{bmatrix} 0.9507 & 0.0045 & 0.0000 \\ 0.0045 & 0.9584 & -0.0464 \\ 0.0000 & -0.0464 & 0.9473 \end{bmatrix},$$

$$\|e^-_{\gamma,KF,LO}\|^2_{H_\gamma} > 4.9122e-004, \text{where } H_\gamma = \begin{bmatrix} 0.9953 & 0.0050 \\ 0.0050 & 0.9948 \end{bmatrix},$$

respectively. After we use this triggering event to decide the transmission time, the resulting average transmission period for the elevation, pitch and travel subsystems are 0.8824s, 0.2256s and 0.2970s, respectively. These average period is used as the transmission period for the periodically triggered state estimator. The system performances of both event triggered and periodically triggered state estimator are shown in Figure 5.6, and the transmission intervals of periodic and event triggered transmission are given in Figure 5.7.

There are three plots in Figure 5.6. In each plot, the x-axis indicates the time, red line indicates the commanded signal given by users, and the green and blue lines represent the performances of the periodically triggered and event triggered state estimator, respectively. The top plot gives the elevation performances of both transmission methods. Its y-axis denotes the elevation angle. We can see that both transmission methods give almost the same elevation performance. The second plot gives the performances of pitch given by periodic transmission and

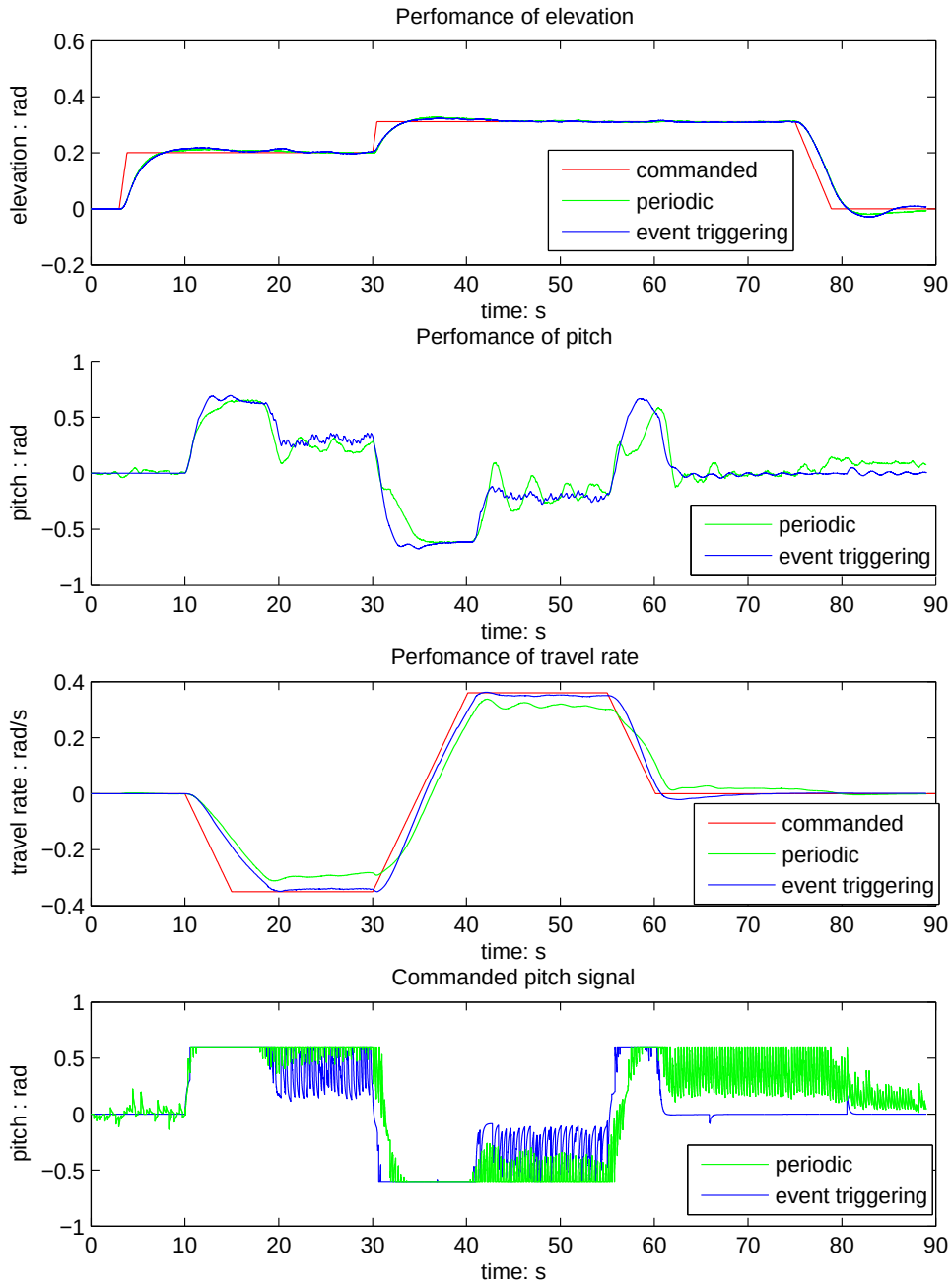

Figure 5.6. Performances of event and periodically triggered state estimators

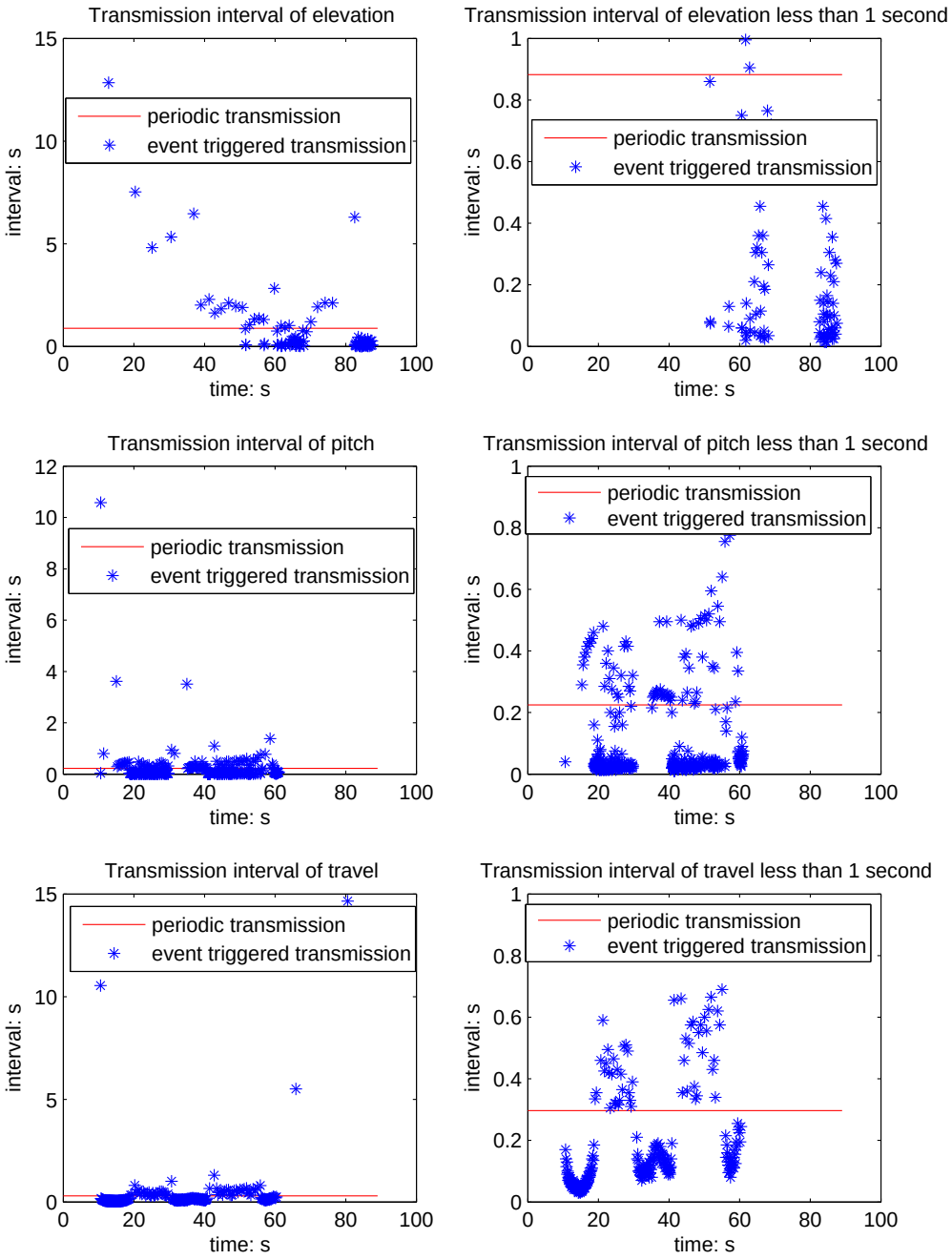

Figure 5.7. Intervals of event and periodically triggered state estimators

event triggered transmission. Its y-axis is the pitch angle. We can see that the pitch angle given by the periodic transmission keeps oscillating with the amplitude of about 0.15 rad when the travel rate is commanded to be a constant, while the oscillation of pitch angle given by event triggered transmission is so small that it can be neglected. The third plot is the performances of travel rate given by both transmission methods. It is easy to see that event triggered transmission provides less oscillation and less static error than the periodic transmission. Therefore, we can conclude that with the same average transmission period, event triggered state estimator offers better overall performance of the 3DOF helicopter than the periodic transmission.

The bottom plot of Figure 5.6 draws the commanded pitch signals of periodic and event triggered transmissions. Although the commanded pitch signal is not an aspect of the helicopter performance, it can provide us better understanding of the behavior of the transmission intervals of pitch which will be discussed later. The commanded pitch signal is calculated using the control input of the travel subsystem (see Equation (5.5)), and is limited in the rang $[-0.6, 0.6]$. The control input of travel depends on the remote state estimate of travel (see Equation (5.4)). The remote state estimate of travel equals to the filtered state when transmission in travel subsystem occurs, and the filtered state oscillates quickly because of the noises in the travel subsystem. Therefore, the commanded pitch signal oscillates quickly if it is in the range $[-0.6, 0.6]$ and the transmissions of travel subsystem occur very often. The analysis is demonstrated by the bottom plot in Figure 5.6 and the plots in bottom row of Figure 5.7. For the periodic transmission, since the transmission of travel subsystem occurs periodically, the commanded pitch oscillates most of the time except the time when the commanded pitch is out of

the range $[-0.6, 0.6]$, which is the transition period of the travel system. For event triggered transmission, we can see that when there is no transmission in the travel subsystem, the commanded pitch is smooth. When there is frequent transmission of travel subsystem, the oscillation appears except the time when the commanded pitch is out of the range $[-0.6, 0.6]$, which is the transition period of the travel subsystem.

Figure 5.7 shows the intervals of the periodic and event triggered transmissions. There are six plots in this figure. The left column gives the full views of the transmission intervals, while the right column enlarges the interval range $[0, 1]$ of the left column. The x-axes of all plots indicate the time, red lines indicate the intervals of periodic transmission, and the blue stars indicate the intervals of event triggered transmissions.

The plots in the first row are the transmission intervals of the elevation subsystem. The elevation subsystem has the fewest transmissions during the three subsystems, because the elevation subsystem is stable by itself and decoupled from the other systems with local information only. Since the coupled part in elevation subsystem only involves the pitch, as long as the remote estimate of pitch is accurate enough, the transmissions of elevation can be very few. The analysis above is reflected in the plots of transmission intervals of elevation which are in the first row. From $t = 0s$ to $t = 10s$, there is no transmission at all because both pitch and the pitch estimate in remote observer are 0 during the period of time. From $t = 10s$ to $t = 60s$, most of transmission intervals are greater than 1 second, because the remote estimate of pitch is very close to the pitch signal due to the frequent transmissions of the pitch subsystem during this period. From $t = 60s$ to the end, the transmissions of elevation become much more frequent than before,

because the pitch subsystem stop transmitting, and the remote estimate of pitch is not accurate enough any more.

The plots in the second row are the transmission intervals of the pitch subsystem. We notice that during all the transmissions of the pitch subsystem, the most frequent transmissions occur when the travel rate is commanded to be a constant, which are the time period from $t = 20s$ to $t = 30s$ and the time period from $t = 40s$ to $t = 55s$. That is because the commanded pitch angle has very frequent changes during these two time periods (See the bottom plot of Figure 5.6). If the commanded signal changes very frequently, the system is always in the transition process. Therefore, the pitch subsystem transmits very often during these periods.

The plots in the bottom row are the transmission intervals of the travel subsystem. It is easy to see that the most frequent transmissions occurs at the time periods from $t = 10s$ to $t = 20s$, from $t = 30s$ to $t = 40s$ and from $t = 55s$ to $t = 60s$. These time periods are the transition time periods of the travel subsystem. Once the travel subsystem are in the static processes, which are almost the time periods when travel rate is commended to be a constant, the transmissions are less often then the transmissions in the transition processes.

5.4 Summary

In this chapter, we apply the event triggered state estimator in chapter 4 to a highly nonlinear 3DOF helicopter. The system performance of the event triggered state estimator is compared against the system performance of a periodically triggered state estimator, when both of them have the same average transmission period. Our experimental results show that the event triggered state estimator offers better overall performance than the periodically triggered state estimator.

CHAPTER 6

FUTURE WORK

In this chapter, we discuss the work to be done in the future. There are three objectives. We first consider how to construct decoupled suboptimal triggering events to bound the mean square state discounted by the cost of transmission in event triggered output feedback systems. In these output feedback systems, the whole control loop, which is from sensor to controller and from controller to actuator, is closed over network. By 'decoupled', we mean the communication in each link is decoupled with the other and both the sensor and the controller can decide when to transmit data by their local information. The second objective is to analyze the impact of data packet dropout and network delays on the event triggered output feedback systems. The third is to design distributed suboptimal triggering events to bound the mean square estimation error discounted by the cost of transmission in large scale systems. In these distributed state estimation systems, each sensor can only observe part of the state, and must decide when to send its data to the controller only using local information.

6.1 Decoupled Optimal Triggering Events for Output Feedback Systems with Infinite Horizon

6.1.1 Introduction and Prior Work

This work will study the decoupled optimal triggering events to minimize the mean square state discounted by the cost of transmission in output feedback systems. In these output feedback systems, the whole control loop, which is from sensor to controller and from controller to actuator, is closed over the communication network. By 'decoupled', we mean the transmission of one link doesn't trigger the transmission of the other and both the sensor and the controller can decide when to transmit data using their local information. In most prior work considering event triggered output feedback systems [9, 24, 30, 53], the controller and the actuator are assumed to be connected directly. This assumption restricts the controller in a neighborhood of the actuator. Another work in [14] did consider when the whole control loop was networked, but the transmissions of both the outputs of the plant and the controller were synchronized. These restrictions are removed in our framework, which makes our work more general and easier to be extended to the large scale distributed systems.

6.1.2 Problem Statement

Consider a controllable and observable linear discrete time process, whose control loop is closed over the network. A block diagram of the closed loop system is shown in Figure 6.1. This closed loop system consists of a discrete time linear *plant*, a *sensor subsystem*, a *controller subsystem* and an *actuator*.

The plant, sensor subsystem and the remote observer in the controller subsystem are the same as described in Chapter 4 except that the communication

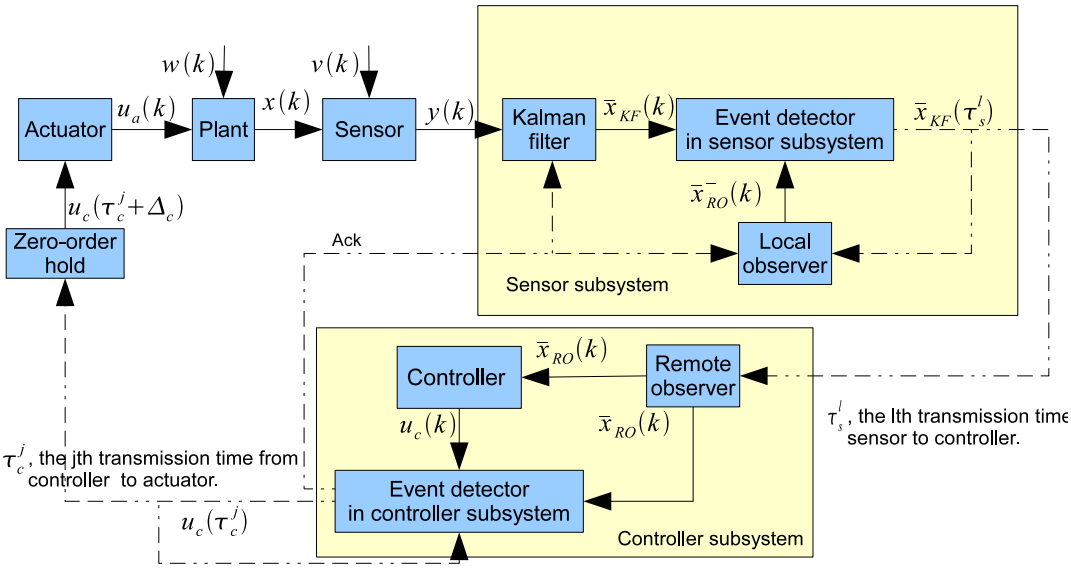

Figure 6.1. Event triggered output feedback control systems

error $n(k) = 0$ and there is a control input $u_a(k)$. Let S_s be the triggering set in sensor subsystem. To distinguish the triggering set in controller subsystem from the triggering set in sensor subsystem, we use S_c to denote the triggering set in controller subsystem.

The controller subsystem which is in the bottom part of Figure 6.1 have three components, the remote observer as defined in Chapter 4, a controller and an event detector in controller subsystem. The remote state estimate $\overline{x}_{RO}(k)$ is fed into the controller. Its output is $u_c(k) = K\overline{x}_{RO}(k)$, where K is the controller gain such that $A+BK$ is stable. Notice that this control input is not the actual control input fed into the plant.

Let's define an increasing and forward progressing time sequence $\{\tau_c^j\}_{j=1}^{\infty}$, where τ_c^j is the jth time when the control input is sent to the actuator from the controller. The *e*vent detector in the controller subsystem transmits the current

control input $u_c(k)$ to the actuator when $[\overline{x}_{RO}(k)\ u_c(k)\ u_c(\tau_c^{j(k-1)})]^T$ lies outside of a triggering set S_c, where $\tau_c^{j(k)}$ is the last transmission time and $j(k) = \max\{j : \tau_c^j \leq k\}$. Once the current control input is sent to the actuator, an acknowledgement is transmitted to the sensor subsystem to let it know that the control input has been updated. When the sensor subsystem receives the acknowledgement, it can use $\overline{x}_{RO}(k)$ generated in the local observer to get the new control input.

The actuator feeds the control input received from the controller subsystem to the plant. Let $u_a(k)$ denote the actual control input applied to the plant. When $u_c(\tau_c^j)$ is transmitted, the actuator updates $u_a(k)$ to be $u_c(\tau_c^j)$, and holds this value until the next transmission occurs. $u_a(k)$, therefore, takes the form

$$u_a(k) = u_c(\tau_c^j), \forall k \in [\tau_c^j, \tau_c^{j+1}).$$

The transmissions from sensor to controller and from controller to actuator are limited in the sense that the average sampling periods in the links from sensor to controller and from controller to actuator are greater than or equal to $T_s \geq 1$ and $T_c \geq 1$ steps, respectively. We express these communication requirements as

$$\min\{t : E(e^-_{KF,RO}(t + \tau_s^\ell)) \notin S_s\} \geq T_s, \forall \ell \in \mathbb{Z}^+, \tag{6.1}$$

$$\min\{t : E\left(\begin{bmatrix} \overline{x}_{RO}(t + \tau_c^j) \\ u_c(t + \tau_c^j) \\ u_c(\tau_c^j) \end{bmatrix}\right) \notin S_c\} \geq T_c, \forall j \in \mathbb{Z}^+, \tag{6.2}$$

where $e^-_{KF,RO}(k) = \overline{x}_{KF}(k) - \overline{x}^-_{RO}(k)$.

The average cost is defined as

$$J(S_s, S_c) = \lim_{N\to\infty} \frac{1}{N} \sum_{k=0}^{N-1} E\left(c(x(k), S_s, S_c)\right),$$

where the cost function c is

$$c(x(k), S_s, S_c) = \|x(k)\|_Z^2 + \lambda_s 1(e_{KF,LO}(k) \notin S_s) + \lambda_c 1\left(\begin{bmatrix} \overline{x}_{RO}(t+\tau^j) \\ u_c(k) \\ u_c(\tau_c^j) \end{bmatrix} \notin S_c\right),$$

and $\|x\|_Z^2 = x^T Z x$.

Our objective is to design the triggering sets S_s and S_c to minimize the average cost $J(S_s, S_c)$ subject to the communication requirements in (6.1) and (6.2).

6.1.3 Possible Solutions and Challenging Issues

Let $\overline{e}_{RO}(k) = x(k) - \overline{x}_{RO}(k)$. We notice that $\overline{e}_{RO}(k)$ and $\overline{x}_{RO}(k)$ are uncorrelated. The expect value of the cost function c is

$$E(c(x(k), S_s, S_c)) = J_s(\overline{e}_{RO}(k), S_s) + J_c(\overline{x}_{RO}(k), S_c), \tag{6.3}$$

where

$$J_s(\overline{e}_{RO}(k), S_s) = E(c_s(\overline{e}_{RO}(k), S_s)),, \tag{6.4}$$

where $c_s(\overline{e}_{RO}(k), S_s) = \|\overline{e}_{RO}(k)\|_Z^2) + \lambda_s 1(e_{KF,RO}(k) \notin S_s$ and

$$J_c(\overline{x}_{RO}(k), S_c) = E(\|\overline{x}_{RO}(k)\|_Z^2) + \lambda_c 1 \left(\begin{bmatrix} \overline{x}_{RO}(t+\tau^j) \\ u_c(k) \\ u_c(\tau_c^j) \end{bmatrix} \notin S_c \right). \tag{6.5}$$

From Equation (6.3), if $\overline{e}_{RO}(k)$ doesn't rely on S_c and $\overline{x}_{RO}(k)$, and $\overline{x}_{RO}(k)$ doesn't rely on S_s and $\overline{e}_{RO}(k)$, then we can say that $J_s(\overline{e}_{RO}(k), S_s)$ and $J_c(\overline{x}_{RO}(k), S_c)$ are completely separated. However, the separation doesn't exist, because $\overline{x}_{RO}(k)$ is closely related to S_s, which is shown in Equation (4.2).

The triggering event of sensor subsystem, decoupled with the triggering event of controller subsystem, can be designed the same as the triggering event in Chapter 4. From some analysis, we know that $\overline{e}_{RO}(k)$ doesn't rely on S_c and $\overline{x}_{RO}(k)$. We can also see that $c_s(\overline{e}_{RO}(k), S_s)$ shares the same form as the cost function in Chapter 4. So the same method can be used to obtain the decoupled suboptimal triggering event of sensor subsystem.

The decoupled triggering event of controller subsystem is more difficult to obtain. Since $\overline{x}_{RO}(k)$ is closely related to S_s, the next step is to see how $\overline{x}_{RO}(k)$ relies on S_s, and to find a way to remove the impact of S_s to $\overline{x}_{RO}(k)$. To find the optimal or suboptimal triggering set, we always need to calculate the expect value of a value function h or an approximated value function f at the next step based on the current information (see Lemma 4.2.1 and 4.2.2). Suppose the current step is k. The remote state estimate at the next step $k+1$, $\overline{x}_{RO}(k+1)$ depends on not only $\overline{x}_{RO}(k)$ but also $e_{KF,RO}(k)$ and S_s. So the main difficulty lies on how to bound the expect value of the value function h or the approximated value function f at the next step $k+1$ only using $\overline{x}_{RO}(k)$. If it can be done, then a decoupled

triggering event of controller can be derived.

6.2 Decoupled Event Triggered Output Feedback Systems with Delays and Dropouts

6.2.1 Introduction and Prior Work

It's well known that communication over networks is not always reliable. Although we've properly designed the triggering event such that the bandwidth of the network is not exceeded, it's still possible to have time delays and packet dropouts in the network. So we would like to know how delays and dropouts influence the design of the triggering event and the performance of the output feedback systems. There is several prior work concerning about this issue. [46–48] discuss the impact of delays and dropouts on state feedback control systems. In these works, the network used User Datagram Protocol (UDP). With UDP packets, the sensor subsystem is not notified whether transmissions succeed. To guarantee the asymptotic stability of the state feedback systems, bounds on the delays and consecutive dropouts are obtained. [31] use the transmission Control Protocol (TCP) to analyze the state feedback systems with delays and dropouts. With TCP packets, an acknowledgements are sent back if transmissions succeed. [31] considered the design of suboptimal event based controllers in the presence of packet loss and delayed acknowledgement for linear stochastic systems. The design objective consisted of a quadratic cost reflecting the control performance discounted by communication price. Based on various restrictions on the control design, optimal solutions within the corresponding class of event based controller were derived.

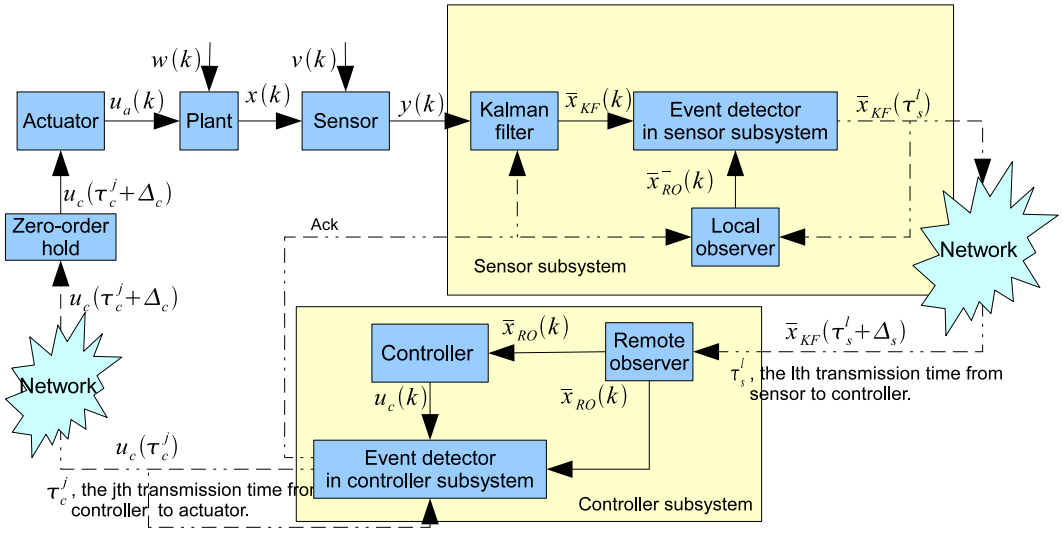

Figure 6.2. Structure of output feedback systems with delays and dropouts

6.2.2 Problem Statement

Consider the same framework as in Section 6.1 with UDP as the communication protocol in the whole control loop.

Since there are delays and dropouts, when sensor decides to transmit, $\overline{x}_{KF}$ together with a time stamp is sent to the remote observer. When remote observer receives information, it will check the time stamp first. If this information is more recent than the previously received information, it will accept it and update its state estimate $\overline{x}_{RO}$ according to the newly received state information and its time stamp. Otherwise, the newly received information is discarded. The discarded information can be seen as a packet dropout. Notice that by checking the time stamp in the packet received at step k and comparing it with the current time, remote observer can get the delay of this packet. We denote the delay of the packet received at step k as $\Delta_s(k)$. To express the behavior of the remote observer

formally, we have

$$\overline{x}_{RO}^{-}(k) = A\overline{x}_{RO}(k-1) + u_a^{'}(k-1)$$

$$\overline{x}_{RO}(k) = \begin{cases} A^{\Delta_s(k)}\overline{x}_{KF}(k-\Delta_s(k)) + \sum_{i=k-\Delta_s(k)}^{k-1} A^{k-1-i}Bu_a^{'}(i), \\ \text{if information received by the remote observer is the latest;} \\ \overline{x}_{RO}^{-}(k), \qquad \text{otherwise,} \end{cases}$$

where $u_a^{'}(k) = u_c(\tau_c^{j(k)})$ for all $k \in [\tau_c^{j(k)}, \tau_c^{j(k)+1})$

When controller decides to transmit, $u_c(k)$ together with a time stamp is transmitted. When actuator receives information, it checks the time stamp first. If this information is more recent than the previously received information, the actuator will accept it and update the control input $u_a(k)$ to be the newly received data. Otherwise, the newly received information is discarded. Let $\Delta_c(k)$ denote the delay of the information received at step k. $u_a(k)$ can be written as

$$u_a(k) = \begin{cases} u_c(k-\Delta_c(k)), & \text{if the actuator receives the latest information;} \\ u_a(k), & \text{otherwise.} \end{cases}$$

The communication requirement, average cost and cost function are defined the same as in Section 6.1. With the network delays and packet dropouts, our objective is to find the optimal triggering sets S_s and S_c to minimize the average cost subject to the communication requirements (6.1) and (6.2).

6.2.3 Problem Analysis and Challenging Issues

The expect value of the cost function is first analyzed. With delays and dropouts, the remote state estimation error $\overline{e}_{RO}(k)$ is correlated with the remote

state estimate $\overline{x}_{RO}(k)$. We can obtain an upper bound on the expect value of the cost function by the fact that $2E(xy^T) \leq E(xx^T) + E(yy^T)$. The upper bound on the expect value of the cost function is

$$E(c(x(k), S_s, S_c)) \leq 2J_s(\overline{e}_{RO}(k), S_s) + 2J_c(\overline{x}_{RO}(k), S_c),$$

where J_s and J_c are defined as Equation (6.4) and (6.5), respectively. So if the variances of $\overline{e}_{RO}(k)$ and $\overline{x}_{RO}(k)$ are bounded, then the average cost is bounded.

Next, $\overline{e}_{RO}(k)$ is studied to find the sufficient conditions to guarantee that the variance of $\overline{e}_{RO}(k)$ is bounded. The behavior of $\overline{e}_{RO}(k)$ is given below.

$$\overline{e}^-_{RO}(k) = A\overline{e}_R(k-1) + B\tilde{u}_a(k-1) + w(k-1)$$

$$\overline{e}_{RO}(k) = \begin{cases} A^{\Delta_s(k)}\overline{e}_{KF}(k - \Delta_s(k)) + \sum_{i=k-\Delta_s(k)}^{k-1} A^{k-1-i}[B\tilde{u}_a(i) + w(i)] \\ \text{if information received by the remote observer is the latest;} \\ \overline{e}^-_{RO}(k), \qquad \text{otherwise,} \end{cases}$$

where $\tilde{u}(k) = u_a(k) - u_a^{'}(k)$. So as long as $\Delta_s(k)$, the variance of $\overline{e}_{KF}(k)$ and $\tilde{u}(k)$ are bounded, and the consecutive receiving time is finite, the variance of $\overline{e}_{RO}(k)$ is bounded. $\overline{e}_{KF}$ has the dynamics of

$$\overline{e}_{KF}(k) = (A - \overline{L}CA)\overline{e}_{KF}(k-1) + (I - \overline{L}C)w(k-1) + (B - \overline{L}CB)\tilde{u}(k-1) - \overline{L}v(k).$$

So if $A - \overline{L}CA$ is stable, and $\tilde{u}(k)$ is bounded, the variance of $\overline{e}_{KF}$ is bounded. Therefore, we can conclude that if $A - \overline{L}CA$ is stable, $\Delta_s(k)$ and $\tilde{u}(k)$ are bounded, and the consecutive receiving time is finite, then the variance of $\overline{e}_{RO}(k)$ is bounded.

Finally, we would like to see how we can guarantee that the variance of $\overline{x}_{RO}(k)$ is bounded. Let's assume that the controller is properly designed such that $A + BK$

is stable, $\Delta_c(k)$ is finite, the triggering event is properly designed such that $\tilde{u}(k)$ is bounded. Are these assumptions sufficient to guarantee that the variance of $\overline{x}_{RO}(k)$ is bounded? The answer is no. Consider the case when $A + BK$ has its eigenvalues very close to the unit circle and Δ_s is always very long. In this case, the controller is not aggressive enough to counterbalance the impact of the delays, and $\overline{x}_{RO}(k)$ can not be bounded.

Therefore, in the closed loop system, the controller, triggering events, communication bandwidth and delays are related with each other. So we need to co-design both the controller and the triggering events such that the average cost is minimized subject to the limited communication bandwidth while there are finite delays in the communication networks.

6.3 Distributed Event Triggered State Estimation Problem in Large Scale Systems

6.3.1 Introduction and Prior Work

This work considers large scale systems with a lot of sensors and very few actuators. The whole system is observable, but for each sensor, the state is only partial observable. It is very possible that the information or part of the information of several sensors are the same. *Data centers* are built to collect information from all sensors, and make a full estimate of the state. Another task of data center is to assign the bandwidth to sensors such that the sensors with more important information have more bandwidth. To save communication resource and energy, each sensor uses event triggering to send its local information to a data center. The triggering event in each sensor is based on local information only. Our objective is to design this distributed triggering event for each sensor to minimize the mean

square estimation error of the whole state discounted by the cost of transmission while the bandwidth of each sensor is not exceeded.

This framework is different from the framework in most prior work. The prior work discussing distributed event triggered estimation or control problems mainly considered multi-agent systems [12, 13, 25, 43, 46–48, 51]. In these systems, every agent could apply a control input to its subsystem. There were no data centers, so each agent needed to gather information from its neighbors. But sometimes, not all the useful information could be offered by neighbors, so each agent must broadcast both local information and the information received which may be also necessary for the other agents. Compared with the framework in the prior work, our framework is more organized. In our system, the leader, which is the data center, talks with every sensor, and therefore has global information. With the global information, the data center can efficiently estimate the state of the system.

6.3.2 Problem Statement

Consider a discrete linear time invariant system with N sensors detecting its measurements. The process state $x : \mathbb{Z}^+ \to \mathbb{R}^n$ and the measurement of sensor i $y_i : \mathbb{Z}^+ \to \mathbb{R}^{m_i}$ satisfy

$$\begin{aligned} x(k) =& Ax(k-1) + Bu(k-1) + w(k-1), \\ y_i(k) =& C_i x(k) + v_i(k), \forall i = 1, \ldots, N, \end{aligned}$$

for $k \in \mathbb{Z}^+$. A, B and C_i are real $n \times n$, $n \times p$ and $m \times n$ matrices, respectively. $u : \mathbb{Z}^+ \to \mathbb{R}^p$ is the control input. w and v_i are independent zero mean white Gaussian random process. We assume that the measurement noise processes v_i for $i = 1, \ldots, N$ are independent with each other. The whole system is observable,

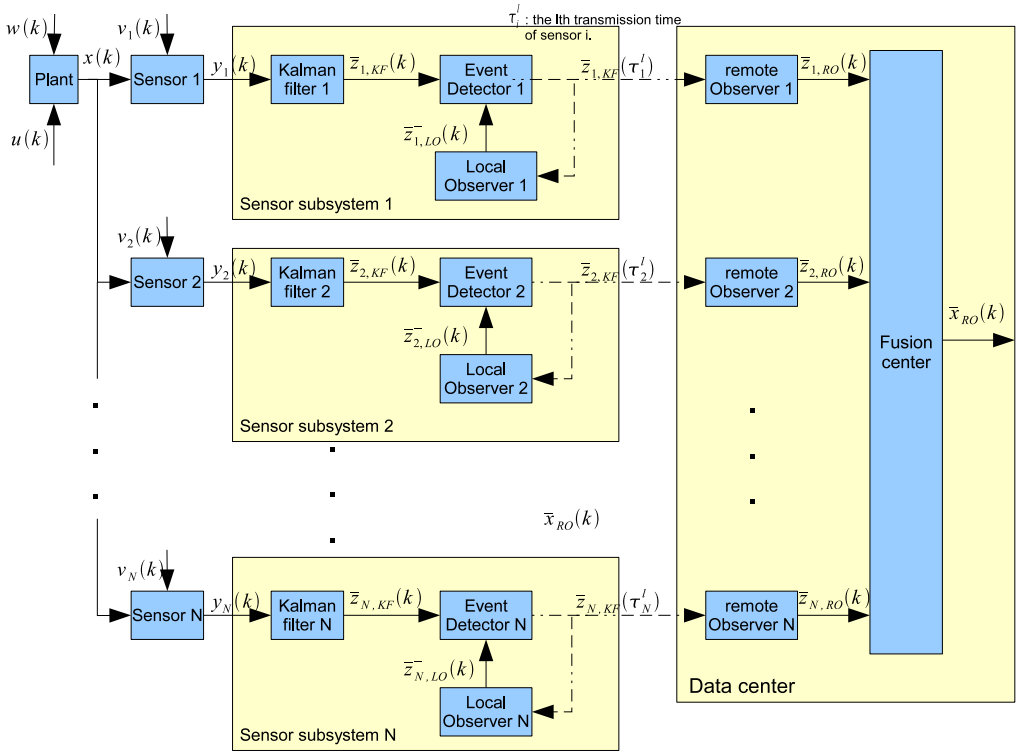

Figure 6.3. Distributed event trigged state estimation problem in large scale systems

i.e. $\left[A, \begin{bmatrix} C_1 \\ \vdots \\ C_N \end{bmatrix}\right]$ is observable, but for each sensor, the state may be only partial observable. A block diagram of the whole system is shown in Figure 6.3.

The output of each sensor is fed into a sensor subsystem. If one sensor can detect the full state x, then the sensor subsystem and the corresponding remote observer in data center are the same as in Chapter 4. Otherwise, we first derive a

standard form of unobservable system [4] for sensor i, which is

$$\begin{bmatrix} z_{i,o}(k) \\ z_{i,u}(k) \end{bmatrix} = \begin{bmatrix} A_{i,o} & 0 \\ A_{i,12} & A_{i,u} \end{bmatrix} \begin{bmatrix} z_{i,o}(k-1) \\ z_{i,u}(k-1) \end{bmatrix} + \begin{bmatrix} B_{i,o} \\ B_{i,u} \end{bmatrix} u(k-1) + \begin{bmatrix} w_{i,o}(k) \\ w_{i,u}(k) \end{bmatrix}$$
$$y_i(k) = [C_{i,o}\ 0] \begin{bmatrix} z_{i,o}(k) \\ z_{i,u}(k) \end{bmatrix} + v_i(k),$$

where $z_{i,o} \in \mathbb{R}^{n_i \leq n}$ is the observable mode at sensor i, and $[A_{i,o}, C_{i,o}]$ is an observable pair. The sensor subsystem then can be built the same as the one in Chapter 4 based on the dynamics

$$\begin{aligned} z_{i,o}(k) &= A_{i,o} z_{i,o}(k-1) + B_{i,o} u(k-1) + w_{i,o}(k-1) \\ y_i(k) &= C_{i,o} z_{i,o}(k) + v_i(k). \end{aligned} \tag{6.6}$$

The sensor subsystem consists of a Kalman filter that produces $\overline{z}_{i,o,KF}(k) \in \mathbb{R}^{n_i}$, and local observer that produces $\overline{z}^{-}_{i,o,LO}(k) \in \mathbb{R}^{n_i}$ and an event detector which decides when to send $\overline{z}_{i,o,KF}(k) \in \mathbb{R}^{n_i}$ to the corresponding remote observer in data center. The remote observer in data center is also the same as in Chapter 4 based on the dynamics (6.6).

The data center has two components: remote observers as mentioned above and a fusion center. The fusion center takes the data from the remote observers, and generates a remote state estimate $\overline{x}_{RO}(k)$ using the Bayes least square estimator, i.e. $\overline{x}_{RO}(k) = E(x(k)|\overline{z}_{1,o,RO}(k), \ldots, \overline{z}_{N,o,RO}(k))$.

The network between the sensors and the data center has limited bandwidth. The data center needs to assign the bandwidth to sensors such that the more 'important' sensors have more bandwidth.

Our objective is to design the distributed triggering event for each sensor that only relies on the local information to minimize average mean cost while the bandwidth of the whole system is not exceeded, i.e.

$$J(\{S_i\}_{i=0}^{N}) = \lim_{M\to\infty} \frac{1}{M} \sum_{k=0}^{M-1} E(c(x(k), \overline{x}_{RO}(k))),$$

where S_i is the triggering event for sensor i, the cost function c is defined as

$$c(x(k), \overline{x}_{RO}(k)) = \|x(k) - \overline{x}_{RO}(k)\|_Z^2 + \sum_{i=1}^{N} \lambda_i 1(\text{transmission occurs at sensor } i), \tag{6.7}$$

, λ_i is the communication price for the ith sensor, and $1(\cdot)$ is a characteristic function.

6.3.3 Challenging Issues

The first issue is how to deal with the coupling between sensors. Since all the noises in the system are Gaussian and $\overline{x}_{RO}$ is a Bayes least estimate over the information of all remote observers, the remote state estimation error $\overline{e}_{RO}(k)$ must be some linear combination of the remote state estimation errors in all the remote observers, $\overline{e}_{RO,i}(k) = z_{i,o}(k) - \overline{z}_{i,o,RO}(k)$ for $i = 1, \cdots, N$. So the expect value of the cost function involves the variance of the remote state estimation error of each sensor and the covariance between the remote state estimation errors of two different sensors. This covariance is the coupling between sensors. So to derive the distributed triggering events, we need to bound the coupling between two sensors with decoupled information of these two sensors.

The second issue is how to assign the limited bandwidth to all of the sensors. Assume that sensor i has the bandwidth β_i, the average mean cost of sensor

i is $c_i(\beta_i)$, and the average mean cost of the whole system is some function of the average mean cost of each sensor, $f(c_1, c_2, \cdots, c_N)$. Then the assignment of bandwidth can be solved by solving the following optimal problem.

$$\min_{\{\beta_i\}_{i=1}^N} f(c_1(\beta_1), c_2(\beta_2), \cdots, c_N(\beta_N))$$
$$\text{subject to } \sum_{i=1}^{N} \beta_i \leq \beta,$$

where β is the bandwidth of the whole system. So if we can obtain c_i and f, the bandwidth assignment can be done at least numerically.

The interesting questions are how the average mean cost increases with respect to the number of sensors, and how we can assign the bandwidth in a recursive way such that there won't be too much computation effort to reassign the bandwidth when a new sensor is added or one of the sensors is broken.

APPENDIX A

PROOFS

In order to prove theorem 2.2.1, we still need two lemmas. The two lemmas show some properties of $e^{-}_{KF,RO}(r)$, $e_{KF,RO}(r)$ and $\overline{e}_{KF}(r)$.

Lemma A.0.1. *$\overline{e}_{KF}(k)$ is independent with $e^{-}_{KF,RO}(j)$ and $e_{KF,RO}(j)$ for any $j \leq k$.*

Proof. It's easy to see that $e^{-}_{KF,RO}(j)$, $e_{KF,RO}(j)$ and $\overline{e}_{KF}(k)$ are Gaussian. $\overline{e}_{KF}(k) = E(x(k)|\mathscr{F}(k))$ is the Bayes least square (BLS) estimation error. A property of BLS estimation is that estimation error is uncorrelated with any function of the measurements from step 0 to step k. As we know, $e^{-}_{KF,RO}(j) = \bar{x}(j) - \overline{x}^{-}_{RO}(j)$ and $e_{KF,RO}(j) = \bar{x}(j) - \overline{x}_{RO}(j)$ are functions of measurements from step 0 to step j. So as long as $j \leq k$, we know $\overline{e}_{KF}(k)$ is uncorrelated with $e^{-}_{KF,RO}(j)$ and $e_{KF,RO}(j)$. Since $e^{-}_{KF,RO}(k)$, $e_{KF,RO}(k)$ and $\overline{e}_{KF}(k)$ are Gaussian, we also know they are statistically independent. So $\overline{e}_{KF}(k)$ is independent with $e^{-}_{KF,RO}(j)$ and $e_{KF,RO}(j)$ for any $j \leq k$. □

Lemma A.0.2. *The sequence $\{I^{-}(0),\ I(0),\ I^{-}(1),\ I(1), ..., I(k-1),\ I^{-}(k),\ I(k), ..., I(M)\}$ is Markov.*

Proof. The dynamics of $e^-_{KF,RO}(k)$ and $e_{KF,RO}(k)$ are summarized below

$$\begin{aligned} e^-_{KF,RO}(k) =& \overline{x}_{KF}(k) - \overline{x}^-_{RO}(k) \\ =& Ae_{KF,RO}(k-1) + L(k)A\overline{e}_{KF}(k-1) + L(k)(w(k)+v(k)) \end{aligned} \tag{A.1}$$

$$e_{KF,RO}(k) = \begin{cases} e^-_{KF,RO}(k) & \text{if } e^-_{KF,RO}(k) \in S^b_k \\ 0 & \text{otherwise} \end{cases} \tag{A.2}$$

From lemma A.0.1, we know that $\overline{e}_{KF}(k-1)$ is independent of $e_{KF,RO}(k-1), e^-_{KF,RO}(k-1), \ldots, e^-_{KF,RO}(0)$. We also know that $w(k)$ and $v(k)$ are independent of $e_{KF,RO}(k-1), e^-_{KF,RO}(k-1), \ldots, e^-_{KF,RO}(0)$. Therefore

$$r(k) = L(k)Ae_{KF,RO}(k-1) + L(k)(w(k)+v(k))$$

is also independent of $e_{KF,RO}(k-1), e^-_{KF,RO}(k-1), \ldots, e^-_{KF,RO}(0)$. Note that the number of transmissions

$$b(k+1) = \begin{cases} b(k)-1 & \text{if } e^-_{KF,RO}(k) \notin S^{b(k)}_k \\ b(k) & \text{otherwise} \end{cases}$$

with $b(0) = \overline{b}$. So $b(k+1)$ is a function of $b(0)$ and $e^-_{KF,RO}(j)$ for $j \leq k$. This means that $r(k)$ is also independent of $b(j)$ for $j \leq k+1$. So we can conclude $r(k)$ is independent of the information sets, $I(k-1), I^-(k-1), \ldots, I^-(0)$.

Consider the conditional probability density function $f(I^-(k) \,|\, I(k-1), I^-(k-1), I(k-2), \ldots, I^-(0))$. From equation (A.1) and since $I^-(k) = (e^-_{KF,RO}(k), b(k))$, we see that

$$f(I^-(k) \,|\, I(k-1), I^-(k-1), \ldots, I^-(0))$$

$$=f(e^-_{KF,RO}(k), b(k) \,|\, I(k-1), I^-(k-1), \ldots, I^-(0))$$
$$=f(Ae_{KF,RO}(k-1) + r(k), b(k) \,|\, I(k-1), I^-(k-1), \ldots, I^-(0))$$

This shows that $I^-(k) = (A\overline{e}_{KF}(k-1)+r(k), b(k))$ is a linear combination of $I(k-1) = (e_{KF,RO}(k-1), b(k))$ and $u(k)$. We showed above that $r(k)$ is independent of $I(k-1), I^-(k-1), \ldots, I^-(0)$. So the conditional probability may be written as

$$f(I^-_k \,|\, I(k-1), I^-(k-1), \ldots, I^-_0) = f(I^-(k) \,|\, I(k-1))$$

which implies that $I^-(k), I(k-1), I^-(k-1), \ldots, I^-_0$ are Markov.

A.1 Proof of Theorem 2.2.1

Proof.

$$\begin{aligned} h(\zeta, b; r) &= \min_{\mathcal{S}^b_r} E\left(\sum_{k=r}^{M} \|\overline{e}_{RO}(k)\|_2^2 \,|\, I^-(r) = (\zeta, b)\right) \\ &= \min_{S^b_r} g(\zeta, b, S^b_r) \end{aligned}$$

where $g(\zeta, b, S^b_r) = \min_{\mathcal{S}^b_r - S^b_r} E\left(\sum_{k=r}^{M} \|\overline{e}_{RO}(k)\|_2^2 | I^-(r) = (\zeta, b)\right)$.

Now we are going to calculate $g(\zeta, b, S^b_r)$ in two cases: $\zeta \in S^b_r$ and $\zeta \notin S^b_r$. Here, the first case is explained explicitly. Because the second case can be derived similarly, we only give the final result.

If $\zeta \in S^b_r$,

$$g(\zeta, b, S^b_r) = \min_{S^b_r(r+1), \cdots, S^b_r(M)} E\left(\sum_{k=r}^{M} \|\overline{e}_{RO}(k)\|_2^2 | e^-_{KF,RO}(r) = \zeta \in S^b_r, b(r) = b)\right)$$

Because the condition $e^-_{KF,RO}(r) = \zeta \in S^b_r, b(r) = b \Leftrightarrow e_{KF,RO}(r) = \zeta, b(r+1) =$

b and $e^-_{KF,RO}(r) = \zeta, b(r) = b$,

$$\begin{aligned} g(\zeta, b, S_r^b) &= \min_{\mathcal{S}_r^b - S_r^b} E\left(\sum_{k=r}^{M} \|\overline{e}_{RO}(k)\|_2^2 | I(r) = I^-(r) = (\zeta, b)\right) \\ &= \min_{\mathcal{S}_r^b - S_r^b} E\left(\sum_{k=r}^{M} \|\overline{e}_{RO}(k)\|_2^2 | I(r) = (\zeta, b)\right). \end{aligned}$$

Since $b(r+1) = b$ which means b transmissions remaining at step $r+1$, only $\mathcal{S}_{r+1}^b$ can influence the value of the expectation.

$$\begin{aligned} & g(\zeta, b, S_r^b) \\ = & \min_{\mathcal{S}_{r+1}^b} E\left(\sum_{k=r}^{M} \|\overline{e}_{RO}(k)\|_2^2 | I(r) = (\zeta, b)\right) \\ = & tr(\overline{P}(r)) + \|\zeta\|_2^2 + \min_{\mathcal{S}_{r+1}^b} E\left(\sum_{k=r+1}^{M} \|e_{KF,RO}(k)\|_2^2 | I(r) = (\zeta, b)\right) \\ = & tr(\overline{P}(r)) + \|\zeta\|_2^2 + \min_{\mathcal{S}_{r+1}^b} E\left(E\left(\sum_{k=r+1}^{M} \|e_{KF,RO}(k)\|_2^2 | I_{r+1}^- = \right.\right. \\ & \left.\left. (e^-_{KF,RO}(r+1), b), I(r) = (\zeta, b)\right) | I(r) = (\zeta, b)\right) \\ = & tr(\overline{P}(r)) + \|\zeta\|_2^2 + E\left(\min_{\mathcal{S}_{r+1}^b} E\left(\sum_{k=r+1}^{M} \|e_{KF,RO}(k)\|_2^2 | I^-(r+1) = \right.\right. \\ & \left.\left. (e^-_{KF,RO}(r+1), b)\right) | I(r) = (\zeta, b)\right) \\ = & tr(\overline{P}(r)) + \|\zeta\|_2^2 + E\left(h(e^-_{KF,RO}(r+1), b; r+1) | I(r) = (\zeta, b)\right) \\ = & h_{nt}(\zeta, b, r). \end{aligned}$$

The fourth equality holds because the information set sequence $\{I^-(k), I(k)\}_{k=0}^M$ is Markov and $e^-_{KF,RO}(r+1)$ is independent with $\mathcal{S}_{r+1}^b$.

If $\zeta \notin S_r^b$, we can show that

$$\begin{aligned} g(\zeta, b, S_r^b) =& tr(\overline{P}(r)) + E\left(h(e^-_{KF,RO}(r+1), b-1; r+1) | I(r) = (0, b-1)\right) \\ =& h_t(\zeta, b, r) \end{aligned}$$

With the value in both cases, we conclude that $g(\zeta, b, S_r^b) = h_{nt} 1_{\zeta \in S_r^b} + h_t 1_{\zeta \notin S_r^b}$, and the value function $h(\zeta, b; r) = \min\{h_{nt}(\zeta, b, r), h_t(b, r)\}$ with $S_r^{b*} = \{\zeta : h_{nt}(\zeta, b, r) \leq h_t(\zeta, b, r)\}$.

There are two initial conditions for the recursive equation. One is the case when there is no remaining transmissions, $h(\zeta, 0; r)$. The other is the case when the number of remaining transmissions is the same as the remaining steps,$h(\zeta, b; r)$ for $b \in [1, \overline{b}]$ and $r = M + 1 - b$. Both of them can be calculated directly. □

A.2 Proof of Corollary 2.2.2

Proof. The symmetric property can be established from algebraic derivation.

To prove the non-decreasing property in one direction, we can first assume it's not true. The conclusion based on the assumption will be there exist an observer which can give even smaller mean estimation error than Kalman filter, which means that the assumption we made is false and the corollary is proved.

We've know that Kalman filter is the optimal observer(both local and remote) for this problem. Now let's suppose that there exists $d \in \mathbb{R}^n$ and $\alpha_1 > \alpha_2 \geq 0$, such that

$$h(\alpha_1 d, b; r) < h(\alpha_2 d, b; r) \tag{A.3}$$

The main idea of the derivation is to show that based on the supposition, the kalman filter does not give the minimum mean square estimation.

Inequality (A.3) indicates that

$$h(\alpha_1 d, b; r) = h_{nt}(\alpha_1 d, b, r) < h_t(\alpha_1 d, b, r). \tag{A.4}$$

Together with $h(\alpha_2 d, b; r) \leq h_{nt}(\alpha_2 d, b, r)$ and (A.3), we can see that

$$h_{nt}(\alpha_1 d, b, r) \leq h_{nt}(\alpha_2 d, b, r). \tag{A.5}$$

Since $\alpha_1 > \alpha_2 \geq 0$, from (2.2.1),

$$E\left(h(\alpha_1 Ad + L(r)\delta y(r), b; r+1)\right) < E\left(h(\alpha_2 Ad + L(r)\delta y(r), b; r+1)\right)$$

If the local and remote observer are designed as

$$\overline{x}_{KF}(k) = A\overline{x}_{KF}(k-1) + L(k)(y(k) - CA\overline{x}_{KF}(k-1)) + \frac{\alpha_1 - \alpha_2}{\alpha_2} Ae_{KF,RO}(k-1),$$

when $e_{KF,RO}(k-1) = \alpha_2 d$, then

$$\begin{aligned} & h'_{nt}(\alpha_2 d, b, r) \\ = \;& \alpha_2^2 \|d\|_2^2 + tr(\overline{P}(r)) + E(h(\alpha_1 Ad + L(r)\delta y(r), b; r+1)) \\ < \;& h_{nt}(\alpha_1 d, b; r). \end{aligned}$$

From equation (A.4) and the property that $h_t(\zeta, b, r)$ is independent with ζ, we know that

$$h'_{nt}(\alpha_2 d, b, r) < h_t(\alpha_2 d, b, r)), \tag{A.6}$$

so $h'(\alpha_2 d, b; r) = h'_{nt}(\alpha_2 d, b, r)$. From (A.5), $h'(\alpha_2 d, b; r) < h_{nt}(\alpha_2 d, b, r)$. Together with (A.6), we conclude that $h'(\alpha_2 d, b; r) < h(\alpha_2 d, b; r)$, which indicates that

the Kalman filter is not the optimal observer in this problem. This conclusion contradict the fact that Kalman filter can give the minimum mean square error estimation, so the supposition is wrong. □

A.3 Proof of Corollary 2.2.3

Proof. $S_r^{0*} = \mathcal{R}, \forall r = 0, 1, ..., M$, and $\theta_r^0 = \infty$. $S_r^{b*} = \{0\}, \forall r = M + 1 - b, ..., M$, and $\theta_r^b = 0$, $\forall r = M + 1 - b, ..., M$. For the other cases,

$$S_r^{b*} = \{\zeta : \zeta^2 + E_{e^-_{KF,RO}(r+1)}(h(e^-_{KF,RO}(r+1), b; r+1)|I(r) = (\zeta, b)) \leq E_{e^-_{KF,RO}(r+1)}(h(e^-_{KF,RO}(r+1), b-1; r+1)|I(r) = (0, b-1))\}.$$

From corollary 2.2.2 we can show that the second term is a constant and the first term is symmetric about y-axis and increasing about $|\zeta|$. So S_r^{b*} must be in the form of $[-\theta_r^b, \theta_r^b]$. □

A.4 Proof of Theorem 2.3.1

Proof. First, we can see that the initial condition of $\bar{h}_t = h_t$ satisfies equation (2.12) and the initial condition of $\bar{h}_{nt} = h_{nt}$ satisfies equation (2.11) by assuming that $\Lambda_{r,j}^0 = \mathbf{0}$ and $c_{r,j}^0 = \infty$ for $j = 2, \cdots, l_r^0$. We also assumes that $\rho_r^0 = \infty$

Now assume that

$$\begin{aligned} \bar{h}_{nt}(\zeta, k, r+1) &= \min_{j=1,\cdots,M-k-r} (\zeta^T \Lambda_{r+1,j}^k \zeta + c_{r+1,j}^k) \\ \bar{h}_t(\zeta, k, r+1) &= \rho_{r+1}^k \end{aligned}$$

are the upper bounds of $h_{nt}(\zeta,k,r+1)$ and $h_t(\zeta,k,r+1)$ for both $k=b$ and $b-1$.

$$
\begin{aligned}
&h_{nt}(\zeta,b,r)\\
\leq& tr(\overline{P}(r))+\zeta^T\zeta+E(\bar{h}(\zeta,b;r+1)|I(r)=(\zeta,b))\\
\leq& tr(\overline{P}(r))+\zeta^T\zeta+\min\{\\
&\min_{j=1,\cdots,M-b-r} E(e^{-T}_{KF,RO}(r+1)\Lambda^b_{r+1,j}e^-_{KF,RO}(r+1)+c^b_{r+1,j}|e_{KF,RO}(r)=\zeta),\rho^b_{r+1}\}\\
=&\min\{\min_{j=1,\cdots,M-b-r}(\zeta^T(A^T\Lambda^b_{r+1,j}A+I)\zeta+\sigma^b_{r+1}+tr(\overline{P}(r)))\\
&,\zeta^T\zeta+\rho^b_{r+1}+tr(\overline{P}(r))\}\\
=&\bar{h}_{nt}(\zeta,b,r),
\end{aligned}
$$

and

$$
\begin{aligned}
&h_t(\zeta,b,r)\\
\leq& tr(\overline{P}(r))+E(\bar{h}(\zeta,b-1;r+1)|I(r)=(0,b-1))\\
\leq& tr(\overline{P}(r))+\min\{\\
&\min_{j=1,\cdots,M+1-b-r} E(e^{-T}_{KF,RO}(r+1)\Lambda^{b-1}_{r+1,j}e^-_{KF,RO}(r+1)+c^{b-1}_{r+1,j}|e_{KF,RO}(r)=0),\rho^{b-1}_{r+1}\}\\
=& tr(\overline{P}(r))+\min\{\sigma^{b-1}_{r+1,1},\cdots,\sigma^{b-1}_{r+1,M+1-b-r},\rho^{b-1}_{r+1}\}\\
=&\begin{cases} tr(\overline{P}(r))+\sigma^{b-1}_{r+1,1}, & \text{if } b=1;\\ tr(\overline{P}(r))+\min\{\sigma^{b-1}_{r+1,1},\cdots,\sigma^{b-1}_{r+1,\ell^b_r},\rho^{b-1}_{r+1}\}, & \text{otherwise.}\end{cases}\\
=&\bar{h}_t(\zeta,b,r)
\end{aligned}
$$

The forth equality holds because $c^0_{r,j}=\rho^0_r=\infty$. □

Lemma A.4.1. *$\{I^-(k),I(k)\}_{k=0}^M$ is Markov.*

Proof. $I(k)=\left(\begin{bmatrix}\overline{x}_{KF}(k)\\ e^-_{KF,RO}(k)1_{q^-(k)\notin S^{b_k}_k}\end{bmatrix},b_k-1_{q^-_k\notin S^{b_k}_k}\right)=f(I^-(k))$. So it's easy

to see that $p(I(k)|I^-(k),\cdots,I_0^-) = p(I(k)|I^-(k))$.

$I_{k+1}^- = \big(\overline{A}q(k), b_{k+1}\big) + \big(\overline{L}_{k+1}r(k), 0\big)$, where $r(k) = CA\overline{e}_{KF}(k) + Cw(k+1) + v(k+1)$, $\overline{e}_{KF}(k) = x(k) - \overline{x}_{KF}(k)$ is the local state estimation error. Because $r(k)$ is independent with $I(k), I^-(k),\cdots,I^-(0)$. So $p(I^-(k+1)|I(k),\cdots,I^-(0)) = p(I^-(k+1)|I_k)$. □

A.5 Proof of Theorem 3.2.1

Proof. By the definition of the value function, we have

$$h(\theta, b; r) = \min_{S_r^b}(h_{nt}(\theta, b, r)1_{\theta\in S_r^b}, h_t(\theta, b, r)1_{\theta\notin S_r^b}),$$

where

$$h_{nt}(\theta, b, r) = \min_{\mathcal{S}_r^b - S_r^b} E(\sum_{k=r}^{M} p(k)^T Z p(k)|I^-(r) = (\theta, b))1_{\theta\in S_r^b},$$
$$h_t(\theta, b, r) = \min_{\mathcal{S}_r^b - S_r^b} E(\sum_{k=r}^{M} p(k)^T Z p(k)|I^-(r) = (\theta, b))1_{\theta\notin S_r^b}.$$

Consider h_{nt} first,

$$h_{nt}(\theta, b, r) = \min_{\mathcal{S}_r^b - S_r^b} E(\sum_{k=r}^{M} p(k)^T Z p(k)|I^-(r) = (\theta, b), \theta \in S_r^b).$$

The condition is equivalent with $I^-(r) = I(r) = (\theta, b)$, because $\theta \in S_r^b$ means no transmission at step r. With lemma $A.4.1$, we can derive that

$$h_{nt}(\theta, b, r) = \min_{\mathcal{S}_r^b - S_r^b} E(\sum_{k=r}^{M} p(k)^T Z p(k)|I(r) = (\theta, b)).$$

We can pull the cost at the rth step out of the minimum, and the remaining costs are only related with $\mathcal{S}_{r+1}^b$, so

$$h_{nt}(\theta, b, r) = \theta^T Z\theta + \beta(r) + \min_{\mathcal{S}_{r+1}^b} E(\sum_{k=r+1}^{M} p(k)^T Z p(k) | I(r) = (\theta, b))$$

With lemma 6.1 and some mathematical deduction, we are able to show equation(3.4) holds.

Follow the same steps, (3.5) can be shown.

Initial conditions are given for two cases: $b = 0$ and $b + r = M + 1$. For the first case, $h_{nt}(\theta, 0, r) = \theta^T \Lambda_{r,1}^0 \theta + c_{r,1}^0$ and $h_t(\theta, 0, r) = \eta^T \Psi_r^0 \eta + d_r^0$ where

$$\begin{aligned}
\Lambda_{r,1}^0 =& \sum_{k=r}^{M} (\overline{A}^T)^{k-r} Z \overline{A}^{k-r}, \\
c_{r,1}^0 =& \sum_{k=1}^{M} (\beta(k) + \sum_{j=r}^{k-1} tr(R(j)\overline{L}^T(j+1)(\overline{A}^T)^{k-j-1} Z \overline{A}^{k-j-1} \overline{L}(j+1))), \\
\Psi_r^0 =& 0, \\
d_r^0 =& \infty.
\end{aligned}$$

For the second case, $h_t(\theta, M + 1 - r, r) = \eta^T \Psi_r^{M+1-r} \eta + d_r^{M+1-r}$, where

$$\begin{aligned}
\Psi_r^{M+1-r} =& \sum_{k=r}^{M} ((A + BK)^T)^{k-r} Z_{11} (A + BK)^{k-r}, \\
d_r^{M+1-r} =& \sum_{k=r}^{M} \Bigg(\beta(k) + \sum_{j=r}^{k-1} tr(R(j) L^T(j+1)((A + BK)^T)^{k-j-1} \\
& Z_{11} (A + BK)^{k-j-1} L(j+1)) \Bigg).
\end{aligned}$$

□

A.6 Proof of Lemma 3.3.2

Proof. For $b = 1$, it's easy to show that $\overline{h}_t(\theta, 1, r) = \eta^T \Psi_r^1 \eta + d_r^1$ where Ψ_r^1 and d_r^1 satisfy equation (3.12) and (3.13) respectively.

With the initial condition at step M, we are able to show that at step $M-1$, $\overline{h}_{nt}(\theta, 1, M-1) = \theta^T \Lambda_{M-1,1}^1 \theta + c_{M-1,1}^1$ where $\Lambda_{M-1,1}^1$ and $c_{M-1,1}^1$ satisfy equation (3.10) and (3.11) respectively. Now suppose that for $b = 1$ and step $r+1$, equation (3.7) holds with $\Lambda_{r+1,j}^1$ and $c_{r+1,j}^1$ defined as (3.10) and (3.11).

$$h_{nt}(\theta, 1, r) = \theta^T Z \theta + \beta(r) + E(h(q_{r+1}^-, 1, r+1) | I(r) = (\theta, 1)),$$

where $E(h(q_{r+1}^-, 1, r+1) | I(r) = (\theta, 1))$

$$\begin{aligned}
&\leq E(\min\{\overline{h}_{nt}(q_{r+1}^-, 1, r+1), \overline{h}_t(q_{r+1}^-, 1, r+1)\} | I(r) = (\theta, 1)) \\
&\leq \min\{E(\overline{h}_{nt}(q_{r+1}^-, 1, r+1) | I(r) = (\theta, 1)), E(\overline{h}_t(q_{r+1}^-, 1, r+1)\} | I(r) = (\theta, 1))\} \\
&\leq \min\{\min_{j=1,\cdots,\rho_{r+1}^1} \theta^T \tilde{\Lambda}_{r,j}^1 \theta + \tilde{c}_{r,j}^1, \theta^T \tilde{\Lambda}_{r,i_{r+1}^1+1} \theta + \tilde{c}_{r,i_{r+1}^1+1}^1\},
\end{aligned}$$

where $\tilde{\Lambda}_{r,j}^1 = \Lambda_{r,j} - Z$ and $\tilde{c}_{r,j}^1 = c_{r,j} - \beta(r)$ for all $j = 1, \cdots, \rho_r^1$.

By now, we've shown that lemma 3.3.2 is true for $b = 1$. Before we go to the case of $b > 1$, we find that

$$\Lambda_{r,j}^b(1,1) = \Psi_r^b = \sum_{k=r}^{M} ((A + BK)^T)^{k-r} Z_{11} (A + BK)^{k-r}, \tag{A.7}$$

which can be shown by mathematical induction. $\Lambda_{r,j}^b(1,1)$ means the left upper $n \times n$ matrix of $\Lambda_{r,j}^b$.

Now, suppose lemma 3.3.2 and equation (A.7) are both true for $b-1$ where $b > 1$. $h_t(\theta, b, r) = \eta^T Z_{11} \eta + \beta(r) + E(h(q_{r+1}^-, 1, r) | I^-(r) = (\theta, b))$. The expectation

part is

$$\leq \min\Big\{\eta^T(A+BK)^T\Psi_{r+1}^{b-1}(A+BK)\eta + d_{r+1}^{b-1} + tr(\overline{\Psi}_{r+1}^{b-1})\ ,$$
$$\min_{j=1,\cdots,\rho_{r+1}^{b-1}}\Big[\eta^T(A+BK)^T\Lambda_{r+1,j}^{b-1}(1,1)(A+BK)\eta + c_{r+1,j}^{b-1} + tr(\overline{\Lambda}_{r+1,j}^{b-1})\Big]\Big\}.$$

Because (3.8), the upper bound above can be simplified as

$$\eta^T(A+BK)^T\Psi_{r+1}^{b-1}(A+BK)\eta + \min\{\hat{\Lambda}_{r+1}^{b-1}, \hat{\Psi}_{r+1}^{b-1}\}$$

Therefore, $\overline{h}_t(\theta, b, r) = \eta^T\Psi_r^b\eta + d_r^b$, where$\Psi_r^b = Z_{11} + (A+BK)^T\Psi_{r+1}^{b-1}(A+BK)$ and $d_r^b = \min\{\hat{\Lambda}_{r+1}^{b-1}, \hat{\Psi}_{r+1}^{b-1}\} + \beta(r)$.

We can also show that $\overline{h}_{nt}(\theta, b, r)$ is specified as equation (3.7) and the Λ and c are specified as (3.10) and (3.11) respectively. The proof is the same as for $b = 1$.

By mathematical induction, we still have equation (A.7) for $b > 1$.

Therefore, lemma 3.3.2 and equation (A.7) are still true for $b > 1$. □

A.7 Proof of Theorem 4.3.1

A.7.1 Proof of Part 1)

To prove the first part, the communication requirement (4.3) needs to be rewritten as

$$E(\|e_{KF,LO}^{-}(k)\|_H^2) \leq \lambda + tr(ZN) - \zeta(k),$$

for any $k = \tau^\ell + 1, \cdots, \tau^\ell + T_r - 1$ and any $\ell \in \mathbb{Z}^+$. By applying $\zeta(k)$ into the inequality above, we can conclude that as long as

$$\begin{aligned}\lambda \geq &(1+\delta^2)tr(HU^-_{KF,LO}(k)) + tr(ZU^-_{LO,RO}(k)) + tr(HR) \\ &- tr(ZN), \forall k = \tau^\ell + 1, \cdots, \tau^\ell + T_r - 1,\end{aligned}$$

the communication requirement (4.3) can be guaranteed. Because during the inter sample interval, no transmission occurs, $U^-_{KF,LO}(k)$ and $U^-_{LO,RO}(k)$ is iteratively calculated under the condition that there is no transmission from $\tau^\ell + 1$ to $\tau^\ell + T_r - 1$. Let $t = k - \tau^\ell$.

$$U^-_{KF,LO}(k) = \sum_{i=1}^{t-1} A^{t-i} R (A^T)^{t-i},$$

and

$$U^-_{LR,RO}(k) = A^t N (A^T)^t.$$

Therefore, if the inequality (4.15) holds, the communication requirement (4.3) can be satisfied.

A.7.2 Proof of Part 2)

To prove part 2), it is sufficient to show that the inequality (4.9) holds for any k with f_k defined in Theorem 4.3.1 and

$$\overline{J}_k = E(f_k(e^-_{KF,LO}(k+1)) | e_{KF,LO}(k) = 0).$$

In the case of $\|e^-_{KF,LO}(k)\|^2_H \leq \lambda + tr(ZN) - \zeta(k)$, no transmission occurs at

step k, so the right side of the inequality (4.9)

$$
\begin{aligned}
=&\|e^-_{KF,LO}(k)\|^2_Z + tr(ZU^-_{LO,RO}(k)) \\
&+ E(f_{k+1}(e^-_{KF,LO}(k+1))|e_{KF,LO}(k) = e^-_{KF,LO}(k)) \\
\leq&\|e^-_{KF,LO}(k)\|^2_H + \|e^-_{KF,LO}(k)\|^2_{A^THA-H+Z} + \zeta(k+1) \\
&+ tr(HR) + tr(ZU^-_{LO,RO}(k)) \\
\leq&\|e^-_{KF,LO}(k)\|^2_H + \delta^2(\lambda + tr(ZN) - \zeta(k)) \\
&+ tr(HR) + tr(ZU^-_{LO,RO}(k)) + \zeta(k+1) \\
=&\|e^-_{KF,LO}(k)\|^2_H + \zeta(k) + \zeta(k+1) \\
\leq& f_k(e^-_{KF,LO}(k) + \overline{J}_{k+1}.
\end{aligned}
$$

The first equality is taken from (4.6), the second step is derived from $E(\min(f,g)) \leq \min(E(f), E(g))$, the third step is derived from the fact that $\|e^-_{KF,LO}(k)\|^2_H \leq \lambda + tr(ZN) - \zeta(k)$, and the fourth step is derived from how we define the $\zeta(k)$.

In the case of $\|e^-_{KF,LO}(k)\|^2_H > \lambda + tr(ZN) - \zeta(k)$, transmission occurs, and the right side of inequality (4.9)

$$
\begin{aligned}
=&\lambda + tr(ZN) + E(f_{k+1}(e^-_{KF,LO}(k+1))|e_{KF,LO}(k) = 0) \\
\leq& f_k(e^-_{KF,LO}(k)) + \overline{J}_{k+1}
\end{aligned}
$$

Since the inequality (4.9) holds in any condition, from Lemma 4.2.2, we know that $J_a(\{S(k)\}_{k=0}^{\infty})$ is bounded above by $\overline{J}_a(\{S(k)\}_{k=0}^{\infty})$ defined in (4.16).

A.7.3 Proof of Part 3)

If a lower bound on the optimal cost is found, an upper bound of the difference between the cost of quadratic sets and the optimal sets can be derived. The lower bound on the optimal cost is given in Lemma A.7.1.

Lemma A.7.1. *The optimal cost J_a^* is bounded below by*

$$\lim_{N\to\infty} \frac{1}{N} \sum_{k=1}^{N} E(g_k(e^-_{KF,LO}(k))|e_{KF,LO}(k-1)=0),$$

where $g_k(\theta) = \min\{\|\theta\|_Z^2 + tr(ZU^-_{LO,RO}(k)), \lambda + tr(ZN)\}$.

Proof. Let's define

$$\underline{J}_{k+1} = E(g_{k+1}(e^-_{KF,LO}(k+1))|e_{KF,LO}(k)=0).$$

By Lemma 4.2.3, if

$$\underline{J}_{k+1}(e^-_{KF,LO}(k)) + g_k(e^-_{KF,LO}(k)) \le G\left(g_{k+1}(e^-_{KF,LO}(k))\right),$$

Lemma A.7.1 is true. The left side of the inequality equals

$$\begin{aligned}
&\min\{\|e^-_{KF,LO}(k)\|_Z^2 + tr(ZU^-_{LO,RO}(k)) \\
&+ E(g_{k+1}(e^-_{KF,LO}(k+1))|e_{KF,LO}(k)=0), \\
&\lambda + tr(ZN) + E(g_{k+1}(e^-_{KF,LO}(k+1))|e_{KF,LO}(k)=0)\},
\end{aligned}$$

and the right side of the inequality equals

$$\begin{aligned}
&\min\{\|e^-_{KF,LO}(k)\|^2_Z + tr(ZU^-_{LO,RO}(k)) \\
&+ E(g_{k+1}(e^-_{KF,LO}(k+1))|e_{KF,LO}(k) = e^-_{KF,LO}(k)), \\
&\lambda + tr(ZN) + E(g_{k+1}(e^-_{KF,LO}(k+1))|e_{KF,LO}(k) = 0)\}.
\end{aligned}$$

So as long as we can show that

$$\begin{aligned}
&E(g_{k+1}(e^-_{KF,LO}(k+1))|e_{KF,LO}(k) = 0) \\
\leq &E(g_{k+1}(e^-_{KF,LO}(k+1))|e_{KF,LO}(k) = e^-_{KF,LO}(k)),
\end{aligned}$$

the inequality (4.11) holds.

First, we realize that

$$g_k(\alpha d_1 + \beta_1 d_2) \geq g_k(\alpha d_1 + \beta_2 d_2) \tag{A.8}$$

if $\beta_1 \geq |\beta_2|$ and $d_1^T Z d_2 = 0$ where d_1 and d_2 are linearly independent.

Second, we'd like to show some properties of the normal probability density function. Let $\mathcal{N}_\theta(\mu, R)$ be the normal probability density function of random variable θ with mean μ and variance R, and R^+ denote the generalized inverse [32] of R. We can always construct a basis of $\mathbb{R}^n$, $\{\varepsilon_i\}_{i=1}^n$, where $\varepsilon_1 = Ad_1$, $(Ad_2)^T\varepsilon_2 \geq 0$, and $\varepsilon_j^T R^+ \varepsilon_j = 0$ for any $i \neq j$. Let

$$p(\theta) = \mathcal{N}_\theta(A(\alpha d_1 + \beta_1 d_2), R) - \mathcal{N}_\theta(A(\alpha d_1 + \beta_2 d_2), R),$$

where d_1, d_2, α, β_1, and β_2 are defined in (A.8). We can show that

$$p(z + \frac{\beta_1 + \beta_2}{2} b_2 \varepsilon_2 + \rho \varepsilon_2) = -p(z + \frac{\beta_1 + \beta_2}{2} b_2 \varepsilon_2 - \rho \varepsilon_2), \tag{A.9}$$

where $z^T R^+ \varepsilon_2 = 0$, $b_2 = (Ad_2)^T \varepsilon_2 \geq 0$ and $\rho \geq 0$. Let $Ad_2 = \sum_{i=1}^{n} b_i \varepsilon_i$. To show (A.9) is true, we first show that

$$\begin{aligned}
& p\left(z + \frac{\beta_1 + \beta_2}{2} b_2 \varepsilon_2 + \rho \varepsilon_2\right) \\
=& \mathcal{N}_z\left(\alpha \varepsilon_1 - \sum_{i \neq 2} b_i \varepsilon_i - (-\frac{\beta_1 - \beta_2}{2} + \rho)\varepsilon_2\right) \\
& - \mathcal{N}_z\left(\alpha \varepsilon_1 - \sum_{i \neq 2} b_i \varepsilon_i - (\frac{\beta_1 - \beta_2}{2} + \rho)\varepsilon_2\right),
\end{aligned}$$

and then show that

$$\begin{aligned}
& p(z + \frac{\beta_1 + \beta_2}{2} b_2 \varepsilon_2 - \rho \varepsilon_2) \\
=& \mathcal{N}_z\left(\alpha \varepsilon_1 - \sum_{i \neq 2} b_i \varepsilon_i + (\frac{\beta_1 - \beta_2}{2} + \rho)\varepsilon_2\right) \\
& - \mathcal{N}_z\left(\alpha \varepsilon_1 - \sum_{i \neq 2} b_i \varepsilon_i + (-\frac{\beta_1 - \beta_2}{2} + \rho)\varepsilon_2\right).
\end{aligned}$$

Because $\varepsilon_j^T R^+ \varepsilon_j = 0$ for any $i \neq j$, the equation (A.9) can be proven. Moreover,

$$p(z + \frac{\beta_1 + \beta_2}{2} b_2 \varepsilon_2 + \rho \varepsilon_2) \geq 0, \text{if } \rho \geq 0 \tag{A.10}$$

Finally, with the property of (A.9), we can show that

$$
\begin{aligned}
& E(g_{k+1}(e^-_{KF,LO}(k+1))|e_{KF,LO}(k)=\theta) \\
& - E(g_{k+1}(e^-_{KF,LO}(k+1))|e_{KF,LO}(k)=0) \\
=& \int_{\theta_i, i\neq 2}\int_{\theta_2\geq 0}\Bigg[g_k(\sum_{i\neq 2}\theta_i\varepsilon_i + (\theta_2+\frac{\beta_1+\beta_2}{2}b_2)\varepsilon_2) \\
& -g_k(\sum_{i\neq 2}\theta_i\varepsilon_i + (-\theta_2+\frac{\beta_1+\beta_2}{2}b_2)\varepsilon_2)\Bigg] \\
& \cdot p(\sum_{i\neq 2}\theta_i\varepsilon_i + (\theta_2+\frac{\beta_1+\beta_2}{2}b_2)\varepsilon_2)d\theta_2\cdots d\theta_n \\
\geq & 0,
\end{aligned}
$$

where $\theta_i = \frac{\theta^T\varepsilon_i}{\|\varepsilon_i\|}$. The last inequality above is derived from the inequalities (A.8) and (A.10). □

Now that both the upper and lower bounds are given, the difference between them can be shown to be bounded by $\min\{D_1, D_2\}$, where D_1 and D_2 are defined in Theorem 4.3.1.

First, we know from part 2) of Theorem 4.3.1 and Lemma A.7.1 that

$$
\begin{aligned}
& J_a(\{S(k)\}_{k=0}^{\infty}) - J_a^* \leq J_a(\{S(k)\}_{k=0}^{\infty}) - J_a^* \\
\leq & \lim_{M\to\infty}\frac{1}{M}\sum_{k=1}^{M} E\left[(f_k-g_k)(e^-_{KF,LO}(k))|e_{KF,LO}(k-1)=0\right] \\
\leq & \lim_{M\to\infty}\frac{1}{M}\sum_{k=1}^{M}\Big[E(\|e^-_{KF,LO}(k)\|_Y^2|e_{KF,LO}(k-1)=0) \\
& \max\{\zeta(k)-tr(ZU^-_{LO,RO}(k)),0\}\Big] \\
= & tr(YR) + \lim_{M\to\infty}\frac{1}{M}\sum_{k=1}^{M}\max\{\zeta(k)-tr(ZU^-_{LO,RO}(k)),0\}.
\end{aligned}
$$

The third inequality is derived by considering the four conditions which are

$$\|\theta\|_Z^2 + tr(ZU_{LO,RO}^-(k)) \lneqq \lambda + tr(ZN)$$

and

$$\|\theta\|_H^2 + \zeta(k) \lneqq \lambda + tr(ZN)$$

and realizing that $H - Z \leq Y$ and $Y \geq 0$.

Next, noticing that

$$J(\{S(k)\}_{k=0}^{\infty}) \leq \lambda + tr(ZN)$$

and

$$J^* \geq \min\{tr(ZU_{LO,RO}^-(k)), \lambda + tr(ZN)\},$$

$J(\{S(k)\}_{k=0}^{\infty}) - J^*$ is bounded above by D_2.

Therefore, part 3) is proven.

BIBLIOGRAPHY

1. A. Anta and P. Tabuada. Self-triggered stabilization of homogeneous control systems. In *American Control Conference, 2008*, pages 4129–4134. IEEE, 2008.

2. A. Anta and P. Tabuada. On the benefits of relaxing the periodicity assumption for networked control systems over CAN. In *2009 30th IEEE Real-Time Systems Symposium*, pages 3–12. IEEE, 2009.

3. A. Anta and P. Tabuada. To sample or not to sample: Self-triggered control for nonlinear systems. In *Automatic Control, IEEE Transactions on*, volume 55, pages 2030–2042. IEEE, 2010.

4. P. Antsaklis and A. Michel. *Linear systems*. Birkhauser, 2005. ISBN 0817644342.

5. A. Arapostathis, V. Borkar, E. Fernández-Gaucherand, M. Ghosh, and S. Marcus. Discrete-time controlled Markov processes with average cost criterion: a survey. ISR; TR 1991-109, 1991.

6. K. Årzén. A simple event-based PID controller. In *Proc. 14th IFAC World Congress*, volume 18, pages 423–428, 1999.

7. K. Astrom and B. Bernhardsson. Comparison of Riemann and Lebesgue sampling for first order stochastic systems. In *Decision and Control, 2002, Proceedings of the 41st IEEE Conference on*, volume 2, pages 2011–2016. IEEE, 2002. ISBN 0780375165.

8. K. Baheti and H. Gill. Cyber-Physical Systems. 2010.

9. L. Bao, M. Skoglund, and K. Johansson. Encoder˜ Decoder Design for Event-Triggered Feedback Control over Bandlimited Channels. In *American Control Conference, 2006*, pages 4183–4188. IEEE, 2006. ISBN 1424402093.

10. A. Bose. Smart transmission grid applications and their supporting infrastructure. In *Smart Grid, IEEE Transactions on*, volume 1, pages 11–19. IEEE, 2010.

11. R. Cogill, S. Lall, and J. Hespanha. A constant factor approximation algorithm for event-based sampling. pages 51–60. Springer, 2010.

12. D. Dimarogonas and K. Johansson. Event-triggered cooperative control. In *European Control Conference*, pages 3015–3020, 2009.

13. D. Dimarogonas and K. Johansson. Event-triggered control for multi-agent systems. In *Decision and Control, 2009 held jointly with the 2009 28th Chinese Control Conference. CDC/CCC 2009. Proceedings of the 48th IEEE Conference on*, pages 7131–7136. IEEE, 2009.

14. M. Donkers and W. Heemels. Output-based event-triggered control with guaranteed L8-gain and improved event-triggering. In *Proceedings of the 49th IEEE Conference on Decision and Control*, 2010.

15. W. Heemels, J. Sandee, and P. Van Den Bosch. Analysis of event-driven controllers for linear systems. In *International Journal of Control*, volume 81, pages 571–590. Taylor & Francis, 2008.

16. O. Imer. *Optimal estimation and control under communication network constraints*. PhD thesis, University of Illinois at Urbana-Champaign, 2006.

17. O. Imer and T. Basar. Optimal estimation with limited measurements. In *Decision and Control, 2005 and 2005 European Control Conference. CDC-ECC'05. 44th IEEE Conference on*, pages 1029–1034. IEEE, 2005. ISBN 0780395670.

18. O. Imer and T. Basar. Optimal estimation with scheduled measurements. In *Appl. Comput. Math*, volume 4, pages 92–101, 2005.

19. P. A. . Information. Cyber-Physical Systems. In *The National Science Foundation*, 2009.

20. E. Lee. Cyber physical systems: Design challenges. In *11th IEEE Symposium on Object Oriented Real-Time Distributed Computing (ISORC)*, pages 363–369, 2008.

21. M. Lemmon. Event-triggered feedback in control, estimation, and optimization. In *Networked Control Systems*, pages 293–358. Springer, 2011.

22. L. Li and M. Lemmon. Event-Triggered Output Feedback Control of Finite Horizon Discrete-time Multi-dimensional Linear Processes. In *Proceedings of the 49th IEEE Conference on Decision and Control*, 2010.

23. L. Li and M. Lemmon. Performance and average sampling period of sub-optimal triggering event in event triggered state estimation. In *submitttted to conference of decision and control*. IEEE, 2011.

24. L. Li, M. Lemmon, and X. Wang. Event-triggered state estimation in vector linear processes. In *American Control Conference (ACC), 2010*, pages 2138–2143. IEEE, 2010.

25. J. Lunze and D. Lehmann. A state-feedback approach to event-based control. In *Automatica*, volume 46, pages 211–215. Elsevier, 2010.

26. M. Mazo and P. Tabuada. On event-triggered and self-triggered control over sensor/actuator networks. In *Decision and Control, 2008. CDC 2008. 47th IEEE Conference on*, pages 435–440. IEEE, 2008.

27. M. Mazo and P. Tabuada. Input-to-state stability of self-triggered control systems. In *Decision and Control, 2009 held jointly with the 2009 28th Chinese Control Conference. CDC/CCC 2009. Proceedings of the 48th IEEE Conference on*, pages 928–933. IEEE, 2009.

28. M. Mazo Jr, A. Anta, and P. Tabuada. On self-triggered control for linear systems: Guarantees and complexity. In *European control conference*. Citeseer, 2009.

29. M. Mazo Jr, A. Anta, and P. Tabuada. An ISS self-triggered implementation of linear controllers. In *Automatica*, volume 46, pages 1310–1314. Elsevier, 2010.

30. A. Molin and S. Hirche. Structural characterization of optimal event-based controllers for linear stochastic systems. In *Proceedings of the 49th IEEE Conference on Decision and Control*, 2010.

31. A. Molin and S. Hirche. Suboptimal Event-based Control of Linear Systems over Lossy Channels. In *Proceedings of the 2nd IFAC Workshop on Distributed Estimation and Control in Networked Systems*, 2010.

32. R. Penrose. A generalized inverse for matrices. In *Mathematical proceedings of the Cambridge philosophical society*, volume 51, pages 406–413. Cambridge Univ Press, 1955.

33. M. Rabi. *Packet based inference and control*. PhD thesis, 2006.

34. M. Rabi and K. Johansson. Event-triggered strategies for industrial control over wireless networks. In *Proceedings of the 4th Annual International Conference on Wireless Internet*, pages 1–7. ICST (Institute for Computer Sciences, Social-Informatics and Telecommunications Engineering), 2008.

35. M. Rabi and K. Johansson. Scheduling packets for event-triggered control. In *Proc. of 10th European Control Conf*, pages 3779–3784.

36. M. Rabi, G. Moustakides, and J. Baras. Multiple sampling for estimation on a finite horizon. In *Decision and Control, 2006 45th IEEE Conference on*, pages 1351–1357. IEEE, 2006. ISBN 1424401712.

37. M. Rabi, K. Johansson, and M. Johansson. Optimal stopping for event-triggered sensing and actuation. In *Decision and Control, 2008. CDC 2008. 47th IEEE Conference on*, pages 3607–3612. IEEE, 2008.

38. M. Rabi, G. Moustakides, and J. Baras. Adaptive sampling for linear state estimation. In *Arxiv preprint arXiv:0904.4358*, 2009.

39. J. Sandee, W. Heemels, and P. van den Bosch. Event-driven control as an opportunity in the multidisciplinary development of embedded controllers. In *American Control Conference, 2005. Proceedings of the 2005*, pages 1776–1781. IEEE, 2005. ISBN 0780390989.

40. J. Sandee, W. Heemels, and P. van den Bosch. Case studies in event-driven control. In *Hybrid Systems: computation and control*, pages 762–765. Springer, 2007.

41. P. Tabuada. Event-triggered real-time scheduling of stabilizing control tasks. In *Automatic Control, IEEE Transactions on*, volume 52, pages 1680–1685. IEEE, 2007.

42. P. Tabuada and X. Wang. Preliminary results on state-trigered scheduling of stabilizing control tasks. In *Decision and Control, 2006 45th IEEE Conference on*, pages 282–287. IEEE, 2006. ISBN 1424401712.

43. X. Wang and M. Lemmon. Decentralized event-triggered broadcasts over networked control systems. In *Hybrid Systems: computation and control*, pages 674–677. Springer, 2008.

44. X. Wang and M. Lemmon. Event design in event-triggered feedback control systems. In *Decision and Control, 2008. CDC 2008. 47th IEEE Conference on*, pages 2105–2110. IEEE, 2008.

45. X. Wang and M. Lemmon. State based self-triggered feedback control systems with L2 stability. In *17th IFAC world congress*. Citeseer, 2008.

46. X. Wang and M. Lemmon. Event-triggering in distributed networked control systems. In *Automatic Control, IEEE Transactions on*, number 99, pages 1–1. IEEE, 2009.

47. X. Wang and M. Lemmon. Event-triggering in distributed networked systems with data dropouts and delays. In *Hybrid Systems: Computation and Control*, pages 366–380. Springer, 2009.

48. X. Wang and M. Lemmon. Finite-gain l2 stability in distributed event-triggered networked control systems with data dropouts. In *the European Control Conference*, 2009.

49. X. Wang and M. Lemmon. Self-Triggered Feedback Control Systems With Finite-Gain L_2 Stability. In *Automatic Control, IEEE Transactions on*, volume 54, pages 452–467. IEEE, 2009.

50. X. Wang and M. Lemmon. Self-triggered feedback systems with state-independent disturbances. In *American Control Conference, 2009. ACC'09.*, pages 3842–3847. IEEE.

51. X. Wang and M. Lemmon. Asymptotic stability in distributed event-triggered networked control systems with delays. In *American Control Conference (ACC), 2010*, pages 1362–1367. IEEE, 2010.

52. Y. Xu and J. Hespanha. Optimal communication logics in networked control systems. In *Proceedings of the IEEE Conference on Decision and Control*, volume 4, pages 3527–3532, Nassau, Bahamas, 2004.

53. H. Yu and P. Antsaklis. ISIS Technical Report: Event-Triggered Real-Time Scheduling For Stabilization of Passive/Output Feedback Passive Systems. In *isis*, page 001, 2010.

This document was prepared & typeset with LaTeX 2ε*, and formatted with* NDdiss2ε *classfile (v3.0[2005/07/27]) provided by Sameer Vijay.*